Improving the arm-hand coordination in neuroprosthetics control with prior information from muscle activity

Thèse N° 9429

Présentée le 17 mai 2019

à la Faculté des sciences et techniques de l'ingénieur
Laboratoire d'algorithmes et systèmes d'apprentissage
Programme doctoral en robotique, contrôle et systèmes intelligents

pour l'obtention du grade de Docteur ès Sciences

par

Iason BATZIANOULIS

Acceptée sur proposition du jury

Prof. J. D. R. Millán-Ruiz, président du jury
Prof. A. Billard, directrice de thèse
Prof. L. J. Hargrove, rapporteur
Prof. B. Argall, rapporteuse
Prof. S. Micera, rapporteur

2019

ÉCOLE POLYTECHNIQUE
FÉDÉRALE DE LAUSANNE

Abstract

Humans use their hands mainly for grasping and manipulating objects and for performing simple and dexterous tasks. The loss of a hand can significantly affects one's working status and independence in daily life. A restoration of the grasping ability is important to improve the quality of the daily life of the individuals with motion disorders. Although neuroprosthetic devices restore partially the lost functionality, the user acceptance is low, possibly due to the artificial and unnatural operation of the devices. We seek to improve the user acceptance of prosthetic devices, hence we developed control approaches that enable a seamless and more natural operation of hand prostheses.

The motion of an able hand, when grasping an object, is divided into two phases: (i) the reaching phase, i.e., when the hand approaches the object, and (ii) the grasping phase, i.e., when the hand closes and touches the object. During the reaching phase, the configuration of the fingers changes continuously as the hand moves closer to the object. The closure of the hand is coupled with the arm extension, resulting in a smooth coordination of the arm, hand and finger. However, current approaches in neuroprosthetic control enable the hand closure activation only after the completion of the reaching phase. These approaches offer a very limited coordination between the prosthesis and the user's intention. We introduce an alternative method for controlling prosthetic devices, based on an early detection of the grasping intention, thus enabling a faster activation of the device, hence improving coordination between the user's arm and the prostheses.

In the first part of thesis, we focus on the identification of the grasping intention for the reach-to-grasp motion with able-bodied individuals. We propose an Electromyographic (EMG)-based learning approach that decodes the grasping intention at an early stage of reach-to-grasp motion, i.e., before the final grasp/hand pre-shape takes place. In this approach, the utilization of Echo State Networks encloses efficiently the dynamics of the muscle activation, enabling a fast identification of the grasp type in real-time. We also examine the impact of different object distances and speeds on the detection time and accuracy of the classifier. Although the distance from the object has no significant effect, rapid motions influence significantly the performance.

In the second part of this thesis, we evaluate and extend our approach on four

real end-users, i.e., individuals with amputations below the elbow. For addressing the variability of the EMG signals, we separate the reach-to-grasp motion into three phases, with respect to the arm extension. A multivariate analysis of variance on the muscle activity reveals significant differences among the motion phases. We examine the classification performance on these phases and compare the performance of different pattern-recognition methods. An on-line evaluation with an upper-limb prosthesis shows that the inclusion of the reaching motion in the training of the classifier substantially improves the classification accuracy.

In the last part of the thesis, we further explore the concept of motion phases on the EMG signals and its potential for addressing the variability of the signals. We model, over the different phases of the overall motion, the dynamic muscle contractions of each class with Gaussian distributions. We extend our previous analysis by providing insights on the Linear Discriminant Analysis (LDA) projection and by quantifying the similarity of the distributions of the classes (i.e., grasp types) with the Hellinger distance. We notice larger values of the Hellinger distance and, thus, smaller overlaps among the classes with the segmentation to motion phases. A LDA classifier with phase segmentation affects positively the classification accuracy.

Keywords: Neuroprosthetics control, Pattern recognition, Biomedical signals, Electromyography, Machine learning, Signal processing

Résumé

Les humains utilisent leurs mains principalement pour saisir et manipuler des objets et pour effectuer des tâches simples et habiles. La perte d'une main peut affecter de manière significative le statut professionnel et l'indépendance de la personne au quotidien. Une restauration de la capacité de saisie est importante pour améliorer la qualité de vie quotidienne d'une personne handicapée. Malgré que les appareils neuroprothétiques restaurent partiellement la fonctionnalité perdue, l'acceptation de l'utilisateur est faible, probablement à cause des mouvements non naturels que ces appareils produisent. Nous cherchons à améliorer l'acceptation des appareils prothétiques par les utilisateurs. C'est pourquoi nous avons développé des approches de contrôle permettant un fonctionnement transparent et naturel des prothèses de la main.

Le mouvement d'une main lors de la saisie d'un objet est divisé en deux phases: (i) la phase d'atteinte, c'est-à-dire lorsque la main s'approche de l'objet, et (ii) la phase de saisie, c'est-à-dire lorsque la main se ferme et touche l'objet. Pendant la phase d'atteinte, la configuration des doigts change continuellement à mesure que la main se rapproche de l'objet. La fermeture de la main est couplée à l'extension du bras, ce qui permet une coordination harmonieuse du bras, des mains et des doigts. Cependant, les approches actuelles en matière de contrôle neuroprothétique ne permettent l'activation de la fermeture de la main qu'après la fin de la phase d'atteinte. Ces approches offrent une coordination très limitée entre la prothèse et l'intention de l'utilisateur. Nous introduisons une nouvelle méthode de contrôle des prothèses, basée sur une détection rapide de l'intention de saisir, permettant ainsi une activation plus rapide de la fermeture de la main, améliorant ainsi la coordination entre le bras de l'utilisateur et les prothèses.

Dans la première partie de la thèse, nous nous concentrons sur l'identification de l'intention de saisie pour atteindre et saisir des objets avec des personnes valides. Nous proposons une approche d'apprentissage basée sur l'électromyographie (EMG) qui décrypte l'intention de saisir à un stade précoce du mouvement, c'est-à-dire avant que le mouvement du bras ne se termine. Dans cette approche, l'utilisation des "Echo State Networks" enferme efficacement la dynamique de l'activation musculaire, ce qui permet une identification rapide du type de saisie en temps réel. Nous examinons également l'impact de différentes distances d'objet et vitesses du mouvement sur le temps de détection et la

précision du classificateur. Bien que la distance par rapport à l'objet n'a pas d'effet significatif, des mouvements rapides ont une influence importante sur les performances.

Dans la deuxième partie de la thèse, nous évaluons notre approche à quatre utilisateurs handicapés; plus précisément des personnes amputées au-dessous du coude. Pour remédier à la variabilité des signaux EMG, nous séparons le mouvement en trois phases, par rapport à l'extension du bras. Une analyse de variance multivariée sur l'activité musculaire révèle des différences significatives entre les phases de mouvement. Nous examinons les performances de classification sur ces phases et comparons les performances de différentes méthodes de reconnaissance de formes. Une évaluation en temps réél avec une prothèse du membre supérieur montre que l'inclusion du mouvement d'atteinte dans les données du classificateur améliore considérablement la précision de la classification.

Dans la dernière partie de la thèse, nous explorons plus en détail le concept de phases de mouvement sur les signaux EMG et son potentiel pour traiter la variabilité des signaux. Nous modélisons, au cours des différentes phases du mouvement, les contractions musculaires dynamiques de chaque classe avec des distributions gaussiennes. Nous étendons notre analyse précédente en fournissant des informations sur la projection de l'Analyse Discriminante Linéaire (ADL) et en quantifiant la similarité des distributions des classes (c'est-à-dire des types de saisie) avec la distance de Hellinger. Nous remarquons des valeurs plus grandes de la distance de Hellinger et, par conséquent, des chevauchements moins importants entre les classes avec la segmentation du mouvement complet en différentes phases. Un classifieur ADL avec segmentation de phase affecte positivement la précision de la classification.

Mots Clés: Contrôle des neuroprothèses, Reconnaissance de formes, Signaux biomédicaux, Électromyographie, Apprentissage automatique, Traitement du signal.

Ό,τι δε συνέβη ποτέ, είναι ό,τι
δεν ποθήσαμε αρκετά
(Whatever didn't happen is
whatever we didn't desire enough)

Nikos Kazantzakis

Acknowledgments

In the end of a long journey, it is difficult to remember all the people I met and interacted and all the events that happened. However, some thank-yous are ought to be given.

First, I would like to express my profound gratitude to my thesis advisor Prof. Aude Billard who gave me the opportunity to work towards a Ph.D. degree. This thesis would not have been possible without her believing in me, supporting me and never ceasing to challenge me. I am more than grateful to her for providing me with constructive feedback on my work and guidance.

I would also like to thank Prof. Levi Hargrove who gave me the opportunity to visit his lab and evaluate my research with end-users, but also his advice during this stay. This experience has indeed "opened my eyes" on what would be effective in clinical applications. Also, I would like to thank Prof. Silvestro Micera for our collaboration and his valuable advice during the beginning of my PhD. I would also like to thank them, together with Prof. Brenna Argall, for their insightful comments and feedback on my thesis. Furthermore, I am grateful to Prof. José del R. Millán, who served as a president of my committee, but also for our collaboration almost throughout my Ph.D.

I would also like to thank the lab's secretary, Joanna Erfani, and the secretary of my doctoral program, Ms Corrine Lebet, for taking care of the administrative aspects of my Ph.D.

The most important of a lab is its members and I am grateful to be in a lab with great people. I would like to thank the first person who I met when I first arrived to the lab, Sahar El-Khoury. I appreciate her help during my first steps as a researcher but also her support and friendship. Also, I would like to thank the former members of the lab: Klas, Miao, Ashwini and Suphi for welcoming me in the lab. I really enjoyed the discussions with Guillaume and Felix over a glass (or more) of beer. Nicolas was the best on "stealing" beers from people when they were not looking! Having beers and barbeques in the terrace with colleagues is one of my best memories from the lab!

There are other members of the lab who I didn't have the chance to spend more time with, such as Denys, Andrew, Laura, Jose, Nili, Joao, Hang, Ravin, Seungu, Joel, Lucia, Murali, Jordi, Kevin, Brice and Suphi, but hanging out with them made my lab-life more enjoyable. I am very lucky to be a colleague with

people who know how to make interesting conversations on various topics: Mahdi (trolling everyone), Baptiste (huge movie fan), Konstantinos (with a solution on everything), Lukas (a famous ski instructor), Micheal (who could join us a bit more for lunch), David (who is always in for anything), Kunpeng (dedicated to object manipulation n^{o}1), Anais (always excited), Salman (who loves jogging), Jacob (rumors have it that he can do a hundred push-ups in a row), Saurav, Bernardo (deep knowledge on Apple devices), Diego-Felipe (huge discussion on which is his preferable name), Farshad (dedicated to object manipulation n^{o}2) and Aileen (my research inheritor?). Many thanks and a big hug to Sina and Leonardo for their help and the discussions during lunch breaks, I have really enjoyed them.

I would also like to give my appreciation to my friends who supported me during my Ph.D. I would like to thank Nadia for the amazing times inside and outside of the lab and for all the discussions about research and life, and life in research. I would like to deeply thank Illaria and Walid for being so kind and supportive and helping me keep going. I really appreciate this, guys. Lastly, I would like to thank Professor Athanasios for tolerating my grouchiness in the office but also for educating me with his deep knowledge on Greek cult culture.

I would have never accomplished this task without the endless support, love and encouragement of my family. I would be never be the person that I am without my parents never losing their faith in me. I cannot be more grateful to my sister, Elena, for always being there for me, offering valuable advice and support throughout my life.

Lastly, but most importantly, I would like to thank my partner in life, Eirini, for her endless patience and love, her understanding and continuous support during my ups and downs. Without her being next to me, I wouldn't be able to complete this work.

Table of Contents

Acknowledgments . . . . . **vii**

1 Introduction **1**
1.1 Motivation 1
1.2 Problem Statement and Approach 2
1.2.1 The role of Pattern Recognition in Prosthetic Devices for the upper-limb 5
1.3 Main Contributions and Thesis Outline 6
1.4 Publications, Source code and Multimedia 9

2 Background **11**
2.1 Human-Hand Motion During the Reaching Phase 11
2.2 Decoding Hand Postures from Electromyography 12
2.2.1 Electromyographic features 14
2.2.2 Machine-learning methods in neuroprosthetics control . . 15
2.3 EMG-decoding on Individuals with Transradial Amputations . . 16

3 EMG-Based Decoding of Grasp Gestures in Reaching-to-Grasping Motions **21**
3.1 Introduction 21
3.2 Methods 23
3.2.1 Participants 23
3.2.2 Experimental Protocol 24
3.2.3 Apparatus and pre-processing 25
3.2.4 Preshape Criteria 26
3.2.5 Classification Method 27
3.2.6 Online Robotic Implementation 28
3.3 Results 29
3.3.1 Reach-to-Grasp classification strategy 29
3.3.2 Decreasing the number of EMG channels 32
3.3.3 Generalization on different distances 33
3.3.4 Speed effect 36
3.3.5 Classification rate Vs Hand preshape 37
3.3.6 Online Robotic Implementation 40
3.4 Discussion 41
3.5 Conclusion 46

4 Decoding the Grasping Intention from Electromyography during Reaching Motions **47**
4.1 Introduction 47
4.2 Methods 49
4.2.1 Experimental Protocol 49

4.2.2 Apparatus and Pre-processing . . . 50
4.2.3 Phases of the Motion . . . 51
4.2.4 Classification Methods for Decoding the Grasping Intention 52
4.2.5 Physical Prosthesis Control . . . 53
4.3 Results . . . 54
4.3.1 Kinematics of the Elbow Joint Angle and Quality of the EMG signals . . . 54
4.3.2 Phases of the Motion . . . 55
4.3.3 Decoding the Grasping Intention . . . 57
4.3.4 On-line Evaluation . . . 61
4.4 Discussion . . . 62
4.5 Conclusion . . . 66

5 Reach-to-grasp motions: Towards a Dynamic Classification Approach for Upper-Limb Prostheses . . . 67
5.1 Introduction . . . 67
5.2 Methods . . . 68
5.2.1 Experimental protocol . . . 68
5.2.2 Apparatus . . . 69
5.2.3 Phases of the motion and classification method . . . 69
5.3 Results . . . 70
5.3.1 Phases of the motion and Hellinger distance . . . 71
5.3.2 Classification performance . . . 72
5.4 Discussion . . . 72
5.5 Conclusion . . . 74

6 Conclusion . . . 75
6.1 Main Contributions . . . 75
6.2 Limitations and Future Work . . . 76
6.3 Concluding Summary . . . 80

Appendices . . . 81

A Supplementary Materials for Chapter 4 . . . 83

B Student Projects Supervised by the Author . . . 89

References . . . 95

Curriculum Vitae . . . 107

Chapter 1

Introduction

1.1 Motivation

Robotic systems were introduced in our daily lives for more than a decade. As their popularity increases, robotic and automated systems' functionalities are being improved, offering various solutions and improving the quality of life. An important application of robotic systems includes the rehabilitation of patients with motor disorders of the upper limb.

The loss of a hand affects all aspects of life (Freeland and Psonak (2007)). It has been reported that between 37% (Ziegler-Graham et al. (2008)) to 61% (K. Oltstlie et al. (2011)) of upper-limb amputations concern below-elbow amputations due to trauma (Ziegler-Graham et al. (2008)). More than one third of the amputee population are below 45 years old (Ziegler-Graham et al. (2008); K. Oltstlie et al. (2011)) and the large majority of them are in early retirement (K. Oltstlie et al. (2011)). Therefore, restoring their lost abilities would provide them a better quality of life and increase their opportunities for active employment.

Grasping is one of the most important functionalities of the hand. Human-hand dexterity makes it capable of adapting to the various tasks and characteristics of objects. When dining, for example, we grasp differently the forks from the knives and glasses, or we select different grasp types depending on if we want to relocate a cup or to drink from it. Indeed, grasping is such a natural activity that it is very hard to even imagine the consequences of losing this functionality. Hence, restoring the grasping ability could, indeed, improve the quality of life of people with upper-limb amputations.

Neuroprosthetic devices are used to partially restore motor abilities lost after pathologies or trauma (Lambercy et al. (2011)). Despite the potential benefits of the prosthetic rehabilitation, a large number of people with upper-limb amputations do not use a prosthesis (Raichle et al. (2008)). Recent studies (Biddis (2010); Oltstlie et al. (2012)), examining the causes of rejection, report that the main reason for secondary, i.e., after a period of usage, prosthesis rejection is a dissatisfaction with the prosthetic comfort, function or control. Moreover, it has been reported (Biddis (2010)) that functionality is one of the priorities for the acceptability of a wearable robotic device, and that inconvenient and

Figure 1.1: Commercially available prosthetic devices. a) the Bebionic hand[1], b) the i-limb ultra hand[2], c) the Michelangelo hand from Ottobock[3]and d) the Azzurra hand from Prensilia[4]

time-ineffective systems might avert individuals from using a prosthetic device.

In order to increase the user's acceptance, a wearable device should cover a large variety of human motions that correspond to daily tasks. As these devices are in direct contact with the users, they should operate in harmony with the users, following smoothly their movements in a natural way. Hence, it is important that the device reacts promptly to the detection of the movement intention.

Our goal is to improve the performance of the pattern-recognition system on reach-to-grasp tasks and, hence, enhance the coordination between the user and the neuroprosthetic device. Specifically, in order to decode the grasp intention decoding during the reaching phase, we investigate the muscle activity of able-bodied individuals and individuals with below-elbow amputations. An accurate identification of the grasp type in the reaching cycle could enable a prompt activation of the device and improve the coordination with the user.

1.2 Problem Statement and Approach

When humans engage in reach-to-grasp tasks, the hand opens and closes in coordination with the extension of the arm (Rand et al. (2008); Wang and Stelmach (1998)). The motion is distinguished into two phases: (i) the reaching phase, i.e., when the hand approaches the object, and (ii) the grasping phase, i.e., when the hand closes and touches the object. Typically, the hand opens rapidly in the early stages of the reaching motion and decreases its velocity converging towards its final configuration (Jeannerod (1984)). Before forming their final configuration, the formation of the fingers, is defined as hand's pre-shape (Haggard and Wing (1995)). Figure 1.2, illustrates the velocity profiles of the arm's extension and the hand's opening and closure of the able-bodied individuals we studied. These profiles are missing from the functionality of neuroprosthetic devices. Although the time of the activation of a prosthesis depends

[1] www.bebionic.com
[2] http://touchbionics.com/products/active-prostheses/i-limb-ultra
[3] https://www.ottobockus.com/prosthetics/upper-limb-prosthetics/solution-overview/michelangelo-prosthetic-hand
[4] https://www.prensilia.com/

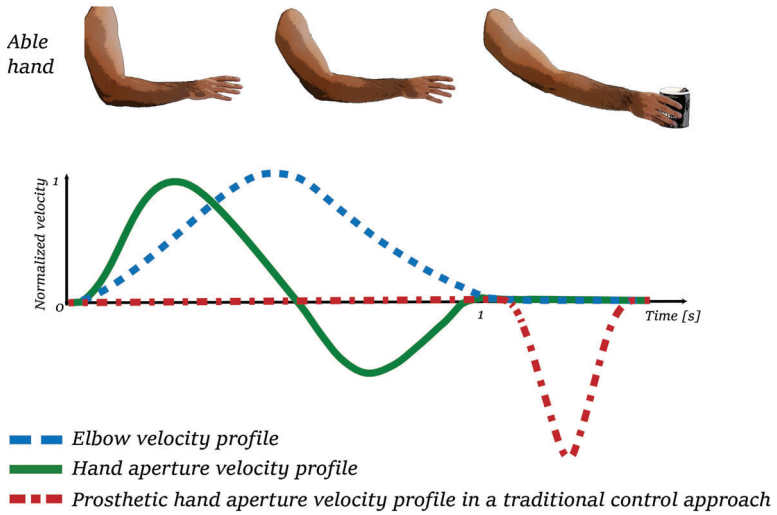

Figure 1.2: An illustration of the functionality of the able hand and a prosthesis. The able hand opens and closes during reaching in coordination with the extension of the arm. Although the time of the activation of a prosthesis depends on the user, the task and the hardware of the prosthetic limb, it generally occurs in the very late stages of the reach-to-grasp cycle and often after the end of the reaching motion.

on the user, the task and the hardware of the prosthetic limb, it generally occurs in the very late stages of the reach-to-grasp cycle and often after the end of the reaching motion. Below, we present the main reason of this limitation.

Neuroprosthetic devices for the upper-limb partially restore the grasping ability of individuals who lost this functionality due to an amputation. In the case of myoprosthesis, the operation of the device involves two principal stages; the identification of the grasping intention (i.e. the grasp type) from the muscle activity of the user and the corresponding activation of the device. The embedded pattern-recognition system, which is responsible for the identification of the grasp type, computes also a measure of confidence for the predicted grasp type. Once the confidence is above a threshold, the prosthetic hand closes immediately, and in a few cases compliantly, to a predefined finger configuration with a fixed speed.

We notice two characteristics regarding this functionality: a) A high accuracy of the pattern recognition system is crucial for the proper operation of the device, and b) the closure of the prosthetic hand occurs regardless of the motion of the arm, with limited or no coordination between them. These characteristics indicate an artificial behavior of the prosthesis as it stays idle in the reaching phase and begins the hand closure only when the object is reached. Figure (1.3) shows an example of this operation from the work of (Kyranou et al. (2016)).

There is a main reason that renders the device idle during reaching: the pattern recognition system fails to identify properly the desired grasp type during the reaching phase. Hence, the system produces a low confidence value for the desired grasp, which is below the selected threshold, and postpones the activa-

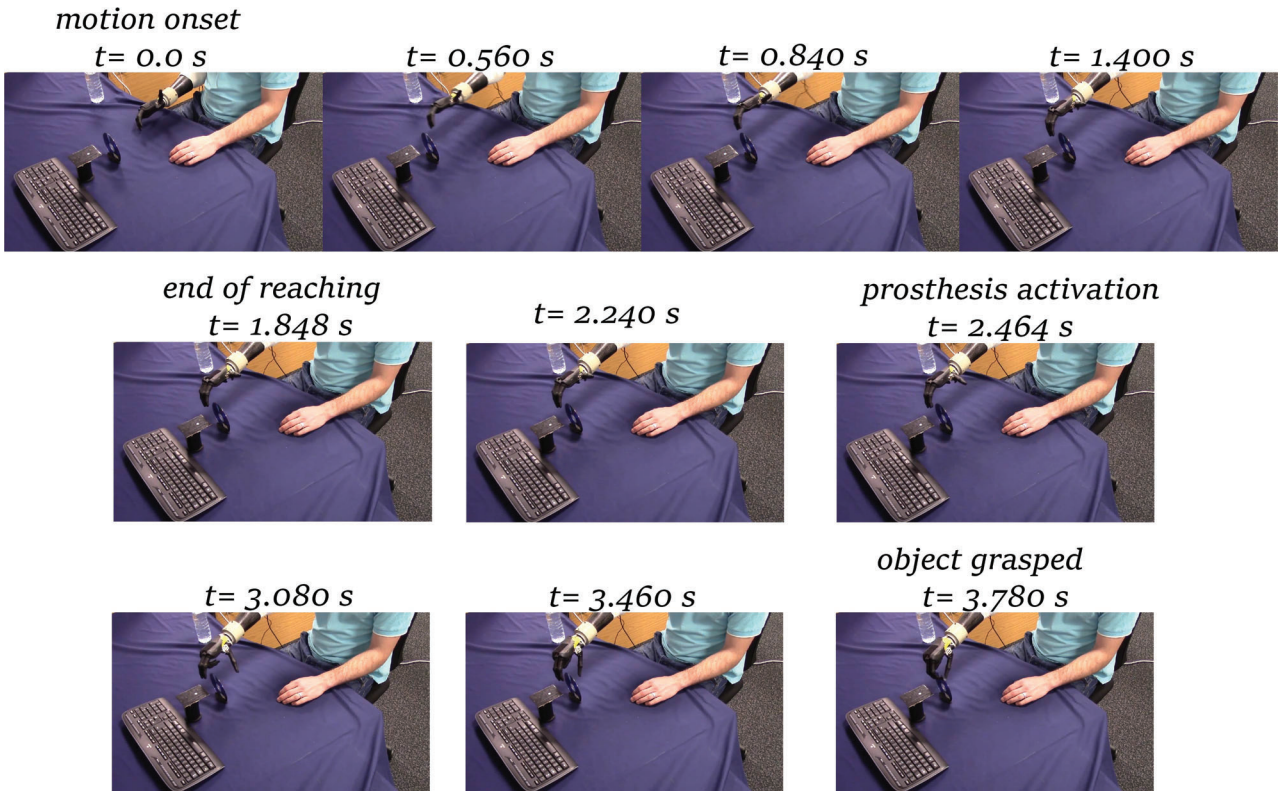

Figure 1.3: An example of traditional control approach from (Kyranou et al. (2016)). The prosthetic device is activated approximately 0.7s after the end of the reaching motion.

tion of the device until it is confident enough for the output.

In this thesis, we address this limitation by focusing on the development of methods and experimental protocols for a successful decoding of the grasping intention during the reaching phase from Electromyography (EMG). An early and accurate prediction of the grasp type during the reaching phase enables a faster activation of the hand prosthesis, thus addressing the aforementioned limitation.

In the first part of the thesis, we investigate the stage where an accurate decoding occurs on able-bodied individuals. In order to do this, we use the hand's preshape and compare it with the classification accuracy. We notice that it is possible to have an accurate decoding of the grasp type in the early stages of the reaching motion and even, in some cases, before the hand's preshape. To demonstrate the feasibility of this approach in neuroprosthetic control, we integrate it in a real-time control of a robotic hand. The high classification accuracy in the early stages of the motion results in a high confidence value that enables an activation of the robotic hand during the reaching phase. As a result, the EMG activity of the arm during reaching is efficient for achieving high accuracy in decoding the grasping intention.

In the second part of the thesis, we evaluate our hypothesis by implementing

the protocol on individuals with below-the-elbow amputations. To address the variability of the EMG signals, we separate the motion into three phases: (1) the first phase - where the velocity of the motion increases, (2) the second phase- where the velocity of the motion decreases, and (3) the third phase - when the reaching motion is complete. We notice significant differences in the EMG activity among these phases. This indicates if we train a classifier in only one phase, it would fail to generalize for the other two. This would result in low classification-confidence value and in delays in the activation of the devices. The inclusion of all the phases in training increases significantly the classification performance and the resulting confidence value. Thus, the device is able to identify the grasp type and to command the prosthesis to close before the end of the reaching motion, i.e., in the second phase. The fast activation of the device improves the coordination with the arm extension and narrows the gap between prosthesis operation and the behavior of an able-hand.

In the third part of the thesis, we further explore the concept of motion phases and its effect in the classification performance. First, we perform a Linear Discriminant Analysis (LDA) for each motion phase and the overall motion. We model the distributions of the classes (i.e., grasp types) on the projected space and quantify the overlap among them. The individual projection on each phase produces overlap smaller than the overall projection hence more distinguished classes. By employing one classifier for each motion phase, we address the variability of the EMG signals and increase the accuracy of the decoder. In this way, we enhance the efficiency of the pattern recognition system and the reliability of the prosthetic device.

1.2.1 The role of Pattern Recognition in Prosthetic Devices for the upper-limb

As previously discussed, the embedded pattern-recognition system is the ”brain” of the prosthetic device. It is responsible for identifying the user's intention and activating the prosthesis. It employs different sensory inputs and processes them for directly relating the sensory patterns to actions for the prosthesis.

Various control methods were developed for intuitively extracting,in a non-invasive or invasive way, the user's intention. In non-invasive control methods, the user's intention could be extracted from electromyography (EMG) (Cipriani et al. (2011)), ultrasound imaging (Gonzales and Castellini (2013)) or force myography (FMG) (Cho et al. (2016)). Surgical methods, such as Targeted Muscle Reinnervation (TMR), could increase the number of degrees of freedom controlled by the EMG activity (Kuiken et al. (2009); Hargrove et al. (2017)).

The accuracy of the pattern recognition system has a significant effect on the efficiency of the prosthesis. To improve the reliability of the system, dif-

ferent machine-learning methods have been investigated, such as LDA (Daley et al. (2012)), Support Vector Machines (SVM) (He et al. (2015)) and Artificial Neural Networks (ANN) (Jiang et al. (2014)). Furthermore, machine-learning approaches are used to control multi-DOF prostheses with fewer independent EMG sites. EMG-based pattern-recognition systems are proposed for the estimation of hand and wrist movements (Smith et al. (2016); Gonzalez-Vargas et al. (2015)) and even individual finger movements (Naik et al. (2016); Khushaba et al. (2012)). Generally, subjects performed muscle contractions while maintaining their arm in a fixed position. Training a classifier in a static position results in classification accuracy lower than when the limb is in positions different than the ones they are trained for and when it performs dynamic motions (Scheme et al. (2011)).

To improve the efficiency of the pattern-recognition system during reaching, we were inspired by the preshape of the hand during reaching. The preshape of the hand is defined as the formation of the fingers before they take the final configuration; this preshaping takes place during the reaching cycle (Supuk et al. (2005)). The posture of the hand can be discriminated well before the contact with the object (Santello et al. (1998)). In other words, the trajectories of the fingers before their closure around the object correspond to an indication of the final grasp type before the grasping phase, i.e., before the fingers are in contact with the object. As the motion is derived from the muscle activity, the grasping intention can be decoded from the EMG signals during the reaching phase. Furthermore, the peripheral nerve function remains functionally intact many years after amputation (Dhillon et al. (2004)); this indicates that this information could be detected from the EMG signals of the residual arm. In this thesis, we explore this assumption and provide evidence that the decoding of the grasping intention from the EMG activity during reaching can be integrated into the control of myo-prosthetic devices.

1.3 Main Contributions and Thesis Outline

In this thesis, we describe the three contributions introduced in the previous section. Here, we present a brief overview of each chapter, as well as the corresponding contributions.

Chapter 2 - Background

In Chapter 2, we present a literature review of the state-of-art approaches, with an emphasis on the decoding, from the muscle activity, of the grasping intention.

Chapter 3 - EMG-Based Decoding of Grasp Gestures in Reaching-to-Grasping Motions

In Chapter 3, we present our first contribution on the decoding of the grasping intention. In particular, we select five grasp types that involve all the fingers and are among the most frequent in our daily lives. We employ Echo State Networks (ESNs), a form of Recurrent Neural Network, for their high performance in classification over stochastic signals (Li et al. (2012); Xu and Han (2016)). The classification accuracy starts at a low level and increases as the hand approaches the object of interest. In all cases, the classification performance reaches a level of high accuracy (i.e., above 90%) $0.5s$ after the motion onset. In order to identify the stage of the reaching phase where the classification reaches high levels of accuracy, we relate the classification performance with the hand's preshape. We select two criteria for the definition of preshape; the hand's aperture (i.e., the distance between the fingertips of the index finger and the hand) and the area enclosed from the fingertips that are involved in the grasp type. In three of the grasp types, before the hand's preshape, the classification accuracy becomes higher than 90%. We notice that the object size has an affect on the classification performance; grasping thin objects with similar grasp types involves a sole closure of the fingers, which starts from the motion onset. In this case, the grasp type could be decoded at a later stage, however, while still in the reaching phase.

As different speeds and distances from the object can require different dynamics, the effect of these factors on the classification accuracy are examined at a next stage. Although the distance from the object has no significant effect, rapid motions dramatically influence the classification. The rapid activation of the arm muscles during rapid motions differentiates the activation of agonist/antagonists muscles, which influences the EMG signals and results in a lower performance.

Furthermore, we integrate this approach in a real-time control of a robotic hand. In this scenario, the robot hand is activated, after a high classification confidence value, and performs the desired grasp type. The on-line evaluation shows a fast and accurate activation of the robot hand that completes its closure before the user reaches the object. This evaluation demonstrates the feasibility of a prompt decoding of the grasping intention from the EMG signals.

Chapter 4 - Decoding the Grasping Intention from Electromyography during Reaching Motions

In Chapter 4, we evaluate this assumption with four individuals with below-the-elbow amputations. The participants perform reach-to-grasp motions for five grasp types with both their intact arm and their phantom limb, attempting to replicate the motion with the phantom limb. We record the activity of muscles of the forearm, as well as the upper arm. To examine more precisely the muscle activity during the motion, we separate the motion into three phases: (1) where the velocity of the motion increases, (2) where the velocity of the motion decreases, and (3) when the reaching motion is complete. We extract time-domain

features from the signals, then model the overall muscle activity of each phase with Gaussian Mixture Models (GMMs), as shown in Figure (1.4). A Multivariate Analysis of Variance (MANOVA) reveals significant differences in the EMG signals among the phases. This indicates limitations on the generalization of a classifier trained solely on one phase.

The classification performance in the three motion phases is examined. We compare the performance of four classification methods; Linear Discriminant Analysis (LDA), Support Vector Machines (SVM) with linear and radial Basis function (RBF) kernels and the ESN approach from Chapter 3. The classification performance for each classifier follows the same profile: There is a poor performance in the first phase, but the performance increases as the hand approaches the object. We notice the largest increase on the second phase. By decreasing the number of classes (i.e., grasp types) to three, the classification accuracy becomes higher than 80% in the second phase, before the end of the reaching motion, for three of the four amputee participants.

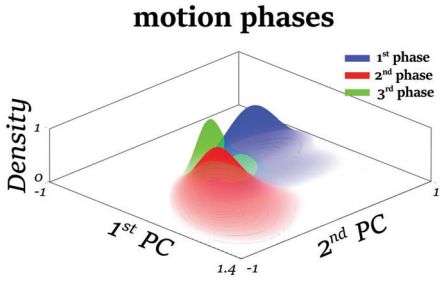

Figure 1.4: The muscular activity of the three phases projected on two principal components and modeled with GMMs

In our real-time evaluation, we highlight the negative impact that the lack of good classification over the entire duration of the reaching motion has in the natural coordination of the motion of the prosthesis with the arm. In particular, the performance of a classifier is compared when it is trained only with one phase (i.e., the third motion phase) against our approach that takes the overall motion into account. Our results show that the muscle contractions when the arm is fixed are different from the contractions when the arm extends, hence the pattern-recognition fails to generalize for the other phases. Therefore, the approach is able to address the problem of dynamically estimating the grasp type and to reduce the time needed for reaching a sufficient classification confidence.

Chapter 5 - Reach-to-grasp motions: Towards a Dynamic Classification Approach for Upper-limp Prosthesis

In Chapter 5, we further investigate the concept of motion phases and their effect on the performance of the patter-recognition system. The same phase segmentation is used as in Chapter 4. We extract time-domain features and perform LDA on the data of each phase and on the overall motion. The projected data of each class (i.e. grasp type) are modeled with Gaussian distributions, and the overlap is quantified with the Hellinger distance. This distance is a bounded metric of similarity between distributions. It reaches its maximum value of 1 when the distributions do not overlap. In the above comparison, we notice values

of the Hellinger distance between the distributions on the LDA space of each phase larger than the overall LDA space. This indicates that the distributions of the classes are better separated in the individual space. Furthermore, the distributions of the classes are better separated in the late stages of the reaching motion, thus producing even larger values of the Hellinger distance.

The better separation of the distribution has an positive effect on the classification performance. By employing one classifier for each phase, we are able to increase the overall accuracy by $6 - 10\%$ on average. As the distributions become more dissociable in the later motion phases, the classification accuracy reaches its highest level ($74.2 \pm 14\%$) in the final phase. These results indicate an improved encapsulation of the EMG patterns on each motion phase.

Chapter 6 - Conclusion

In Chapter 6, we summarize the contributions and their limitations. We discuss potential research directions that could derive from this work.

Chapter 6 - Appendices

In the Appendices, additional materials regarding the contributions are provided. We, also, present a brief description of the projects supervised by the author.

1.4 Publications, Source code and Multimedia

The chapter concerning the contributions of this thesis are published in peer-reviewed journals and at conferences. The context of Chapter 3 is published in (Batzianoulis et al. (2017)). The evaluation with individuals with below-elbow amputations, presented in Chapter 4, is published in (Batzianoulis et al. (2018)). The context of Chapter 5 is published in (Batzianoulis et al. (2019)).

In addition, the author also wrote and coauthored several publications which are not part of this thesis. During his internship before starting his PhD research, which took place in LASA lab of Professor Aude Billard, he published an abstract with the pilot results on the decoding of the grasping intention from the EMG activity (Batzianoulis et al. (2015)). During this period, he also contributed in a study on regressing the wrist position from the EMG signals (El-khoury et al. (2015)). He contributed in a study on the development of a synergistic control method combining the eye-gaze and muscular activity for proximal upper-limb prosthesis, an abstract of which is published in (Krausz et al. (2016)). Furthermore, I participated in a project on developing Inverse Reinforcement Learning (IRL) methods with the employment of electroencephalographic (EEG) signals, the pilot results of which are published in (Iwane et al. (2019)).

The source code of projects mentioned above can be found in this link.

Videos from the projects could be found in these links: first contribution, second contribution, and in LASA's YouTube Channel.

Table 1.1: Links related to the included publications

source code https://github.com/yias?tab=repositories
Chapter 3 https://www.youtube.com/watch?v=58tjelKFhAg&t
Chapter 4 https://www.youtube.com/watch?v=vnBPR9EexYo&t
LASA YouTube Channel https://www.youtube.com/channel/UCqnvGUfdlr94mddDQamEBGA

Chapter 2

Background

In this chapter, we present a literature review of the state-of-art approaches for decoding hand gestures from the muscle activity. The motion of the human hand inspired us and we present briefly studies related with the behavior of the hand in reach-to-grasp motions. Then we focus on the developments in the decoding of the hand posture, grasping intention, and machine-learning algorithms that are used.

2.1 Human-Hand Motion During the Reaching Phase

The human hand is characterized by 21 degrees of freedom (DOFs) controlled by 29 muscles (Jones and Lederman (2006)). Humans are capable of controlling this large number of DOFs and use their hands dexterously due to a multidimensional reduction of the controlled variables operated by the central nervous system. This multidimensional reduction is accomplished through the use of postural synergies Santello and Soechting (1998) , corresponding to a number of hand postures that humans combine when grasping objects.

When reaching to grasp an object, the opening and closing of the hand is in coordination with the motion of the arm (Rand et al. (2008); Wang and Stelmach (1998)). It opens rapidly in the early stages of the reaching cycle, while the fingers converge gradually to their final configuration (Jeannerod (1984); Rand et al. (2008)). The velocity and acceleration profiles of the motion are in harmonic relation with the motion of the fingers and the wrist, and the fingers function in a synergistic manner (Wing and Turton (1986); Santello and Soechting (1998)). It is shown that the reach-to-grasp motion consists of many components (M. Jeannerod (1998); Supuk et al. (2005)). Specifically, the motion can be separated into two phases:(1) the reaching phase, when the hand approaches the object while the fingers are pre-shaping (Supuk et al. (2005)),and (2) grasping phase, where the hand traveled the distance to the object and the fingers take their final form.

In the early stages of the reaching cycle, the hand preshapes according to the selected grasp type. The preshape of the hand is defined as the formation of the

fingers before they take the final configuration (Supuk et al. (2005)). Specifically, the fingers extend to a maximum before they start closing around the object, with respect to its characteristics. Santello et al. (1998) report that the posture of the hand could be discriminated well before the contact with the object. In other words, the trajectories of the fingers before their closure around the object correspond to an indication of the final grasp type before the grasping phase, i.e., before the fingers are in contact with the object. In able-bodied individuals, the hand's preshape occurs at around 60% of the reach-to-grasp motion (Paulignan et al. (1990)).

To capture the preshape, objective metrics are considered. Due to its simplicity, the hand aperture is a commonly used metric for describing the hand preshape (Haggard and Wing (1997)). This metric is defined as the distance of the thumb from the index finger, as these fingers have an important role in the vast majority of grasp types. However, this metric is limited, as the relative motion of these two fingers is not always representative of the grasp type, such as in the lateral grasp. Hence, grasping modes also require the coordination of all the five fingers. To address this limitation, Supuk et al. (2005) propose the area between the fingertips as a metric of preshape. The hand's orientation is another metric of preshape (Roby-Brami et al. (2000)). However, in order for this metric to be considered, different hand orientations should be involved in the grasping.

All the above studies point out the occurrence of continuous motion for the fingers during the reaching phase. This gradual molding of the fingers could be revealed through different patterns of muscle activation during the reaching motion. These patterns can identify the hand's preshape, hence, constitute a direct indication of the grasp type. In this thesis, we exploit this observation and investigate methods for an efficient recognition of the grasping intension during the reaching motion.

2.2 Decoding Hand Postures from Electromyography

It has been extensively demonstrated that a user's motion intention can be accurately detected by surface electromyographic recordings (sEMG) (Novak and Riener (2014)). Different EMG-based systems are proposed for the estimation of hand and wrist movements, and hence used as noninvasive interfaces for controlling exoskeletons (Leonardis et al. (2015)), prosthetic devices (Scheme et al. (2011); Ju and Liu (2014)), computer-animated hands in a virtual environment Sebelius et al. (2005), or for teleoperating robotic arms (Shenoy et al. (2008)). Other studies use various machine-learning methods to decode hand orientations, as well as different combinations of fingers (Shenoy et al. (2008);

Jiang et al. (2005)). Such strategies are useful for accomplishing power grasps that require the simultaneous closure of all fingers on an object. However, these strategies are insufficient to generate differentiated control of all fingers in the variety of pinch grasps used in dexterous objects manipulation, as required for grasping a larger variety of objects.

There are studies focused on the investigation of discrete classifications of wrist flexion/extension (Sebelius et al. (2005); Huang et al. (2005)) and abduction/adduction (Shenoy et al. (2008)), as well as on the use of EMG signals to control wrist exoskeletons (Khokhar et al. (2010); Ziai and Menon (2011)). In (Ma et al. (2015)), the authors use muscles synergies, computed with Non-negative Matrix Factorization (NNMF), to decode four types of hand movements; hand open/close and wrist pronation/supination. Although they report high accuracy when the participants were asked to perform independently each hand motion, the performance drops when they performed simultaneously hand and wrist motion. Indeed, the inclusion of additional degrees of freedom in EMG-based controllers increases the difficulty of a successful estimation of the hand posture.

A few studies focus on the simultaneous and proportional control of the wrist and fingers. A proportional control scheme of 4 DOFs motions by EMG signals is presented in (Muceli and Farina (2012)). Their results show a significant drop of the R^2 coefficient when a dimensionality reduction performed on the extracted features. A simultaneous proportional myoelectric control of 2 DOFs is proposed in (Fougner et al. (2014)), including an online implementation with able-bodied subjects. These approaches use a separate classifier for each DOF to recognize the corresponding motion and achieve dynamic movements in free space with a robotic hand. Those studies focus mainly on the open and closure of the hand, as this motion is an important component of prosthetic devices.

Recent studies investigate the relation between EMG signals and the position of the fingers (Ju and Liu (2014); Naik and Nguyen (2015); Cipriani et al. (2011); Su et al. (2007)). In particular, the authors in (Naik and Nguyen (2015)) report a classification scheme of ten finger flexions, individual finger flexion and simultaneous multiple-finger flexions, using only two sEMG channels. In (Cipriani et al. (2011)) and (Su et al. (2007)), the authors recorded the EMG signals and the fingers' joint angles when performing seven hand gestures, creating a mapping between the fingers' position and the muscular activity.

These studies examine the muscle activity during the motion of wrist and fingers while the rest of the arm remains in a fixed position. Yet, these approaches could be inapplicable on reach-to-grasp motions as muscles from the whole arm are activated in a reaching motions. Training a classifier in a static position, as mentioned above, results in lower classification accuracy when the limb is in different positions or performs dynamic motions (Scheme et al. (2011)). To increase the efficiency of the classification approach, it is important to look into the patterns of the muscular activation. The authors in (Liu et al. (2014)) point

out that the muscle activation differs with respect to the arm position and that examining the EMG patterns is important. This thesis offers an elaboration on the EMG patterns during reach-to-grasp motions, both on able-bodied subjects and individuals with amputation.

2.2.1 Electromyographic features

Feature extraction is very commonly used in the processing of the EMG signals. Those features could be in the time-domain, such as the mean absolute value, the wavelength and the number of slope sign changes, in frequency-domain, such as the power spectral density, the median frequency and the total power of the signal, or autoregressive features. The wavelet transformation is also considered a useful tool as it can provide both time-domain and frequency domain features.

Boostani and Moradi (2003) performed a comparison of 19 features to evaluate their space quality and sparsity. The features were extracted from the forearm muscles of ten individuals with below-elbow amputations, when they contracted these muscles to move their phantom-limbs. The results show that time-domain features produce sufficient sparsity between the classes with the smallest computation time. This is an important indication of their efficiency in real-time control schemes. This outcome is aligned with the results of (Phinyomark et al. (2012)) where the mean absolute value and the waveform length could perform efficiently with an LDA classifier.

The mean absolute value is probably the most frequently used feature and it is often selected as the sole feature for classification (Smith et al. (2016); Cipriani et al. (2011)). Indeed, this feature could encapsulate sufficient information for a high performance. Other studies have suggested a combination of time-domain features as an input to a classifier. A common set of time-main features is the mean absolute value, waveform length, number of zero crossings and slope sign changes (Young et al. (2013); Li et al. (2010); Earley et al. (2016); Geng et al. (2017)). In addition to this set, other features, such as the average amplitude (Fougner et al. (2014)), the integrated absolute value (Carpaneto et al. (2012)) and the variance of the signals (Naik et al. (2016)), are frequently selected. A combination of time-domain features with autoregressive coefficients is used in (Naik et al. (2016); Khokhar et al. (2010); Liu et al. (2014); Krasoulis et al. (2017); Huang et al. (2005)).

Regardless of the classification method, there is no direct conclusion about which are the optimal features for decoding the grasping intention from the muscular activity. Generally, the extraction of time-domain features is sufficient for producing high classification accuracy. Another benefit of time-domain feature is their little requirement of computational power, which makes them efficient for real-time control. Therefore, we employ mainly three time-domain features

in this thesis; the mean absolute value, the waveform length and the number of slope-sign changes.

2.2.2 Machine-learning methods in neuroprosthetics control

After the pre-processing step, the extracted features are introduced to a classifier. However, studies have shown that the introduction of a "pre-classification" step could improve the performance of the pattern-recognition system. Naik et al. (2016) suggest the employment of Independent Component Analysis (ICA) on the features before introducing them to an LDA classifier and they noticed significantly improved results. Besides ICA, dimensionality reduction methods, such as PCA, have also been shown to have beneficial effect on the classification accuracy (Hargrove et al. (2009)).

Undoubtedly, the most common machine-learning method used to decode a user's intention from electromyography is LDA (Young et al. (2013); Li et al. (2010); Earley et al. (2016); Naik et al. (2016); Hargrove et al. (2009); Geng et al. (2017); Krasoulis et al. (2017)). This is mainly because of its simplicity but, most importantly, due to its generally good performance in the analysis of biomedical signals.

However, there are studies that suggest other classification methods. Cipriani et al. (2011) propose that a k-NN method with the 8 nearest neighbors is sufficient to classify efficiently the individual motion of the digits, even for individuals with transradial amputation. Huang et al. (2005) show that GMM could be a good alternative of LDA, as they noticed an improved classification performance. Furthermore, Khokhar et al. (2010), Carpaneto et al. (2012) and He et al. (2015) show that SVM could also be used for decoding the user's intention from electromyography. Jiang et al. (2014) showed significant improvement in the classification performance when using an MLP-ANN instead of LDA.

It is clear that the main steps in the pattern recognition systems is a feature extraction, followed by a classification method. In the large majority of the studies related to EMG decoding, the researcher selects *a-priori* the features extracted from the EMG signals. However, there are machine learning methods that can perform automated feature extraction. For example, Recurrent Neural Networks have been shown to have good performance in time series, letting the feature extraction on the hidden layer. The automated feature-extraction is a techniques that have not been tested yet on the EMG signals. In the Chapters 4 and 5, we employ the echo property of ESN as a method of automated feature-extraction and classification. Echo State Networks have a high-dimensional and sparse hidden-layer, fixed from a random initialization, and optimizing the weights of the output layer. In this method, the introduction of the signals into the hidden equals to a projection to a higher dimensional space.

This could ”linearize” the non-linear signals, enabling an efficient classification accuracy performing a linear regression on the output layer.

2.3 EMG-decoding on Individuals with Transradial Amputations

Most of the studies mentioned above evaluated their control methods on able-bodied individuals. In this subsection, we review studies that performed experiments with individuals with below-elbow amputation.

The vast majority of the commercially-available hand-myoprosthesis, including the most recent devices with enhanced dexterity, still employ *direct-myoelectric-control (DC)* methods, which are offered since the 1970s Graupe and Cline (1975). In DC methods, the EMG signals are generally recorded from one or two pairs of muscle, the agonist-antagonist pairs. Each group is responsible for controlling a motor direction; for example, one for opening and one for closing the fingers. To activate the motor, the user generates specific EMG patterns (i.e., co-contract the muscles) and the recognition of the muscle activation is based on the magnitude of the EMG signal Williams (2004). The extension of this control approach to multiple DoF becomes challenging due to several reasons: To activate the motor of a joint, the contraction of each residual muscle (or group of muscles) should occur independently. Yet, localizing the activation of specific EMG sites is not trivial on amputees. Furthermore, the intuitiveness of the DC approach is very limited in multi-DoF control. In order to drive a particular joint, the user should generate a specific muscle activation, which the amplitude-based recognition system can identify, for switching from the control of one joint to another. Besides the demanding training procedure, this method leads to unintentional toggling between the DoFs potentially creating inconvenience to the user (Kuiken et al. (2016)).

Pattern-recognition (PR) based control approaches are relatively new to clinical practice. As we have seen in the previous sections, the training protocols of the PR-based control follow the reverse principle than the DC approach: Instead of training the user on the muscle-activation patterns and manually setting the threshold for the EMG magnitude, the user contracts the muscles in a natural way whilst a pattern-recognition system is trained on the EMG patterns. Hence, PR-based approaches could offer a more intuitive control of hand prostheses. Recent studies (Kuiken et al. (2016) and Resnik et al. (2018)), that compare the two approaches with individuals with below-elbow amputation, support this hypothesis. They report that, although the PR approach requires longer periods for training and familiarization, it has similar or greater acceptance by the users.

Especially for our study, the use of a DC approach would be counter-intuitive; the user should voluntary co-contract the muscles in a specific pattern and, in

the same time, perform a reaching motion by seamlessly extending the arm. It is clear that those two conditions contradict each other, creating a potential confusion to the user and to the controller. In contrast, we exploit the benefits of pattern-recognition methods to adapt to the EMG patterns generated during the reaching motion and hence improve the intuitiveness of the controller even more.

The research community on neuro-prosthesis control tends to favor the PR-based approaches. We will present below studies that are relevant to ours, such as they too target on a intuitive decoding of the grasping intention and evaluate their approaches with individuals with below-elbow amputation. As we will see, the number of degrees of freedom to control, but also the classification performance, is significantly lower with individuals with amputations than in able-bodied individuals that we saw in the previous section.

For example in (Daley et al. (2012) and He et al. (2015)), the authors performed an off-line analysis on the high-density EMG signals for decoding grasp types and wrist motions with transradial amputees and able-bodied subjects. From the analysis on the participants with transradial amputations, the classifier was able to identify from $1-3$ grasp types and $3-4$ wrist motions. Daley et al. (2012) reported that the average classification accuracy was around 75% across all the tasks for the two participants who lost their hands due a traumatic incident and around 50% for the two participants that have congenital hand-loss. In contrast, the able-bodied participants had a classification accuracy above 81%. It is clear from this comparison that the classification accuracy could vary depending on the condition of the amputation, and, generally, it could differ even more from able-bodied individuals. The classification accuracy depends also on the amputation level; the pattern-recognition system has significantly higher performance on individuals with partial hand amputation than transradial amputation Menon et al. (2017). This indicates that the quality of the EMG signals decreases with more proximal amputations. In some cases, the employment of filtering methods, such as the Common Spatial Patterns (CSP), could improve the performance of the pattern-recognition system (Amsuess et al. (2016)). However, the accuracy degrades exponentially when evaluated over consecutive days He et al. (2015), which is another of the limitations of the PR-based approaches.

Another noticeable characteristic in the studies with amputees is the difference between off-line and on-line performance. For example, Kuiken et al. (2009) reported an offline performance of 94% on a motion test protocol, whilst their on-line performance dropped to 81.2%. Especially when the number of classes (i.e., hand gestures) increases, the decrease could be even more significant; in Li et al. (2010) the classification accuracy dropped from 92.1% (off-line) to 67.4%. This is a clear indication that improvements in the off-line performance are not always correlated with the actual control of prosthesis.

To address this limitation, recent studies introduce additional sensory types, such as near-infrared spectroscopy (Guo et al. (2017) and inertia measure-

ments (Krasoulis et al. (2017); Cognolato et al. (2018)). The results seem promising as the hybrid decoders outperform the EMG-only decoder. An interpretation of these results is that the classifier has a reduced dependency to the noisy EMG signals and, thus, it becomes more robust. However, there is another outcome hidden in these studies; when the classifier is trained solely on the data of the "external" sensors, it has lower performance than the EMG-only classifier. Therefore, the EMG signals contain such a valuable information for the motion intention that it cannot be replaced with other sensory inputs. Thus, the investigation of intelligent methods for addressing the variability of EMG signals is of paramount importance for increasing the robustness of the control approach. In order to achieve this goal, there should be a deeper understanding of the EMG patterns generated from the muscle contractions. This brings us to our next observation.

Experiments in laboratory environments are usually concern only the stationary EMG portions for classification, i.e., the periods where the motion is kept at approximately constant force without movement (Farina et al. (2014)). Yet, reach-to-grasp motions, and also other type of motions, involve dynamic muscle contractions and stationary EMG portions are generated only in specific periods of the overall motion. This makes them rarely representative of the whole motion and has a crucial effect on the classification performance. Nevertheless, research in this field prefer static experimental protocols.

For example, the decoding of the motion intention for the phantom fingers is examined by Naik et al. (2016) and Cipriani et al. (2011). Specifically, Naik et al. (2016) present a method for computing the optimal EMG sites of the forearm employing ICA. Although this work reported up to 92% accuracy, these results involve only off-line analysis. Cipriani et al. (2011) show a teleoperation of a prototype robotic hand by individuals with transradial amputation. The results varied across the participants; the success rate was from 60% to 97%, and the completion time stayed between $0.8s$ to $1.8s$. In both studies, the arm remained in fixed position during the recordings and the testings.

A similar experimental protocol was followed by Amsuess et al. (2014). The authors propose a method for decoding two grasp types and four wrist motions, together with a resting and hand open condition. Their method is based on a combination of LDA and an multilayer perceptron Artificial Neural Network (ANN). In their experimental protocol, the participants performed muscle contractions while maintaining their arms in a fixed position. The four participants with transradial amputations had an average classification performance above 90% overall classes. However, those results could not be compared with the results of this thesis for two reasons: (a) their experimental protocol involves static positions of the arm and (b) the selected classes include the wrist positions and a hand-open condition, without providing specifically any results on the accuracy of the two grasp types.

The effect of dynamic training protocols with transradial amputees have

been examined in (Yang et al. (2017)), (Geng et al. (2017)) and (Kanitz et al. (2018)). The effect of different postures of the arm was examined in (Geng et al. (2017)). In their experimental protocol, the participants performed muscle contractions for hand open/close, wrist pronation/supination and flexion/extension when their arms were resting in five different positions. The classifier performed significantly better when trained on all the arm positions. Extending their hypothesis, (Kanitz et al. (2018)) propose a method for decoding four grasp types, regardless the position of the arm. They investigate, in particular, the onset of the muscle contraction for capturing the temporal information on the muscles for each grasp type for five positions of the elbow joint and four positions of the shoulder joint. Their approach showed promising generability over the different arm positions, when evaluated in a real-time control scheme.

In (Yang et al. (2017)), the authors investigate the classification performance on the prediction of individual digits of the hand: when the decoder is trained on a static position of the arm and when the arm moves. In the dynamic experimental protocol, the arm was extended and the subjects contracted their muscles while moving from one point of a circle to another. Their analysis showed that, when trained on a static arm position and tested on the dynamic protocol, there is a significant decrease in the performance of the decoder, approximately 30%.

Krasoulis et al. (2017) evaluated a hybrid (EMG+IMU) decoder in the real-time control of a prosthesis with two amputee participants who performed reach-to-grasp motions. Similar to other studies we reviewed, the hybrid decoder performed better than the EMG decoder in this test and the results were less accurate than the off-line analysis. This work omitted, however, to report any improvements on the reaction time of the device.

These studies highlight the improvement on the EMG-decoder, when dynamic training protocols are employed. However, they are different with the work presented in this thesis. Specifically, Yang et al. (2017) focus on the decoding of the motion intention of different digits, and no reaching motion was involved in their protocol. Furthermore, none of these studies addresses the delay in the activation of the device. In contrast, in this thesis we develop decoding methods for the grasping intention during the reaching motions and investigate the improvements on the reaction time of prosthetic devices.

Chapter 3

EMG-Based Decoding of Grasp Gestures in Reaching-to-Grasping Motions

In this chapter, we present our first attempt to decode the grasping intention during the reaching phase from electromyography. We base our approach on Echo State Networks and relate the classification performance with the hand preshape. In this way, we identify the stage of the reaching phase where the classification reaches high levels of accuracy. We select two criteria for the definition of preshape: the hand's aperture (i.e., the distance between the fingertips of the index finger and the hand) and the area formed by the fingertips involved in the grasp type. We examine the effect of the motion speed as well as the distance from the object to classification accuracy. We also integrate the decoding approach in a real-time control of a robotic hand to demonstrate the feasibility of the approach for a potential control of a myo-prosthesis.

3.1 Introduction

It has been extensively demonstrated that a user's motion intention can be accurately detected by surface electromyographic recordings (sEMG) (Novak and Riener (2014)). Different sEMG-based systems were proposed for the estimation of hand and wrist movements, and used as non-invasive interfaces for controlling exoskeletons (Khokhar et al. (2010); Ziai and Menon (2011)), prosthetic devices (Nishikawa et al. (1999); Ju and Liu (2014); Fukuda et al. (2003)), computer-animated hands in a virtual environment (Sebelius et al. (2005)), or for teleoperating robotic arms (Fukuda et al. (2003); Shenoy et al. (2008)). The previous studies focused on the investigation of discrete classifications of wrist abduction/adduction (Fukuda et al. (2003); Shenoy et al. (2008)), flexion/extension (Nishikawa et al. (1999); Sebelius et al. (2005); Huang et al. (2005); Kita et al. (2006)) as well as of a different combination of finger motions (Fukuda et al. (2003); Shenoy et al. (2008); Jiang et al. (2005)). These strategies are useful for accomplishing power grasps that require simultaneous closure of all fingers on the object. However, these strategies are insufficient to generate differentiated control of all fingers in the variety of pinch grasps used in dexterous object manipulation, as required by the grasping of a larger variety of objects.

The differentiated control of all fingers is complex to achieve due to the high

dimensionality of the hand control. Indeed, the human hand is characterized by 21 degrees of freedom (DOFs) controlled by 29 muscles Jones and Lederman (2006). It has been hypothesized that humans are capable of controlling this large number of DOFs and use their hands dexterously thanks to a multidimensional reduction of the controlled variables operated by the central nervous system. This multidimensional reduction is accomplished through the use of postural synergies (Santello et al. (1998)), corresponding to a number of hand postures that humans combine when grasping objects. Dalley et al. (2012); Sapsanis et al. (2013); Ouyang et al. (2014); Smith et al. (2008) propose to exploit a mapping between upper limb EMG signals and hand postures, as a strategy to control the large number of the hand's degrees of freedom. However, in these approaches only the grasping phase, i.e., when the fingers have already reached their final configuration, was examined and the subjects were asked to perform the corresponding grasp keeping the upper-arm fixed. Nonetheless, the muscular activity differs between a static and a dynamic position of the arm. During reaching-to-grasp movements, the configuration of the fingers and of the wrist changes simultaneously with the arm's motion, and this might influence the classification performance. This formation of the fingers, before reaching their final configuration, is defined as hand preshape. The hand preshape is in direct relation with the characteristics of the object, specifically to the shape and width of it. In able-bodied subjects, the hand preshape occurs before the hand reaches the object, at around 60% of the reach and grasp motion (Paulignan et al. (1990); Jeannerod (1984); M. Jeannerod (1998); Santello and Soechting (1998)). Therefore, in order to accomplish a smooth control of the grasping gesture, it is crucial to classify the hand posture during the reaching phase before the occurrence of the preshape. Indeed, an accurate estimation of the final grasp posture in the early stages of the reach-to-grasp motion would ensure a faster reactivity of the assistive and the wearable devices. As a result, these devices would increase their effectiveness and usability, and increase the natural transition between the reaching and grasping phase on the prostheses, hence increase their acceptance by patients. However, at the time of the writing only a limited number of studies are focused on the detection of different grasp movements during reaching and grasping motions (González et al. (2010); Liarokapis et al. (2013); Fligge et al. (2000)), and no measurements were performed to assess when a good classification was achieved with respect to the hand preshape .

In this chapter, we propose a novel EMG-based learning approach that decodes the grasping intention of the user at an early stage of the reach-to-grasp motion, i.e., before the final grasp/hand preshape takes place. We also demonstrate the applicability of our work to online applications. This chapter corresponds to the following publication:

Batzianoulis, I., El-Khoury, S., Pirondini, E, Coscia, M., Micera, S. and Billard A., *Emg-based decoding of grasp gestures in reaching-to-grasping motions*,

Grasp types	Fingers involved	Object
Precision disk	5 (all fingers)	Large cylinder (10cm diameter)
Tripod	3 (thumb, index, middle)	Small cylinder (5 cm diameter)
Thumb-2 fingers	3 (thumb, index, middle)	Thin rectangular
Thumb-4 fingers	5 (all the fingers)	Thin rectangular
Thumb-2 fingers	2 (thumb and little finger)	Thin rectangular

Table 3.1: Chosen grasp types Bullock et al. (2013).

Robotics and Autonomous Systems, 2017.

3.2 Methods

3.2.1 Participants

Fourteen healthy young subjects (10 males and 4 females, average age 28.2±3.9) participated in the experiment. All subjects were right-handed, according to the Edinburgh inventory test Oldfield (1971), and they had no prior history of neurological disorders and neuromuscular injuries. They performed the experiments with their dominant arm. The experiment was approved by the BMI Ethics

Committee for Human Behavioral Research of EPFL, and the recordings were carried out in agreement with the Declaration of Helsinki. All subjects gave written consent to participate at the beginning of the experiment.

3.2.2 Experimental Protocol

The subjects were asked to reach and grasp 3 different objects with five different grasp types: precision disk, tripod, thumb-2 fingers, thumb-4 fingers, and ulnar pinch, see Figure (3.1). These grasps were mostly chosen for their common usage in daily life Bullock et al. (2013).

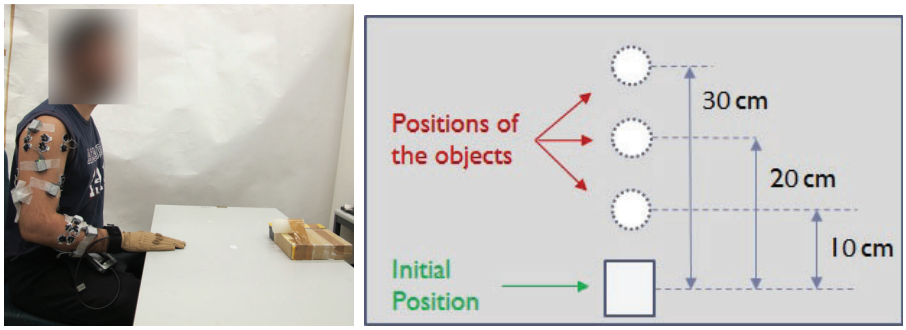

Figure 3.1: (a):The experimental setup showing the electrodes for EMG recording and the CyberGlove for capturing the hand joint angles, (b) the plan showing the initial position of the hand and the three positions of the object

During the experiment, the subjects were seated in front of a table with their elbow flexed at about 90° and their hand placed on the table with the palm downward and the fingers pointing to the object, see Figure (3.1a). The subjects were asked to reach the object and grasp it with a predefined grasp type, keeping the same hand orientation for all the grasp types. The subjects began a self-paced motion, according to the advice of the experimenter, and they had to declare that they grasped the object in order to consider the trial completed. The objects were placed at three different distances (i.e., 30cm, position P1, 20cm, position P2, and 10cm, position P3) from the initial hand position, see Figure (3.1b). All the fourteen subjects performed 20 trials for each of the five grasp types for position P1. After completing this first part of the experiment, six subjects continued the experiment for the positions P2 and P3 performing 15 trials for each grasp type. Three subjects performed additionally fast reach-to-grasp motions for objects placed at position P1; they were asked to perform the motions by extending their arm with an higher acceleration than during the first part of the experiment. The subjects performed all trials for one grasp before moving to the next grasp.

3.2.3 Apparatus and pre-processing

The EMG signals, from 16 upper limb muscles (Table 3.2), were recorded using a Noraxon DTS desktop system, with a sampling rate of 1500 Hz. The electrodes were placed, when it was possible, according to the standard procedure for surface electromyography for non-invasive assessment of muscles (SENIAM) guidelines (Hermens et al. (2000)). At the beginning of the recordings, a manual test for the maximum voluntary contraction (MVC) was performed for each muscle. During the test, the subjects were asked to perform isometric contractions for each muscle. The test was repeated three times for each muscle, with a break after each contraction to prevent muscle fatigue.
The data were filtered with a seventh-order band-pass Butterworth filter between 50 Hz and 500 Hz for the suppression of movement artifacts. To construct a linear envelope, a full-wave rectification was performed, followed by a smoothing with a low-pass seventh-order Butterworth filter with cutoff frequency at 20 Hz. Finally, the resulting EMG signals were normalized by the MVC.

	Muscles
1	Infraspinatus (INFRA)
2	Deltoid Anterior (DANT)
3	Deltoid Medial
4	Deltoid Posterior (DPOS)
5	Biceps Brachii long head (BICL)
6	Triceps Brachii long head (TRIC)
7	Brachialis (BR)
8	Flexor Digitorum Superficialis (FLDS)
9	Extensor Digitorum Communis (EXDC)
10	Flexor Carpi Ulnaris (FLCU)
11	Extensor Carpi Ulnaris (EXCU)
12	Flexor Carpi Radialis (FLCR)
13	Flexor Pollici Brevis (FLPB)
14	Extensor Pollicis Brevis (EXPB)
15	Adductor Pollicis Transversus (ADPT)
16	Abductor Digiti Minimi (ABDM)

Table 3.2: Muscles which activity is captured for the reaching and grasping experiment.

The joint angles of the fingers were measured using the CyberGlove System's CyberGlove[1], with a sampling rate of 100 Hz. The Cyberglove has 22 bend sensors located over the hand joints. As bending can be detected anywhere along the sensor length, the glove can adapt well to different hand sizes, and it needs to be calibrated in order to transform raw sensor values to hand joint angles. Linear regression was used to calibrate the 4 fingers (index, middle, ring, and little), and a data-driven approach was employed to model the non-linear relationship between the thumb sensors and the joint angles. The recorded joint angles were used to compute the fingertip's position with respect to the wrist

[1] www.cyberglovesystems.com

by forward kinematics. More details about the Cyberglove calibration procedure can be found in (de Souza et al. (2014)).

The two data streams were synchronized using a trigger signal provided by an Arduino board. At each trial, the subjects began moving only when instructed to do so by the experimenter. Simultaneously, the experimenter was pressed a button on the console, which generated a trigger pulse that indicated the start of the recording of the Cyberglove data. The trigger pulse was introduced to the Noraxon system as an extra channel. During the offline analysis, all the data were synchronized with respect to the trigger pulse, thus ensuring synchronization between the Cyberglove and the Noraxon system. The onset of the motion was detected from the joint angles of the fingers, as they switched from a resting position to motion generation. This transition results in a change on the angular velocity of the joint angles of the fingers; this change was captured by the Cyberglove and corresponds to the moment $t = 0sec$ on the analysis and the figures.

3.2.4 Preshape Criteria

The preshape of the hand is considered as the formation of the fingers before they reach their final configuration (Haggard and Wing (1995)). In this work, we employed two criteria to identify the occurrence of the hand preshaping (Paulignan et al. (1990),Supuk et al. (2005)). The first criterion is based on the distance between the fingertips of the thumb and the index finger; they are considered to be the fingers that participate in most of the grasp types. For this reason, they provide valuable information for the configuration of the fingers, and in particular for the opening and closing of the hand. In the case of the ulnar pinch, which is performed with the thumb and little finger, we replaced the index finger with the little finger. The first criterion is defined in the literature as the hand's aperture and, in this chapter, we will refer to it as *aperture*.

The second criterion is based on the estimation of the area of the polygon that is described by the fingertips involved in the grasp. For the precision disk and the thumb-4 fingers, the area considered is the one of a pentagon created by the fingertips of all five fingers. For the tripod grasp and the thumb-2 fingers, the area was the surface of a triangle defined by the fingertips of the thumb, index, and middle finger. Finally, for the ulnar pinch, the area was again the surface of a triangle, but consisted of the fingertips of the thumb, the index finger, and the little finger. In the following sections, we will refer to this criterion as *area*.

To estimate the *aperture* and the *area*, we compute the position of the fingertips with respect to the wrist from the data recorded from the Cyberglove. The *aperture* and the *area* vary with respect to the opening and closing of the hand, providing objective information for the determination of the preshaping. In particular, the preshaping is assumed to correspond to the peak value of the aperture and the area, and the grasp is considered complete when these criteria

reach stability.

3.2.5 Classification Method

The preprocessed EMG signals were analyzed using a sliding time-window of $150msec$ with an overlap of $50msec$. In order to embed the specificity of the motion's time evolution, we combined an Echo State Network (ESN) (Jaeger (2001)) to classify the data with the Majority Vote (MV) criterion applied to each time window from the motion onset, as suggested in (Englehart and Hudgins (2003)). The MV criterion assigns a class label to the class that gathers the most votes. The preprocessed EMG data input were provided as input to the ESN, without extracting any feature from the EMG signals. Each ESN entailed 180 sigmoid units, with a transfer function $f = tanh$, and it output 5 classes for each of the 5 grasp types. The activation function of the output units was chosen to be the identity function. The classification for each time window was fed to the MV algorithm, where each vote corresponded to the result of the classification.

As the classification strategy is implemented online, the following analysis was performed in the time domain, thus avoiding time normalization. As the hand's preshape occurs around the 60% of the reaching motion, we chose to analyze the first second of the reaching motion. This approach enables the capture of the hand preshape in different time steps and in relation with the classification rates.

One classifier was trained for each subject. For the first position of the object (P1), the classification machine was built with the 75% of the dataset of 100 trials (i.e., training dataset) and tested in the remaining data (i.e., 25%) by using the cross-validation method. For the generalization over different distances (i.e., positions P2 and P3), two different classifiers were built. In the first case, the training dataset was constituted by the data from two different positions, and the testing dataset included only the data from the remaining positions. In the second case, instead, the classifier was trained on one position and tested in the other two.

In the case of the trials at different speeds, we tried different combinations of training and testing data in order to examine the performance of generalization. First, the classifier was trained with the data of self-paced motions and tested with data on fast motions. For a second step, the classification machine was trained with the data of fast motions and tested with the data of self-paced motions. In the last test, we mixed the data of fast and slow motions, amd the classification machine was trained with 75% of the data and tested with the remaining 25%, following a four-folder cross-validation.

In order to examine the robustness of our approach in clinical conditions, we investigated the classification accuracy with fewer EMG channels as input to the classifier. We first removed the intrinsic muscles of the hand *(Abductor*

Digiti Minimi, Adductor Pollicis Transversus and *Flexor Pollici Brevis*). These three muscles are responsible for the motion of the little finger and the thumb. By removing these muscles from our dataset, we simulated a condition of motor dysfunction in those two fingers. This condition could be a result of either a cervical spinal cord injury in the C8 vertebra or partial amputation of the fingers.

For a second step, we excluded the activity of the *Extensor Pollicis Brevis* that contributes to the flexion and abduction of the thumb, which left us with 12 EMG sites. The exclusion of this muscle, together with the *Adductor Pollicis Transversus* and *Flexor Pollici Brevis*), simulates a total loss of the functionality of the thumb. This condition could derive either from a thumb amputation or a severe cervical injury in the C6 vertebra. Also, the deduction of the most distal muscles from our dataset corresponds to a simulation of hand loss, such as wrist disarticulation.

As a next step, we removed the activity of the *Flexor Carpi Radialis* and the ulnar muscles (*Flexor Carpi Ulnaris* and *Extensor Carpi Ulnaris*), keeping 11 and 9 EMG channels accordingly. These conditions correspond to an amputation on the forearm level (e.g. transradial amputation close to the elbow), where the residual extensor muscles remain active.

Finally, we kept only the 7 EMG muscles that correspond to muscles from the upper arm(i.e *Infraspinatus, Deltoid Anterior, Deltoid Medial, Deltoid Posterior, Biceps Brachii long head, Triceps Brachii long head* and *Brachialis*). In this case, we simulate a more proximal amputation, such as elbow disarticulation, and a total paralysis of the distal upper-limb (e.g., below the elbow) due to an injury in T1 and C6-C8 vertebrae.

3.2.6 Online Robotic Implementation

For the purposes of the online implementation, we use a right Allegro hand from Simlab[2]. This is a humanoid hand with 16 DOFs split equally on 4 fingers. Although it is only an approximate reproduction of the dexterity of the human hand and has more DOFs than currently available assistive devices, it serves as a benchmark for our ability to reproduce grasps with dexterity similar to those generated by humans. The Allegro hand has also the advantage of being controlled at an extremely fast rate (400Hz), which enables demonstrating the benefit of our early pre-shape detection for real-time control of finger closure during the arm movements.

In the online robotic implementation, the EMG signals were acquired using a National Instruments USB-6210 data acquisition board with a sampling rate at 1000Hz. The acquired signals were pre-processed (filtered and rectified as described in previous subsection) and classified using a C++ project of Visual Studio 2013 installed in a desktop computer (Intel Xeon @ 2.27 GHz with

[2]http://www.simlab.co.kr/Allegro-Hand.htm

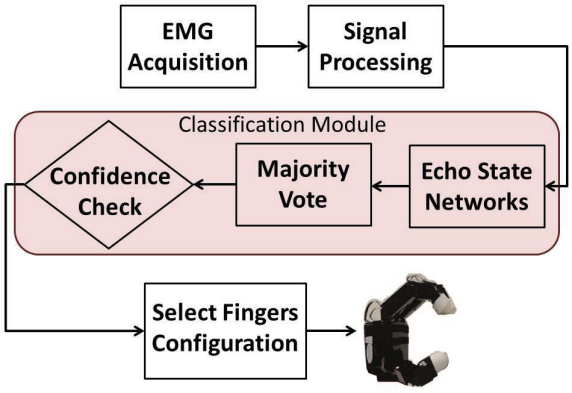

Figure 3.2: Control scheme of the robotic implementation.

Windows 8.1). The classification output for each time window was streamed to a portable computer (Intel i7 @ 2.6 GHz with Ubuntu 14.01) and introduced to the majority vote algorithm. Finally, the corresponded joint angles were imported to the Allegro hand, using ROS. The straight forward control scheme is presented in the Figure (3.2)).

3.3 Results

In order to assess the classification accuracy and the robustness of the results, we defined the success rate as the percentage of movements correctly classified for a specific grasp type on the total number of reach-to-grasp motions corresponding to that specific grasp type (Recall column in Table (3.3)). We also computed the precision measure (i.e., the percentage of trials correctly classified for a specific grasp type on the total number of reach-to-grasp movements classified to the same grasp type) and the F-measure, which corresponds to the harmonic average of the recall and precision values, for each grasp type. An F-measure score of 1 means that each motion belonging to a specific grasp type was perfectly classified as such.

After presenting the Recall, Precision and F-measure values of each time window, we defined the classification performance as the number of correctly classified trials over the total number of trials, for simplicity purposes.

3.3.1 Reach-to-Grasp classification strategy

Table (3.3) shows the average and standard deviation of the classification results across subjects and grasps for 10 different time windows starting from 0.15 to 1.05 seconds with a step size of 100$msec$. The average classification performance among subjects increased during time, as the hand moved closer to the object (see Figure (3.3b)) for all the three positions with a slight decrease only at 450 and 950$msec$ for P1 (see Table (3.3)). In particular, a success rate of $90 \pm 4.5\%$

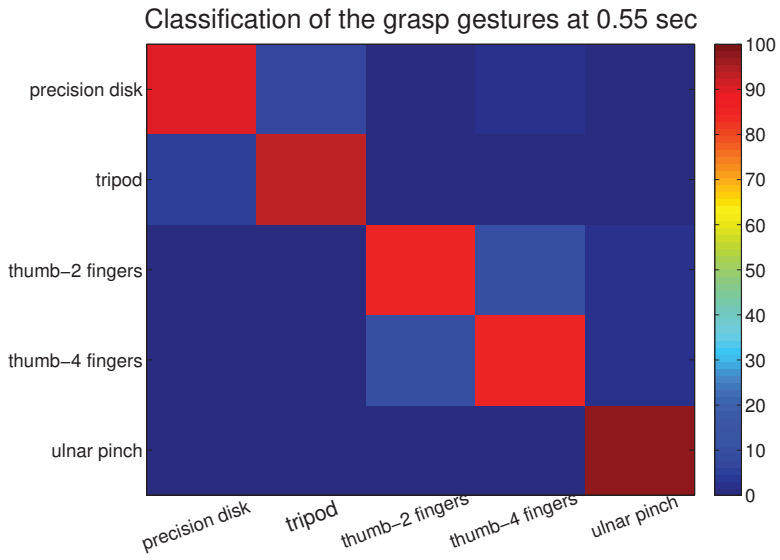

(a)

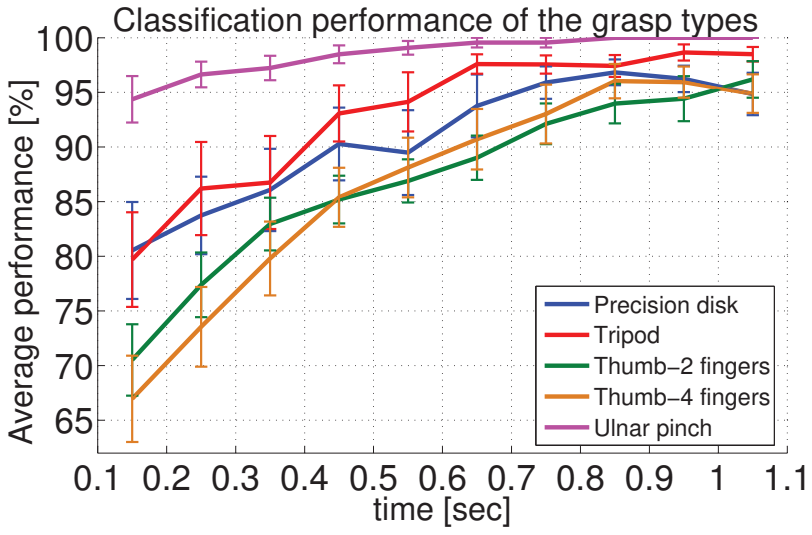

(b)

Figure 3.3: a) Confusion matrix of the classification between grasp types in among the subjects, 0.55 sec after the onset of the motion. Warmer color indicates higher classification performance, b)Average and standard error of the classification performance of all the grasp types among subjects for 30cm distance of the object.

was reached $0.5sec$ after motion's onset (i.e., half-way through the reaching motion). On average, an F-measure of 0.91 was obtained for the five grasp types and for all time windows. However, it was higher than 0.76 already $150msec$ after motion onset, thus showing that an accurate classification of the five grasp types is possible before the grasp occurred.

	ESN MV		
time(s)	Precision	Recall	F-measure
0.15	0.81 ± 0.06	0.84 ± 0.05	0.76 ± 0.08
0.25	0.89 ± 0.04	0.91 ± 0.04	0.88 ± 0.05
0.35	0.87 ± 0.06	0.89 ± 0.06	0.84 ± 0.06
0.45	0.93 ± 0.04	0.94 ± 0.04	0.92 ± 0.04
0.55	0.91 ± 0.06	0.92 ± 0.05	0.90 ± 0.06
0.65	0.95 ± 0.02	0.96 ± 0.02	0.94 ± 0.03
0.75	0.95 ± 0.03	0.95 ± 0.03	0.94 ± 0.03
0.85	0.97 ± 0.02	0.97 ± 0.01	0.96 ± 0.02
0.95	0.96 ± 0.03	0.97 ± 0.02	0.95 ± 0.03
1.05	0.97 ± 0.02	0.98 ± 0.01	0.96 ± 0.02
Total av.	0.92	0.93	0.91

Table 3.3: The average and standard deviation of the classification results across grasp types and subjects. The *Recall* values correspond to the percentage of EMG data correctly classified as a specific grasp type to the total number of reach-to-grasp motions corresponding to the same grasp type. The *Precision* values correspond to the percentage of EMG data correctly classified as a specific grasp type to the total number of reach-to-grasp motions classified to the same grasp type. The $F - measure$ values corresponding to the harmonic average of the recall and precision values. The last row of each of the above tables correspond to the total average across time windows.

Figure (3.3a) shows the confusion matrix averaged across subjects for the five grasp types, $550ms$ after motion onset. This timing was chosen because it corresponded to half-way of the reach-to-grasp motion. Precision disk, tripod and ulnar pinch were distinguishable already at half motion (89.5%,92.7% and 98.3% respectively), whereas thumb-2 fingers and thumb-4 fingers were distinct later in the reaching motion when the hand moved closer to the object(85.1% for both of the classes). As expected from the hand configuration during the grasping, a misclassification tended to occur between tripod and precision disk and between thumb-2 and thumb-4 fingers (85.5% and 85.8% respectively). From Figure (3.3b), we notice that thumb-2 fingers and thumb-4 fingers reach 90% of classification rate $0.7sec$ after the onset of the motion.

Figure 3.4 presents a comparison between two strategies; (a) the classification strategy that we followed in previous paragraphs, over the complete reach-to-grasp motion and (b) the classification performance when one ESN classifier was trained with the last time-window, where the reaching motion is complete.The second strategy shows lower accuracy than the first throughout the motion. Its accuracy reaches 90% only late in the motion, approximately $1s$ after the motion onset. In contrast, the strategy that includes the whole reaching motion presents an accuracy of 90% in a much earlier stage, approximately $0.5s$ after the motion-onset. This outcome indicates that the muscle activity varies during the reaching phase of the motion, as we will see in greater detail in Chapter 4.

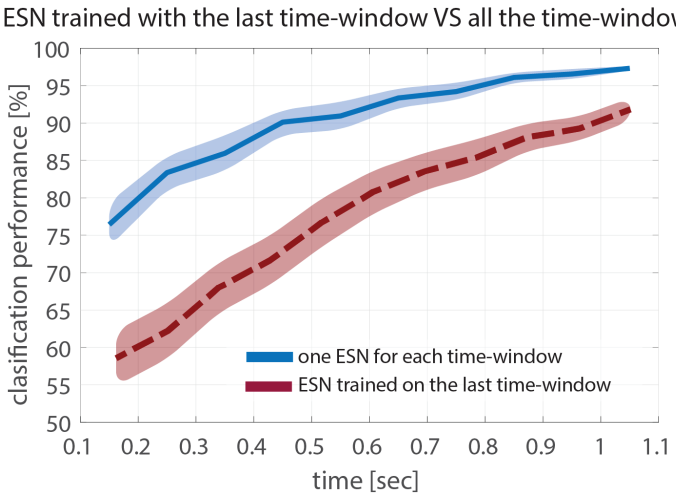

Figure 3.4: The evolution of classification performance and its standard error when training one ESN for each time-window against training an ESN with the final time-window (i.e., the last motion phase). The blue and red lines correspond to the average performance among the subjects for each method, respectively. Accordingly, the blue and red shade-areas correspond to their standard errors.

3.3.2 Decreasing the number of EMG channels

In this subsection, by removing the more distal muscles, we examine the performance of the approach when using a smaller number of EMG sites. As previously stated, for this analysis we kept 13,12,11,9 and 7 muscles from the initial muscle set as input to the classifier.

Figure (3.5) presents the evolution through time of the classification success rates. As depicted, the classification performance decreases as the number of muscles becomes lower. The success rate at $t = 0.55sec$ ($0.55sec$ after the onset of the motion) is between $90.95 \pm 1.85\%$ and $85 \pm 1.9\%$ when using more than 10 muscles, and drops rapidly to $77.65 \pm 2.36\%$ and $68.95 \pm 3.03\%$ when using 9 and 7, muscles respectively.

p values, $t = 0.55sec$ after the motion onset

	16	13	12	11	9
13	0.9435				
12	0.4039	0.9157			
11	0.3743	0.8981	0.9989		
9	0.0004	0.0087	0.1276	0.1424	
7	$< 10^{-3}$	$< 10^{-3}$	$< 10^{-3}$	$< 10^{-3}$	0.0243

Table 3.4: The results from the pairwise comparison of the classification performances, $0.55sec$ after the onset of the motion, when using different muscle groups. The highlighted cells depict the pairs in which the null hypothesis was not rejected at the significant level of 5%.

The one-way analysis of variance (ANOVA) performed on the classification performances rejected the null hypothesis at the significant level of 5% ($p < 10^{-3}$

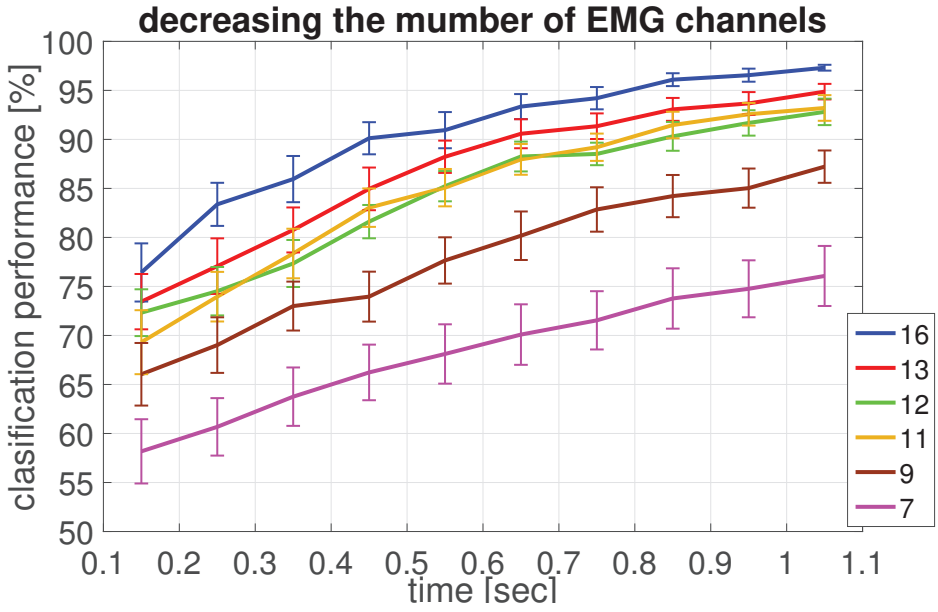

Figure 3.5: The evolution of classification performance and its standard error while reducing the number of EMG sites. The object was 30cm away from the initial position of the hand.

p values, $t = 1.05sec$ after the motion onset

	16	13	12	11	9
13	0.9007				
12	0.3921	0.9493			
11	0.4977	0.9798	0.9989		
9	0.0006	0.0189	0.1715	0.1188	
7	$< 10^{-3}$	$< 10^{-3}$	$< 10^{-3}$	$< 10^{-3}$	0.0001

Table 3.5: The results from the pairwise comparison of the classification performances, 1.05sec after the onset of the motion, when using different muscle groups. The highlighted cells depict the pairs in which the null hypothesis was not rejected at the significant level of 5%.

for $\alpha = 0.05$). The Tables (3.4)) and (3.5)) present the results of the pairwise comparison analysis of the classification performances at the moment of $t = 0.55sec$ and $t = 1.05sec$. As it is shown, the performance decreases significantly when reducing the number of EMG channels from 16 to 9, though it is not significantly different when using $13, 12$ and 11 muscles. A significant drop in performance was observable when using 9 and 7 muscles.

3.3.3 Generalization on different distances

For a second step, we examined the generalization across distances by (i) training the classifier on two positions (i.e., P1 and P2 or P1 and P3) and testing it on the remaining third position (P3 or P2, respectively) and, (ii) training

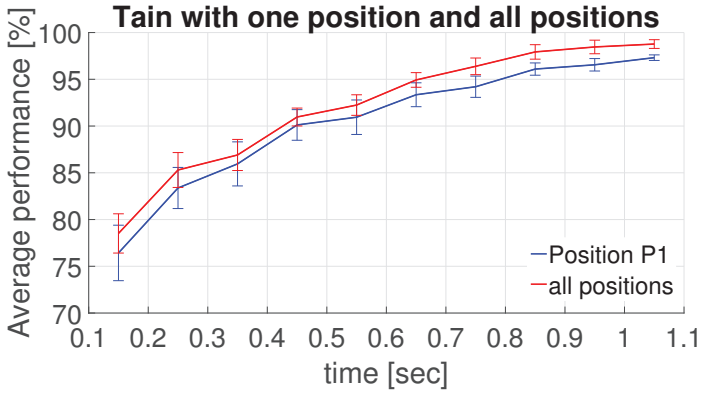

(a)

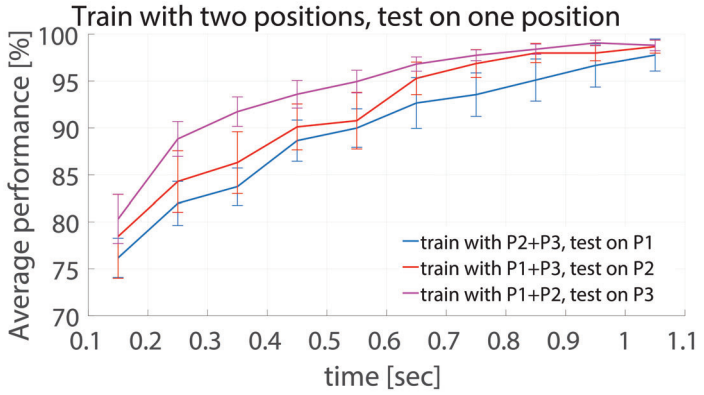

(b)

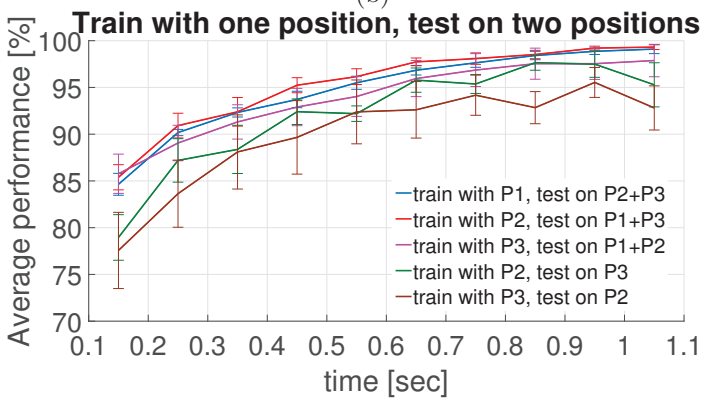

(c)

Figure 3.6: Classification success rate in different distances: (a) Average classification performance and standard error on the reaching motion: The blue line presents the performance of the classification of grasp types on position P1. The red line corresponds to the classification performance when all the positions (P1, P2 and P3) are taken into account, (b) Average classification performance and standard error on training with two positions and testing on the third: The blue line presents the performance when training on reaching motions to two positions P2 and P3 and testing on position P1. Respectively, the red line corresponds to training on positions P1 and P3 and testing on position P2 while the magenta line corresponds to training on positions P1 and P2 and training on position P3, (c) Average classification performance and standard error on training with one position and testing on the other two positions: The blue line presents the performance when training with reaching motions to positions P1 and testing on positions P2 and P3. Respectively, the red line corresponds to training on position P2 and testing on positions P2 and P3, while the magenta line corresponds to training on positions P3 and training on position P1 and P2. The green line corresponds to training with position P2 and testing on position P3. The brown line corresponds to training with position P3 and testing on position P2.

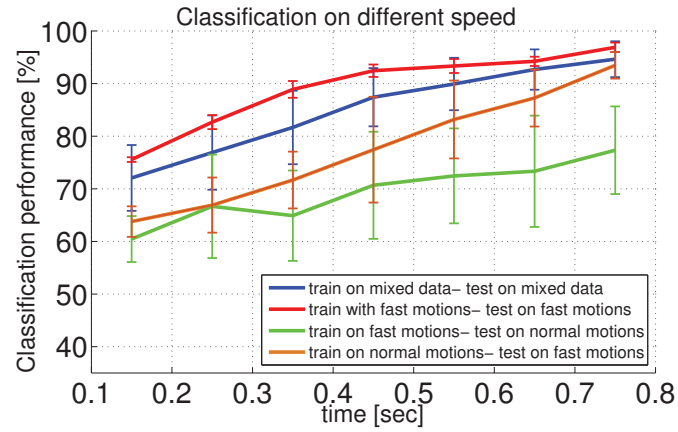

(a)

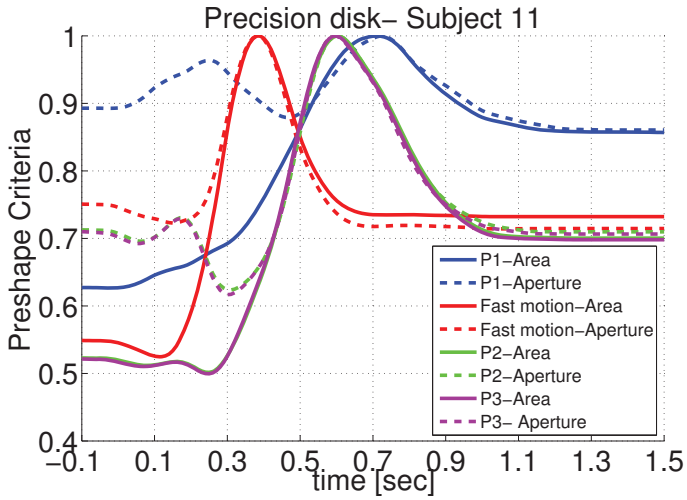

(b)

Figure 3.7: a: Average classification performance and standard error on the fast motions: The red line presents the performance of the classification of grasp types with the data of fast motions. The blue line corresponds to the classification performance when the data of fast motions were mixed with the data of normal motions. The green line corresponds to the performance when training with fast motions and testing on normal motions. The brown line corresponds to the performance when training with normal motions and testing on fast motions. the magenta and cyan vertical lines indicate the peak of the preshape criteria then subject 11 performed the precision disk grasp with fast and normal motions respectively as depicted in Figure (3.7b). b: Preshape criteria on the precision disk of subject 11: The subject opens its fingers sooner in fast motions than it does in normal motions.

the classifier on one position (i.e., P1 or P2 or P3) and testing it on the other two (i.e., P2 and P3 or P1 and P3 or P1 and P2, respectively). The performances were higher when the classifier was trained with a single position, with respect to a classifier trained on two positions (see Figures (3.6b) and (3.6c)). Indeed, the average performance at $0.45sec$ after movement onset was $93.93 \pm 1.7\%$ and $90.78 \pm 2.5\%$, when training on one position and on two positions, respectively. For the classifier trained with two positions, the performance was better when the training set included movements from the farthest distances (i.e., P1 and P2) and the testing set included the shortest distance (i.e., P3) (see Figure (3.6b)). The performance in this case was $93.6 \pm 3.6\%$ after $0.45sec$ from the motion on set. For the classifier trained with a single position, the best classification performance was achieved when the classifier was trained in the middle distance (i.e., P2) and tested on the other two distances (i.e., P1 and P3) (see Figure (3.6c)). In this case, a classification accuracy of $95.2 \pm 2.0\%$ was achieved $0.45sec$ after movement onset. It is worth mentioning that this case (i.e., training with P2 and testing on P1 and P3) presented, as well the smallest standard error when compared to the other generalizations. A one-way analysis of variance on the classification performance at the moments $t = 0.55sec$ and $t = 1.05sec$ after the onset of the motion failed to reject the null hypothesis on the significant level of 5% ($p = 0.12$ and $p = 0.88$ respectively).

3.3.4 Speed effect

In order to further evaluate the generalizability of our approach, we examined the effect of the speed on the classification. We first analysed the differences in finger motions in fast movements with respect to self pace motions. As expected there was a significant difference in the timings of hand opening and closing between motions performed at self-paced speeds and at fast speeds (see Figure (3.7a)). Indeed, the subjects opened and closed their hands in fast motions more rapid than in self-paced motions.

For a first step, we mixed the data of the self-paced and fast motions for training and testing. The classification performance reached $90 \pm 2.3\%$ of success after $0.55sec$ from movement onset. We then compared this first classification with the results obtained from training the classifier in the fast motions and testing it in either for fast or self-paced motions, or training the classifier with the movements at self-selected speed and testing it for the fast motions. As expected when using data from only the fast motions both for training and testing, the classification performance reached an accuracy higher than 90% sooner than when mixing the motions ($0.35sec$ for fast motions, $0.55sec$ for self-paced motions). Whereas the classifiers that were trained and tested in different datasets achieved lower performances than that trained and tested with mixed data. In particular, the accuracy of 90% was achieved $0.7sec$ after motion onset. Moreover, the standard error of these classifiers was higher than 4.5%, which

indicated that the classifier performed significantly better in some subjects than in others.

3.3.5 Classification rate Vs Hand preshape

To quantify how early into the preshape phase, we could detect the grasp intention, we used two criteria: (a) the hand textitaperture: the distance between the fingers involved during the grasp (i.e., thumb and index finger for *precision disk*, *tripod*, *thumb-2 fingers* and *thumb-4 fingers* and thumb and pinky finger for *ulnar pinch* grasp) and (b) the *area* of the fingertips: the surface obtained interconnecting the tips of the fingers involved in each grasp.

It is worth mentioning that the aperture involves solely the behavior of the thumb and index finger. Hence, the area criterion could be more informative of the motion of the fingers, as it encapsulates the behavior of all the fingers involved in the grasp (Supuk et al. (2005)). In order to examine the general trends of the motion of the fingers, we computed the two criteria in normalized time and present the results in Figure (3.8). As it is shown, the preshape is indicated in three grasp types (*precision disk, tripod* and *thumb-4 fingers*) by the peak of the *area* criterion that is followed by a smooth convergence to the final point. In the case of the *thumb-4 fingers* grasp, the start of the preshape phase is also revealed through a peak in the aperture; this peak occurs simultaneously with the peak of the *area* criterion. Both curves then decrease smoothly until full closure onto the final grasp. In the case of *thumb-2 fingers* grasp, it is more difficult to define the moment of preshape occurrence (see the third graph of Figure (3.8a) and (3.8b)), as the fingers begin their motion with a flexion, until the $30-40\%$ of the duration of the self-paced motions. At this point, the value of the area criterion stays approximately stable for a period of time before closing smoothly to the final grasp. During the same period, the value of the aperture criterion decreases, indicating a flexion of the index finger and the thumb. As the thumb-2 fingers grasp involves also the middle finger, the area criterion encapsulates the behavior of the middle finger. In order for the value of the *area* criterion to stay stable while the index finger and the thumb are flexing, the middle finger extends until all the fingers start to close simultaneously. We considered that the preshape occurs when the *area* criterion starts converging smoothly to its final value. Regarding the ulnar pinch, two fingers are involved, the thumb and the little finger. In this case, the *aperture* criterion, which corresponds to the distance between the fingertips of the thumb and the little finger, is more representative of the preshape than the *area* criterion, which involves more fingers. Hemce, we considered that the preshape occurs on the peak of the *aperture* criterion. Figure 3.9 presents the fingers configuration on the initial hand position, on the preshape and in the end of the motion.

Table (3.7) presents the average real time of preshape occurrence as well as the completion time for all the motions. The one-way analysis of variance

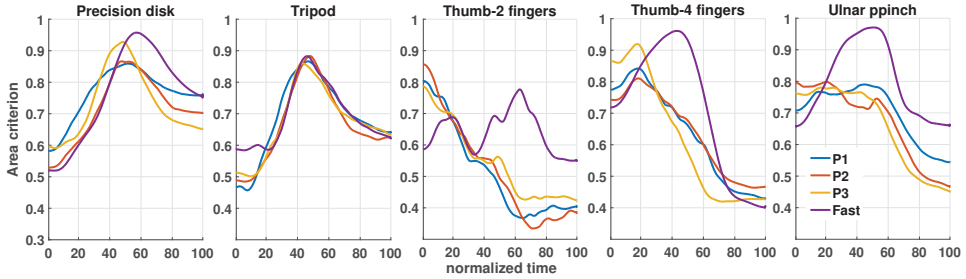

(a) The area criterion

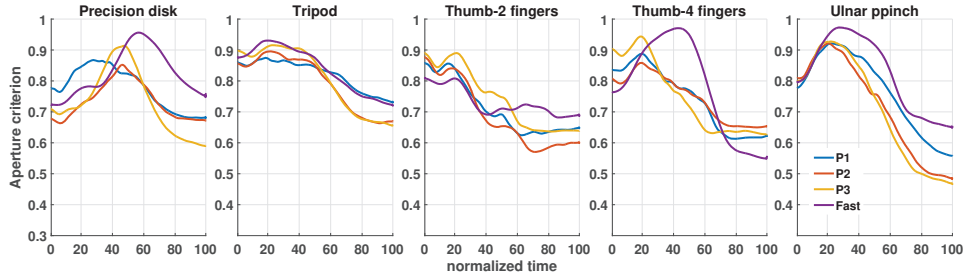

(b) The aperture criterion

Figure 3.8: The average value of preshape criteria across all subjects.

	$P1 = 30cm$	$P2 = 20cm$	$P3 = 10cm$	$Fast$
precision disk	$0.74 \pm 0.17sec$	$0.62 \pm 0.18sec$	$0.52 \pm 0.24sec$	$0.40 \pm 0.25sec$
tripod	$0.71 \pm 0.24sec$	$0.60 \pm 0.17sec$	$0.56 \pm 0.25sec$	$0.53 \pm 0.21sec$
thumb-2 fingers	$0.53 \pm 0.28sec$	$0.48 \pm 0.24sec$	$0.47 \pm 0.24sec$	$0.38 \pm 0.19sec$
thumb-4 fingers	$0.38 \pm 0.2sec$	$0.31 \pm 0.22sec$	$0.30 \pm 0.23sec$	$0.42 \pm 0.22sec$
ulnar pinch	$0.43 \pm 0.21sec$	$0.42 \pm 0.23sec$	$0.42 \pm 0.25sec$	$0.41 \pm 0.12sec$

Table 3.6: The average times and standard deviations of the preshape occurrence per grasp type

(ANOVA) rejected the null hypothesis at a significant level of 5% for the preshape occurrence and the completion time ($p < 0.001$ for $\alpha = 0.05$). A pairwise comparison analysis of the timings of the preshape and task completion shows that the timings are not significantly different between the self-paced motions

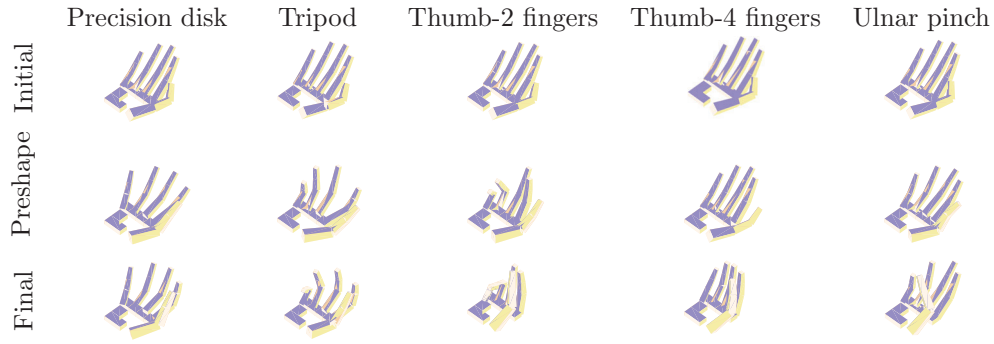

Figure 3.9: Configuration of the fingers in three different moments of the reaching motion: Initial configuration (before the onset of the motion), configuration on the preshape, final configuration (when grasping the object).

	preshape occurrence	completion time
$P1 = 30cm$	$0.56 \pm 0.26sec$	$1.30 \pm 0.27sec$
$P2 = 20cm$	$0.49 \pm 0.21sec$	$1.19 \pm 0.22sec$
$P3 = 10cm$	$0.46 \pm 0.25sec$	$1.14 \pm 0.25sec$
Fast	$0.40 \pm 0.11sec$	$0.83 \pm 0.17sec$

Table 3.7: The average times and standard deviations of the preshape occurrence and task completion on the different motions

preshape occurrence

	$30cm$	$20cm$	$10cm$
$20cm$	10^{-3}		
$10cm$	$< 10^{-3}$	0.91	
Fast	$< 10^{-3}$	$< 10^{-3}$	$< 10^{-3}$

Table 3.8: The results from the pairwise comparison between the timings of the preshape occurrence. The highlighted cells depict the pairs in which the null hypothesis was not rejected at the significant level of 5%.

when the object is placed $20cm$ and $10cm$ away of the initial position of the hand (Tables (3.8) and (3.9)).

After examining the behavior of the fingers, we extracted the timings of the preshape occurrence with a visual inspection of the criteria for each trial. The average and standard deviation of the time of the preshape occurrence and completion time are presented in Table(3.7). As it is shown the preshape occurs on average between $0.46 - 0.56sec$ after the onset of self-paced motions. Figure(3.6a) presents the evolution of the classification performance through real time. As it is shown, the success rate reaches 90% of classification accuracy, on average, at $0.45sec$ after the onset of the self-paced motions. These results suggest that it is possible to classify the grasp type during the preshape of the fingers.

We also compared the classification performance with the preshape occurrence for each grasp type individually. Table (3.6) presents the time of the preshape occurrence for all the grasp types, and Figure (3.3b) presents the evolution of the classification performance for all grasp types in real time. Comparing the time preshape occurrence from Table 6 with the classification results of the Figure (3.3b), we notice that the success rate for the precision disk reaches $89.5 \pm 3.8\%$ of accuracy $0.55sec$ after the onset of the motion, and the corresponding preshape appears $0.74 \pm 0.17sec$ after the motion onset. Concerning the tripod grasp, a $94.1 \pm 2.7\%$ of classification accuracy is observed at $0.55sec$, and the preshape occurs at $0.71 \pm 0.24sec$ after the motion onset. Continuing with the thumb-2 fingers grasp type, a $92.1 \pm 1.8\%$ of classification accuracy is noticed $0.75sec$ after the onset of the motion, and the corresponding preshape occurs $0.53 \pm 0.28sec$ after the motion onset. Regarding the thumb-4 fingers, a $90.7 \pm 2.8\%$ of classification accuracy is noticed 0.65 sec after the onset of the

completion time

	$30cm$	$20cm$	$10cm$
$20cm$	10^{-3}		
$10cm$	$< 10^{-3}$	0.21	
Fast	$< 10^{-3}$	$< 10^{-3}$	$< 10^{-3}$

Table 3.9: The results from the pairwise comparison between the task completion times. The highlighted cells depict the pairs in which the null hypothesis was not rejected at the significant level of 5%.

motion, and the corresponding preshape occurs $0.38 \pm 0.20sec$ after the motion onset. Finally or the ulnar pinch, a $94.46 \pm 2.1\%$ of classification accuracy is noticed $0.15sec$ after the onset of the motion, while the corresponding preshape occurs $0.43 \pm 0.28sec$ after the motion onset. In summary, 90% of classification performance is achieved before the preshape occurrence for three grasp types (precision disk, tripod and ulnar pinch). For the other two, the preshape preceded the 90% of classification accuracy.

3.3.6 Online Robotic Implementation

In order to demonstrate the usability of the proposed approach for the estimation of the final grasp gesture in the early stages of the reaching motion for an assistive or a rehabilitative application, we present here an online robotic implementation of our approach. The system was trained offline, whereas the testing was performed online using the aforementioned control scheme of the Figure (3.2)). We defined a set of desired joint configuration for the 4 fingers of the Allegro hand, so that these correspond to similar postures to the human hand, see Figure 3.11. As soon as the classifier reached the confidence threshold of 0.5, the fingers of the robotic hand were driven to their desired final posture. The confidence of the majority vote was defined as the difference in votes between the two most "popular" classes, divided by the sum of all the votes.

Five able-bodied subjects participated in the online implementation experiment(four males and one female). The subjects performed 15 self-paced reach-to-grasp motions for each grasp type with the objects placed 30 cm away from the initial position of the hand. The recorded dataset, consisting of 75 trials, was used to train the system offline. After the training phase, the subjects performed 30 reach-to-grasp motions for different objects, using a grasp type of their choice, between these five grasp types. The results of the online implementation are presented on the Figure 3.10. The $92.5 \pm 2.9\%$ of the test trials were successful allowing the execution of the correct grasp type. In the $88.58 \pm 3\%$ of the successful trials the robotic hand reached its final configuration before the subject reached the object(see the video[3]and Figure (3.11)). Moreover, all the grasp types have an average success rate above 90% at the end of the motion

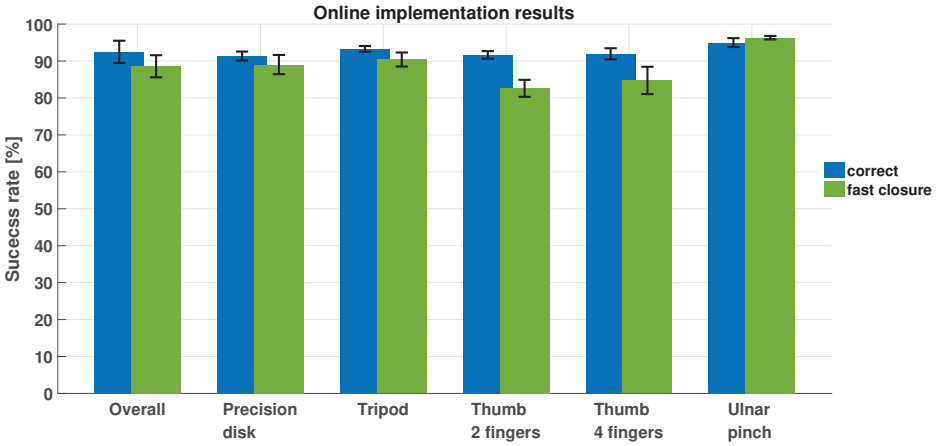

Figure 3.10: Online implementation results.

grasp type	activation time	closure
Precision disk	$0.53 \pm 0.13 sec$	$0.32 sec$
Tripod	$0.54 \pm 0.16 sec$	$0.41 sec$
Thumb-2 fingers	$0.58 \pm 0.25 sec$	$0.41 sec$
Thumb-4 fingers	$0.63 \pm 0.30 sec$	$0.42 sec$
Ulnar pinch	$0.54 \pm 0.12 sec$	$0.41 sec$

Table 3.10: The activation times of the robotic hand for all grasp types in the online implementation. The third column of the table corresponds to time needed for the robotic hand to take its final configuration closing with its maximum velocity.

and above 80% on the early prediction of the grasp type. The lowest performances on the early prediction appear at the *thumb-2 fingers* and *thumb-4 fingers* grasp types with $82.6 \pm 4.3\%$ and $84.75 \pm 3.7\%$, respectively. The highest performance on the early prediction of the grasp type was noticed at the *ulnar pinch* ($96.3 \pm 0.5\%$) followed by the *tripod* grasp ($90.4 \pm 3.3\%$) and *precision disk* ($89.4 \pm 2.3\%$). Table (3.10) presents the average and standard deviation of the activation times of the robotics hand among the correctly classified trials. The average activation time of the robotic hand among all grasp types was $0.54 \pm 0.05 sec$. *Thumb-2 fingers* and *thumb-4 fingers* had the largest variance on the activation time ($0.25 sec$ and $0.3 sec$ respectively).

3.4 Discussion

Previous studies Dalley et al. (2012); Ouyang et al. (2014); Liarokapis et al. (2013); Carpaneto et al. (2012), presented different approaches for mapping EMG signals to reaching and grasping motions, according to object's features and locations and during static or dynamic gestures. In these approaches, the

[3] https://www.youtube.com/watch?v=58tjelKFhAg&t

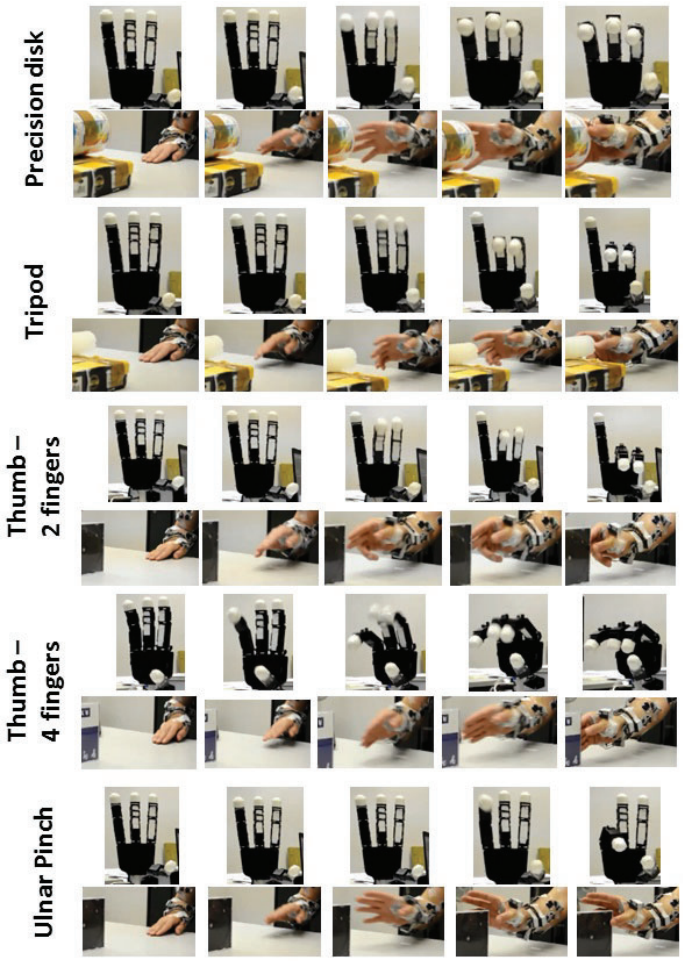

Figure 3.11: Snapshots of the finger motions of the robotic hand and human hand.

system is trained as the subject is asked to perform a grasp type, with or without holding an object, and to stay there for a few seconds. Using this technique, the classifier is able to recognize different grasp types, but only after they are already performed. Transferring this method to an on-line application, the hand should first travel the distance to the object location and then start closing according to the preferred grasp type. This equals a mechanical and unnatural motion in comparison to the seamless natural motion of the human hand. In our approach, the classifier is trained with data of the reaching motion and the classification performance is related to the time of fingers/hand preshape. A decode of the grasping type in the early stages of the motion is important, as it would enable the device to react promptly to the intention of the user. Therefore, we propose an EMG-based learning approach that decodes the grasping intention of the user at an early stage of the reach to grasp motion. Our approach is based on an Echo State Network (ESN) (Jaeger (2001)) combined with a Majority Vote (MV) criterion applied to time windows of $150ms$, from the motion onset to the grasp of the object. We applied the algorithm to an offline classification of five different

grasp types: precision disk, tripod, ulnar pinch, thumb-2 fingers and thumb-4 fingers grasp. Furthermore, we examined whether our approach was robust to different objects' location and to different motion speeds. Indeed, the object's distance and the movement velocity could differentiate the activation of the muscles, especially for the muscles of the upper arm, influencing the classification performance. Finally, we demonstrated in three subjects the usability of our approach for the online control of the Allegro hand.

Reaching-to-grasp motions are decomposed into two phases: (a) the reaching phase, where the hand travels towards the object location, and (b) the grasping phase, where the hand reached the object and the fingers are in contact with the object (Paulignan et al. (1990); Jeannerod (1984); M. Jeannerod (1998)). In a natural self-paced motion the hand spontaneously opens and closes while being in the reaching phase (Paulignan et al. (1990); Jeannerod (1984); M. Jeannerod (1998); Santello and Soechting (1998)). The preshape of the hand is defined as the formation of the fingers before they take the final configuration, and it takes place during the reaching cycle (Supuk et al. (2005)). In particular, the fingers extend to a maximum before they start closing (continuously flex) around the object with respect to its characteristics. It has been reported that the posture of the hand could be discriminated well before the contact with the object (Santello and Soechting (1998)). In other words, the trajectories of the fingers before their closure around the object correspond to an indication of the final grasp type before the grasping phase, i.e. before the fingers are in contact with the object. In this chapter, we showed that this information could be revealed from the muscular activity.

It was shown that the hand's pre-shaping occurs from 60% to 80% of the reach-to-grasp motion, which corresponds to the time instant when the distance between the thumb and the index reached its maximum (Paulignan et al. (1990), Supuk et al. (2005)). Our analysis with normalized time suggests that hand preshape occurs after the 30% with respect to the completion time of the task. We observe that the fingers preshape between the $30 - 60\%$ of the reaching cycle regardless of the distance from the object or the speed of the motion. Furthermore, the initial position of the hand as well as the characteristics of the object could play an important role on the detection of the preshape: For example, when reaching to grasp a thin object by starting from an open-hand configuration, the hand might not need to open more in order to adjust to the size of the object. In this case, detecting the preshape becomes less trivial, and additional principles should be considered for the definition of the preshape. In this chapter, we consider the onset of a smooth closure of the fingers (flexion without extension) as such a principle. Yet, the detection of the preshape becomes more obvious when the task demands large extension of the fingers.

Moreover, Martelloni et al. (2009) suggested that a period between the 25% and the 50% could be sufficient to obtain differences in muscle activity when reaching to grasp three different objects. We expand this suggestion and our

results showed that it is possible to classify five grasp types using EMG data from early stages of the reaching motion. We related the classification performance with the hand's preshape and our offline results showed that a classification rate of 90% was achieved before the hand preshaping for the precision disk, tripod, and ulnar pinch. Whereas, for the thumb-2 fingers and the thumb-4 fingers grasps, instead, the computed hand preshape criteria did not always show a peak, hence the hand preshaping was not always clearly detected.

We evaluated the accuracy of our approach by decreasing the number of EMG channels inserted as input to the classifier. By removing the muscles from the hand and forearm, we kept less information regarding the motion of the fingers, expecting that this would influence negatively the performance. The results showed a significant decrease in the classification performance when using 9 and 7 muscles from the initial muscle set. In particular, the classification performance reduces as the muscles of the hand and forearm are removed, but this does not lead to a significant drop in the performance, as long as we retained at least 7 muscles from the upper arm and 4 from the forearm (i.e *Flexor Digitorum Superficialis, Flexor Carpi Ulnaris, Extensor Digitorum Communis* and *Extensor Carpi Ulnaris*). These results indicate that our method successfully classifies grasps early, without the muscular activity of the more distal muscles. In particular, our classification approach could offer high accuracy in distal amputations, such as wrist disarticulation and transradial amputation, and in SCI cases on low cervical vertebrae (C6-T1). Although the results with less EMG channels are promising, we should keep in mind that the activation of the residual muscles of an amputated arm could be different concluding to a different performance. This aside, our control method performs efficiently with able-bodied users, as presented in the online implementation.

In addition, we examined the proposed approach when the object is placed in different distances. Our results showed no significant differences between the classification performance on different object's distances. This outcome can be explained from the training of the classifier in time steps without normalizing the time. With this approach, we were able to capture enough variability of the EMG activity of motions with different duration and speed. We also took advantage of the short-term memory capacity of the Echo State Networks (ESNs) by avoiding extracting features and treating the signals as time series. This approach imparted a level of tolerance to different muscle activation to the classifier. Furthermore, we evaluated different combinations of training and testing dataset acquired at different object's distances and we concluded that the best performance was achieved when the classifier was trained in the middle distance and tested in distances 10 cm larger or shorter. When we compared the performances between the same training approaches (as presented in 3.6b and 3.6c), we observed the lowest classification performances when the classifier was trained with the shorter distance and tested on further distances. This result suggests a better generalization over the shorter distances than the further

positions. A potential expansion of the generalization would be the inclusion of different positions in space.

Although no significant differences were found when considering different object's distances, as the motion velocities in self-paced motions are slightly different, depending on the object's location, a fast motion influences significantly the classification performance. Although the preshape appears in the same stage on the reaching cycle, regardless of the speed of the motion, we notice that the hand preshapes significantly sooner in time than in self-paced motions. In some cases the fingers follow trajectories different than in self-paced motions. The rapid activation of the arm muscles during fast motions differentiates the activation of agonist/antagonists muscles, influencing the EMG signals and resulting in a lower performance when significantly different velocities were taken into account. A classifier that included different speed motions performed sufficiently well only when the training involved both data form normal and fast motions. The reduction of the performance obtained when the classifier was trained with a single speed motion can cause inconvenient behavior for assistive and prosthetic devices. A cervical injury usually results in low motor functionality also for the upper arm, even in cases where the median and musculocutaneous nerves are intact, and individuals with SCI execute reaching motions in very low speed. Hence, training a decoding system in various speeds could be rather difficult and, in many cases, non-applicable. In contrast, individuals with below-elbow amputation have the ability to extend their arms fast. Therefore, more attention should be paid to the effect of speed on the design of more human-friendly and convenient myo-prosthetic devices. Indeed, seamless control and robot-human interfaces represent two pivotal aspects in robotic-rehabilitation approaches.

For a proof of concept, we integrated our approach in the control of an Allegro hand. After a training phase performed offline including 15 repetitions for each object of the five grasp types, the success rate of classification was around 92.5%. The difference between the offline and online classification performance could be due to different sampling frequency used in the online implementation. This robotic implementation leads to the conclusion that the early estimation of the final grasp from the EMG signals could be applied to a robotic system and, as an extension, could be applied to the control of a prosthetic device or of an exoskeleton. An important extension of the approach is the introduction of a robotic control scheme that derives from the natural motion of the human hand, which would impart a human-like behavior to the robotic device. Additional works could be done to integrate to the robotic system tactile sensors for the attainment of a safe/stable grasp. Indeed, recent developments on the sensory field (D'Anna et al. (2017); Novak et al. (2013)), showed that the design of compliant prosthesis should also include the sensory feedback to the user. This feedback could involve visual and tactile information in order to provide a compliant solution to the demands of the different conditions. A control scheme of an upper arm prosthesis that combines a variety of sensors (e.g EMG, vision,

tactile sensors) would provide a robust use of the device . Moreover, a potential next step would be to include the proposed approach in the control of the fingers' exoskeleton in order to examine any inconvenience that this causes and be further developed on a semi-autonomous control scheme.

Fligge et al. (2000) report that it possible to relate the object's characteristics with the muscular activity. To do so, the decode of the preshape by the EMG signals, as presented in our work, could provide valuable information for object before the contact of the fingers with the object. As this information comes in advance of the contact, it could be used for accomplishment of a safe grasp.

Finally, a further interesting extension of this work is the classification of specific-finger configuration with different hand orientations. In this case, a classifier could tackle the problem of the high dimensionality of the task with the use of postural synergies (Santello and Soechting (1998)), that correspond to a number of hand postures that humans combine when grasping. Furthermore, during grasping different orientations of the hand are used. Young et al. (2013) and Fougner et al. (2014) has reported a successful classification of the simultaneous motion of the wrist and fingers. A potential combination of the decode of the grasping intention of the user with the simultaneous control of the wrist will provide a more natural motion of the wearable device with respect to the human motion.

3.5 Conclusion

In this chapter, we have made a first step towards enabling a more fluent control of prosthesis. Specifically, we have compared the classification accuracy with the hand pre-shape, investigating the stage where the accuracy becomes higher than 90%. The results have shown that it is possible to have high accuracy before the hand preshape and in some cases, such as the precision disk grasp type, before the hand has completed the opening stage. We ave also observed that 90% of accuracy occurs approximately $0.5s$ after the motion onset. Integrating this approach in a real-time control of a robotic hand, we noticed that the robotic hand was activated whilst the user was still in the reaching phase. These results indicate that the EMG activity of the first stages of the reaching phase is sufficient for providing high prediction accuracy. This study is limited, however, by the participation of only able-bodied individuals and, for this reason, we evaluate the assumption with end-users in the next chapter.

Chapter 4

Decoding the Grasping Intention from Electromyography during Reaching Motions

In this chapter, we focus on the evaluation of the decoding approach with four individuals with below-elbow amputations. As the preshape criteria are not applicable in this case, we introduce the concept of motion phases in the control approach. In particular, to better examine the evolution of the classification accuracy over the reach-to-grasp motion, we separate the EMG into phases with respect to the angular velocity of the elbow joint. We perform an analysis in order to explore the differences, among the EMG patterns, in the motion phases and to compare the performance of different classification methods. Furthermore, we investigate the effect of different muscle-groups on the classification accuracy. Lastly, we highlight the benefits of including all the motion phases in the real-time control of a prosthesis and the resulting confidence of the pattern recognition system.

4.1 Introduction

Surface electromyography (EMG) has been widely studied as an intuitive human-machine interface for controlling intelligent external devices, such as prosthetic hands (Novak and Riener (2014); Earley et al. (2016)). As amputees generally have a limited number of independent EMG sites available for controlling a multi-degree of freedom (DOF) prosthesis, we cannot rely on a one-to-one EMG-to-DOF control. Surgical methods, such as targeted muscle reinnervation (TMR) (Miller et al. (2008); Kuiken et al. (2009)) and regenerative peripheral-nerve interfaces (RPNIs) (Urbanchek et al. (2011)), can enable the control of a larger number of DOFs.

Advanced signal-processing approaches could also be used to control multi-DOF prostheses with fewer independent EMG sites. EMG-based pattern recognition systems are proposed for the estimation of, both independent and simultaneous (Fougner et al. (2014); Young et al. (2013)), hand and wrist movements (Smith et al. (2016); Gonzalez-Vargas et al. (2015); Li et al. (2010)). Using extrinsic hand muscles, pattern recognition has effectively classified functional hand-grasp patterns (Smith et al. (2016)) and even individual finger movements (Naik et al. (2016); Khushaba et al. (2012)).

In these previous studies, subjects generally performed muscle contractions

while maintaining their arm in a fixed position. However, training a classifier in a static position, as mentioned above, results in lower classification accuracy when the limb is in different positions or performs dynamic motions (Scheme et al. (2011)).

Reach-to-grasp movements are important activities that require dynamic contraction of the muscles. A few studies have attempted to decode grasping intention from EMG during reach-to-grasp motions, but only with able-bodied subjects (Batzianoulis et al. (2017); Martelloni et al. (2009)). When reaching to grasp an object, the opening and closing of the hand is in coordination with the motion of the arm (Rand et al. (2008); Wang and Stelmach (1998)), see Figure 4.1a. More specifically, the human hand opens rapidly in the early stages of the reaching cycle, whereas the fingers converge gradually to their final configuration (Jeannerod (1984); Rand et al. (2008)).

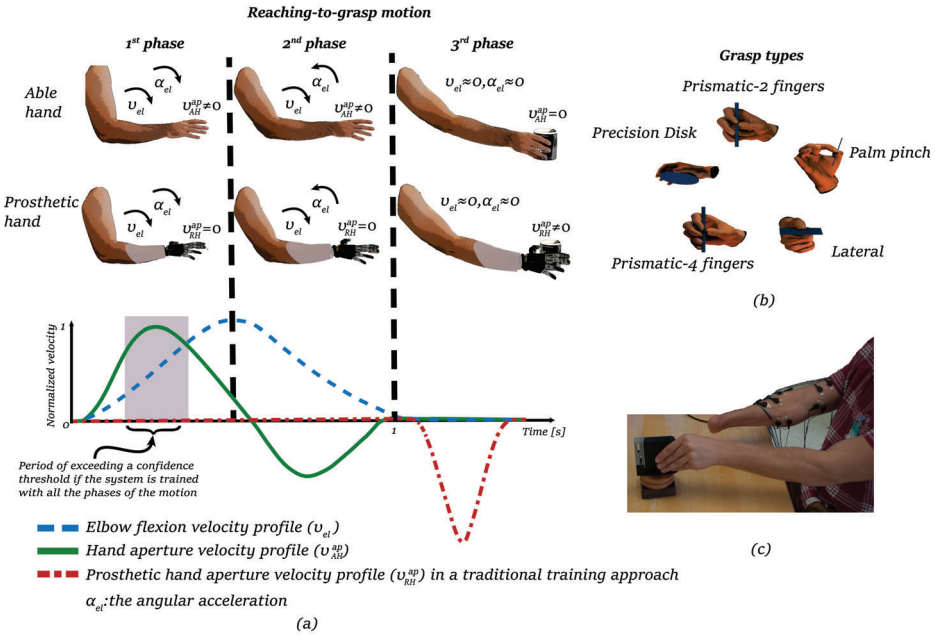

Figure 4.1: a) Typical profiles of velocities of the elbow and hand aperture in abled-bodied subject Rand et al. (2008); Gentilucci et al. (2000); Bongersa et al. (2012) compared to that generated with a traditional prosthetic device, as presented in Ghazaei et al. (2017); Amsuess et al. (2016). During reaching, the aperture of the human hand (solid green line) changes in coordination with the extension of the arm (dashed blue line). In contrast, the prosthetic hand (dash-dotted red line) begins its motion later in the reach-to-grasp cycle, once the elbow is fully extended. In our approach, we separate the reach-to-grasp motion into three phases (denoted by dashed vertical lines) according to the angular acceleration of the elbow joint a_{el}. We distinguish between acceleration, deceleration and rest phases. We present that a pattern recognition system, trained including the reaching motion, could gain efficient prediction confidence early in the reaching motion and, thus, activate faster a prosthetic device. b)) The selected five grasp types used in our classification, following the names and using figures from the taxonomy of Feix et al. (2015). c) Experimental set-up for training the system with amputee subjects in data recordings. EMG-information from the amputated arm are recorded while the subject performs the reach and grasp motion with his/her intact arm.

A self-paced reaching motion of an able-bodied hand could take approximately 1s to complete (Batzianoulis et al. (2017); Haggard and Wing (1995)). In contrast, the activation of prosthetic hands could occur more than one second

after the onset of the motion (Ghazaei et al. (2017); Amsuess et al. (2016)) (see Figure 4.1a). This makes unnatural the actuation of a prosthetic hand, due to the lack of the natural arm-hand coordination. It also slows down the reach-to-grasp motion. It is crucial that prosthetic devices react promptly to human intentions in order to enable natural and intuitive operations (Farrell and Weir (2007)). To convey a seamless coordination between the device and the residual arm, it is important that the device identifies the grasping intention during the reaching phase.

In the previous chapter and in (Batzianoulis et al. (2017)), we showed that the detection of the grasp type in synchrony with the reaching motion could enable a smooth coordination of hand closure with the reaching motion, thus providing a more natural and seamless motion of the arm and a robotic hand. In our approach, the classification performance is related to the occurrence of hand pre-shape during reaching motions, following the natural pre-shape phase as documented in (Jeannerod (1984); Santello and Soechting (1998)). Our prior study was limited to able-bodied subjects. Here, we extend this approach to decoding residual EMG in individuals with a below-elbow amputation. We compare the performance of four different classifiers: LDA, two SVMs, and an Echo State Network (ESN). Additionally, we explore a relationship between classification performance and the phases of the reach-to-grasp motion. This chapter corresponds to the following publication:

Batzianoulis, I., Krausz, N., Simon, A., Hargrove, L. and Billard, A., *Decoding the grasping intention from electromyography during reaching motions*, Journal of NeuroEngineering and Rehabilitation, 2018.

4.2 Methods

4.2.1 Experimental Protocol

Eight able-bodied subjects (6 males and 2 females $25-32$ years old) with no known neurological or physical deficits and four unilateral transradial amputees participated in the experiment. All able-bodied subjects were right-handed and performed the experiment with their dominant hand. All subjects were naive to pattern recognition control, with the exception of three of the amputee subjects. Two of the amputee subjects had undergone a TMR surgery. Table 4.1 presents the demographic information about the amputee subjects.

During the experiment, both the able-bodied subjects and the amputee subjects sat in front of a table, facing a computer screen, with their elbows at a 90^o angle. The able-bodied subjects had their right-hands closed on the table and they were asked to reach the object and grasp it with a predefined grasp type

and to maintain the same wrist orientation for all grasp types. Custom computer software, called Control Algorithms for Prosthetics Systems (CAPS) (Kuiken et al. (2009)), prompted users to initiate the reach-to-grasp motion and to go back to a resting position. Subjects performed the motions at their own pace. They were tasked to reach and grasp an object placed $30cm$ away from the initial position of their hand. Once they had reached the objects, they were asked to remain in the same posture until they received a cue from CAPS to go back to the resting position. The duration of each trial was $4s$ with a $10s$ rest between trials, to avoid fatigue. All subjects performed 30 trials for five grasp types, resulting in 150 trials in total.

In the experiments with the amputee subjects, the subjects were asked to reach the object and grasp it with their intact hand while trying to replicate the motion with their phantom limb, see Figure 4.1c. These subjects started their self-paced motions when cued by the experimenter. Whenever a subject perceived an irregular or unexpected muscle contraction, the experiment was paused and the trial was repeated. Regular breaks were taken in order for the subjects to relax from the stress and effort of contracting their phantom limb. All the amputee subjects were able to complete the experiments.

Table 4.1: Demographic information of the four transradial amputatee subjects. TR1 and TR3 underwent a TMR operation for neuroma pain, not for improving prosthetic control. TR1 is not a user of a myoprosthesis due to financial reasons.

Subject	TMR	User of myoprosthesis	Age	Years since amputation
TR1	Yes	No	25	7
TR2	No	myoelectric prosthesis	53	38
TR3	Yes	myoelectric prosthesis	51	2
TR4	No	myoelectric prosthesis	68	>30

4.2.2 Apparatus and Pre-processing

Custom computer software Kuiken et al. (2009) was used for signal acquisition, with EMG signals acquired at $1000Hz$ with a $30-350Hz$ band-pass filter using TI ADS1298 biosignal amplifiers. The EMG activity of 12 muscles was recorded: *Trapezius (Trap), Deltoid Anterior (DA), Deltoid Medial (DM), Deltoid Posterior (DP), Biceps Brachii long head (BB), Triceps Brachii long head (TB), Brachialis (BR), Flexor Digitorum Superficialis (FDS), Extensor Digitorum Communis (EDC), Flexor Carpi Ulnaris (FCU), Extensor Carpi Ulnaris (ECU), Flexor Carpi Radialis (FCR)* (seven muscles of the upper arm and five muscles of the forearm). To construct a linear envelope, full-wave rectification was performed, followed by smoothing with a low-pass seventh-order Butterworth filter with cut-off frequency at 20Hz. At the end of this step, each chan-

nel was normalized by the maximum value recorded in the trials. A goniometer was placed on the subjects' elbow for measuring the onset and extension of the elbow.

In order to evaluate the quality of the EMG signals, we computed the root mean square of signal-power (P_{rms}), following the method presented in Agostini and Knaflitz (2012). In particular, we accumulated the raw EMG signals of all the trials for each participant and calculated the P_{rms} for each EMG channel. We grouped the 8 able-bodied participants as our control-group. We, then, compared the signal-powers of EMG signals of each amputee participant with our control group.

4.2.3 Phases of the Motion

As illustrated in Figure 4.1a, during a natural reach-to-grasp motion, the opening and closing of the hand is coordinated with the extension of the elbow Rand et al. (2008); Wang and Stelmach (1998). Typically for able-bodied subjects, the hand opens rapidly in the early stages of the reaching motion and decreases its velocity while approaching the object and reaching the final configuration Jeannerod (1984). The hand's velocity peak occurs before the peak velocity of the elbow extension Rand et al. (2008). Thus, the hand reaches its final grasp-posture after the peak velocity of the elbow extension. Because EMG recordings from upper and lower arm muscles encapsulate information on the hand motion, the EMG patterns will likely differ in the different phases, specifically before and after the elbow extension velocity peak. Taking inspiration from this behavior, we divided the reach-to-grasp motion into three phases, with respect to the extension of the elbow joint. The first phase is defined as the interval from motion onset (i.e. when the angular velocity of the elbow joint exceeds a velocity threshold) until the angular velocity of the elbow reaches its maximum. The second phase is the interval between the aforementioned maximum angular velocity and the end of the reaching motion (i.e. when the angular velocity of the elbow drops below a velocity threshold). We define the third phase as the phase after the completion of the elbow extension. More specifically, we selected 25% of the duration of the reaching motion selected after the velocity drops below a threshold. The velocity threshold was set at 10% of the maximum angular velocity recorded for each subject.

We normalized the time of the duration of the reaching cycle. The reaching cycle corresponds to the time interval between the motion onset and the end of the extension of the elbow, i.e. when the angular velocity of the elbow drops below the velocity threshold. We performed a one-way multivariate analysis of variance (MANOVA) on the average values of the 12 EMG channels over the three phases for each grasp type. The Wilks Lambda test and the Pillai-Barlett Trace test were used to compare the results to a significance level of 5%

($a = 0.05$). We present the results in Section III.

To further investigate the three phases, we grouped the EMG signals of the classes together for each phase. The signals were divided into sliding time-windows and the average activity of each channel was extracted, thus creating a vector of N elements (N corresponds to the number of EMG channels). A principal component analysis (PCA) was performed with the data from the third phase, and the data of the two remaining phases were projected into the new hyperplane. The distribution of the data on the first two principal components was fitted to Gaussian Mixture Models (GMMs) for each phase, and the number of Gaussian components was optimized by the Bayesian Information Criterion (BIC). We performed an analysis on the complete muscle set ($N = 12$) and an analysis using only the muscles of the forearm ($N = 5$).

4.2.4 Classification Methods for Decoding the Grasping Intention

The preprocessed EMG signals were analyzed using a sliding time-window of $150ms$ with an increment of $50ms$. The time window and increment lengths were chosen to be between the preferred values for an online implementation, as suggested in (Smith and L. J. Hargrove (2011)). We did not use any dimensionality-reduction method (such as PCA) in this step. For each grasp type, 10 trials were randomly selected as the testing set. The remaining 20 trials of each grasp type constituted the training and validation sets. A four-fold cross-validation was performed to optimize the hyper-parameters for each classification method.

The classification accuracy of four classification methods was compared, specifically for an LDA classifier, an SVM with linear kernel, an SVM with a Radial Basis Function (RBF) kernel and an ESN. For each classification method, one classifier was trained per subject. We did not attempt any inter-subject training. We inserted the classification outcome of each time window into a Majority Vote (MV) algorithm that uses a buffer of $0.5s$ history to predict the winning class.

In the cases of LDA and SVM, we extracted three features for each time window and introduced them into the classifier. Following the previously described methods for EMG pattern recognition (Englehart and Hudgins (2003)), we chose three features; the average activation of each time window, its waveform length, and the number of slope changes. In the case of ESN, we did not perform any feature extraction, treating the problem as a multidimensional time-series problem.

Linear Discriminant Analysis

LDA is one of the most commonly used classification algorithms for biomedical signals, due to its performance and robustness. LDA finds a linearly optimal combination of the features in order to separate the classes. A fitting function estimates the parameters of a Gaussian distribution for each class and finds the probability of each point belonging to a class. Despite the linear nature of LDA, it has been shown to perform well in the classification of EMG signals (Daley et al. (2012)).

Support Vector Machine

We tested two types of kernels, i.e. a linear kernel and an RBF kernel. In the case of the linear kernel, after a grid search, we optimized the penalty factor C. Likewise in the case of the RBF kernel, we optimized by a grid search both the penalty factor C and the γ parameter.

Echo State Networks

ESN (Jaeger (2001)) is an effective recurrent neural network (RNN) that has attracted substantial interest due to its performance in time-series (Li et al. (2012); Xu and Han (2016)). The core of ESN is a large fixed reservoir. The reservoir contains a large number of randomly and sparsely connected neurons. The determination of the readout weights is the only trainable part; the weights can be obtained simply by linear regression. The necessary and sufficient condition for generating the echo state is based on information from the dynamic reservoir, such as the spectral radius of the internal weight-matrix. We optimized the three hyper-parameters; number of neurons, spatial radius and regularization parameter, by a grid search.

4.2.5 Physical Prosthesis Control

For the purpose of the online implementation, we used the RIC hand (Lenzi et al. (2016)), a prototype prosthesis with two degrees of actuation, that is able to perform two grasping postures: hand open, power grasp, and prismatic 2 fingers. Due to its design, the RIC hand can offer access to a low-level control of the actuators. In this control scheme, we control the actuators directly hence avoid any delays that arise from using control interfaces offered by commercial prosthesis. We mounted the prosthesis on a socket fitted to the user's residual forearm and placed a goniometer was placed on the elbow joint to record arm extension. We collected 12 EMG signals from the arm, preprocessed and classified them in real time and inserted the classification output into a majority vote algorithm. The buffer of the majority vote was $0.5s$. Once the majority vote confidence exceeded a threshold of 0.5, i.e. more than half of the votes belonged to the same class, the corresponding command was sent to the prosthesis.

One subject, TR4, participated in a real-time control experiment. During the training phase, we cued the subject to perform 20 reach-to-grasp motions for each trained grasp type. The collected EMG signals were used to train two SVMs with RBF kernels: the first classifier used EMG from all the motion phases, whereas the second classifier was trained with EMG collected after arm extension (only the third phase). During the testing phase, the subject performed two sets of 20 reach-to-grasp trials for each classifier with the prosthesis turned on. Prior to the testing phase, the subject controlled the prosthesis for $10 - 15$ minutes to familiarize themself with the device control. We used two metrics to compare the performance of the classifiers: the classification accuracy, and the time to reach a 0.5 majority-vote confidence level. We performed a two-sample t-test to validate the null hypothesis and to determine if there were significant differences between the results from the two classifiers.

4.3 Results

4.3.1 Kinematics of the Elbow Joint Angle and Quality of the EMG signals

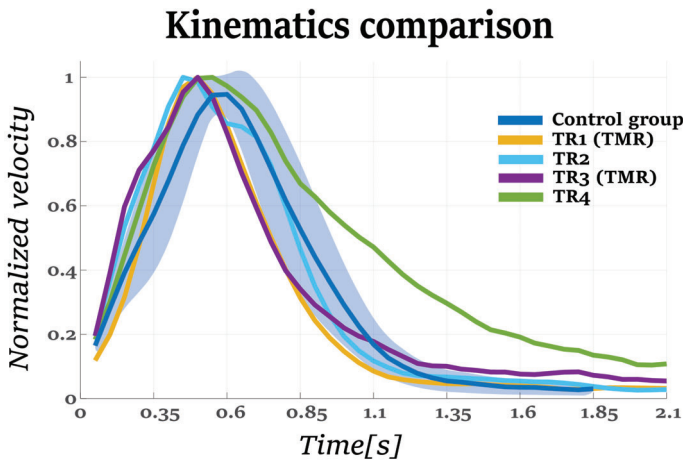

Figure 4.2: The normalized average velocity of the elbow joint angle for the control group and each of the TR subjects. The blue shadow area corresponds to the standard deviation of the normalized velocity across the control group. The peak of the velocity occurs approximately in the same stage for all the participants. TR4 completes the reaching motion later than the other participants.

As a first step of our analysis, we examine the kinematics of the elbow joint angle. Figure 4.2 presents the velocity profiles of the elbow joint for all the participants in our study. All the velocities present approximately the same profile: a rapid acceleration in the first stages of the motion with a smoother deceleration as the arm extension is close to the end. The peak of the velocity

occurs approximately in the same stage for all the participants. An one-sample t-test revealed no significant differences among the moments of the velocity peaks ($p = 0.89$). TR4 completes the reaching motion slower than the rest of the participants.

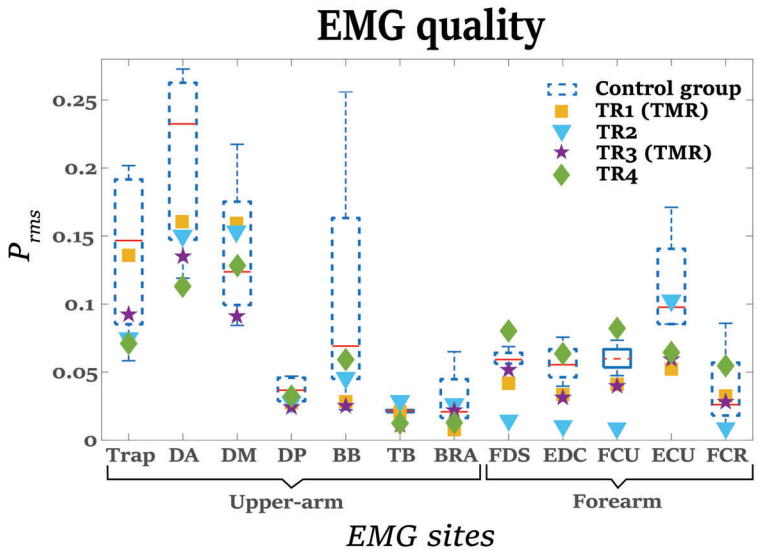

Figure 4.3: The signal-power (P_{rms}) for all the EMG channels recorded in our study. The blue dashed squares correspond to the box-plots of the control group (the red horizontal lines correspond to the medians of the group for each muscle). The orange squares correspond to the P_{rms} of each EMG signal for the subject TR1. The blue triangles, purple stars and green diamonds correspond to the P_{rms} of each EMG signal for the subjects TR2, TR3 and TR4, respectively.

Figure 4.3 shows the root mean square of signal-power (P_{rms}) for the control group and the amputee participants. The P_{rms} of the amputee participants is the same level of the control group for the muscles of the upper-arm (*Trap-BRA*). In contrast to this, their signal-power is generally lower than the control group in the muscles of the forearm. In particular, the difference in the signal-power is more obvious for the muscle ECU, where only the subject TR2 is in the same level as the control group. The signal-power of the other forearm muscles of TR2, however, are in a significantly lower level than the control group. This could be an indication for low classification accuracy for the subject TR2, as we will see later in the subsection 4.3.3.

4.3.2 Phases of the Motion

To examine the muscle-activation patterns during the reaching motion, we divided the recorded EMG signals in two groups: muscles of the forearm and muscles of the upper arm. Figure 4.4 presents representative examples of the average EMG activity of each muscle group in normalized time; the blue color corresponds to the muscles of the forearm and the red color corresponds to the muscles of the upper arm. The vertical dashed lines highlight the average time

of the shift from the 1^{st} phase to the 2^{nd} phase, with the green shaded areas corresponding to the standard deviation of that shift. We calculated these events from the kinematic data recorded by the goniometer. The mean reaching time varied between $0.97 \pm 0.16s$ to $1.26 \pm 0.3s$ for able-bodied subjects and from $1.13 \pm 0.23s$ to $1.7 \pm 0.3s$ for amputee subjects.

We identified the maximum elbow-joint angular velocity at $30 - 45\%$ of the reaching motion for all the participants. Regarding the timing of maximum elbow-joint angular velocity, we found no significant difference between able-bodied and amputee subjects ($p = 0.55, t-value = 1.45$). The activation pattern of the distal muscles (muscles of the forearm) differed between amputee and able-bodied participants. In particular, the activation of the distal muscles in able-bodied subjects occurred earlier than in amputees. The muscular activity of the forearm muscles of able-bodied subjects reached a peak from $20 - 60\%$ of the motion, decreasing as the motion came closer to completion.

The EMG activity of the forearm muscles of the amputee subjects increases gradually during the reaching. Whereas, the proximal muscles remain at a constant level of activation after the maximum angular velocity is reached. This difference in activation timing could have an effect on classification performance.

We compared the average activity across the three phases with a one-way MANOVA. As it rejected the null hypothesis, we found significant differences between the phases ($p < 0.01$, *Degrees of Freedom (DoF)*$= 2$) for all the subjects (able-bodied and amputees). Figure 4.4 presents the Gaussian models of the phases on the first two principal components for the complete muscle-set and the muscles of the forearm, respectively.

Although some models partially overlap, they have different mean values for all subjects, regardless of the muscle-set. In able-bodied subjects, the third-phase models are concentrated around the origin and have standard deviations smaller than the other phase models.

For amputees, the third-phase models are concentrated around the origin, similar to the able-bodied results. However, these models cover an area larger than the corresponding models for the able-bodied subjects. For all amputee subjects, a larger overlap was found between the models first and second phases with a larger distance from the models of third-phase.

By performing a one-way MANOVA, we compared the average muscle activity during the three phases for each class (i.e. grasp type). The one-way MANOVA failed to reject the null hypothesis ($p < 0.001, DoF = 2$); this indicates significant differences between the means of the phase models for all the subjects. The significant differences between the three phases show that the data, from all classes in the space, change continuously, thus reducing the ability for a classifier to generalize across the three phases if it is trained on only one of them.

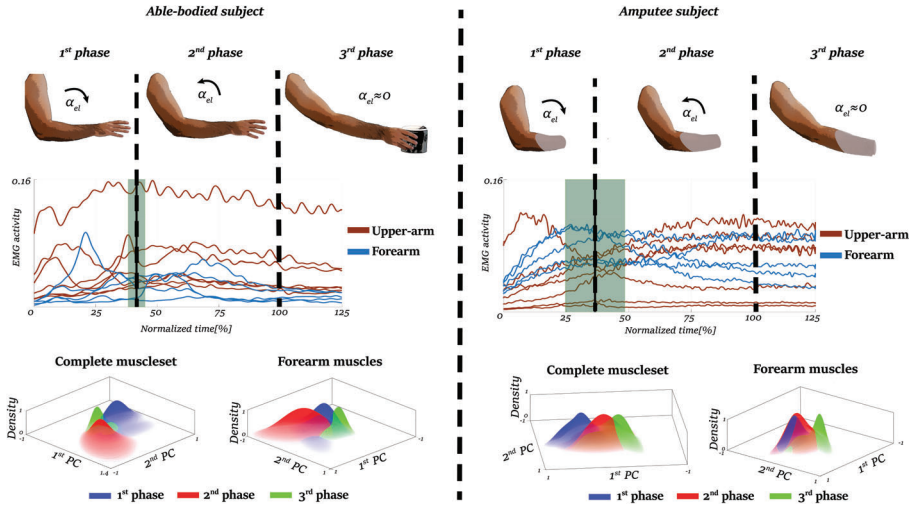

Figure 4.4: Representative examples of the EMG activity and the phases of the motion of the able-body subject 4 (left) and the amputee subject TR4 (right). The graphs in the middle correspond to the linear envelope of the EMG signals of the upper-arm (red lines) and the forearm (blue lines). The grey shadow areas correspond to the standard deviations of the timings where the shifts between the phases occurred. The graphs on the bottom of the figure show a representation with Gaussian Mixture Models (GMMs) of the EMG activity of the three phases projected on the first two components of third phase after performed Principal Component Analysis (PCA). The analysis was performed on the complete muscle set ($N = 12$) and when using only the muscles of the forearm ($N = 5$). The GMR representation shows limited overlap between the three phases, indicating differences on the EMG activity of the phases. Occasionally, an extended overlap occurred between the first and second phases as presented in the bottom-right graph. However, the third phase had rarely overlapped with any of the other two phases.

4.3.3 Decoding the Grasping Intention

In this subsection, we compared the performance of four classifiers (LDA, SVM with linear kernel, SVM with RBF kernel and ESN). Figure 4.5 presents the average classification accuracy of each classifier over a time interval of $2s$. After performing an analysis of variance (ANOVA) for a significance level of 5%-$a = 0.05$, we did not notice any significant differences between the classifiers' performances for each group of classes ($\{p = 0.7$, $F\text{-}value$=0.43$\}$, $\{p = 0.5$, $F\text{-}value$=0.97$\}$ and $\{p = 0.8$, $F\text{-}value$=0.35$\}$ for 5, 4 and 3 classes, respectively). However, the SVM classifier with the RBF kernel performed better than the other classifiers, with $60.45 \pm 8.2\%$, $65.82 \pm 8\%$ and $77.4 \pm 5.88\%$ classification accuracy for 5,4 and 3 classes, respectively; but this difference was not significant. This was followed by the SVM with the linear kernel, the ESN, and the LDA. As the SVM-RBF classifier achieved slightly better performance, the rest of the results correspond to the performance of this classifier.

Figure 4.6 presents the classification performances of the five grasp types in each of the three motion phases. Poor classification performance occurred during the first phase in both amputee and able-bodied subjects. Accuracy improved in the subsequent two phases (see Figure 4.6a and d). The grasp types precision disk, palm pinch and lateral grasp, yielded the best performance in second and

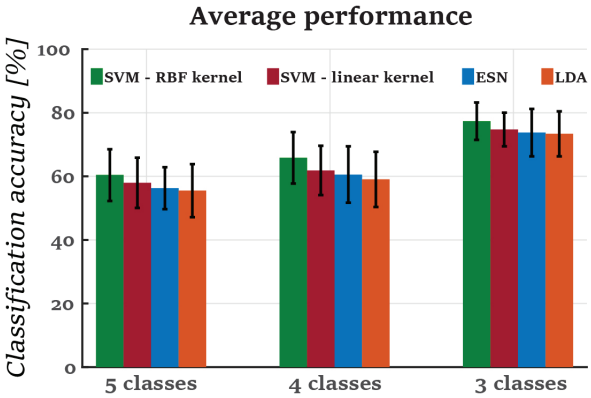

Figure 4.5: The average performance of all the classification models through out the whole trajectory of 2s among all the subjects.No significant differences were noticed between the performances of the classifiers for each group of classes($p = 0.7$, $p = 0.5$ and $p = 0.8$ for 5, 4 and 3 classes respectively.

third phases for amputee subjects (see Figure 4.6b and c). The lateral grasp improved from 58.1±6.2% in the second phase to 60.45±8.2% in the third phase. Accordingly, the precision disk and palm pinch increased from $60.2 \pm 10.2\%$ to $70.5 \pm 1.2\%$ and $68.4 \pm 6.8\%$ to $71 \pm 8.9\%$, respectively. The precision disk and lateral grasp types had the best classification accuracy also for the able-bodied subjects (see Figure 4.6e and f). These grasp types' performances increased from $60.2 \pm 10.2\%$ and $50.8 \pm 9.9\%$ in the second phase to $75.5 \pm 7.6\%$ and $87.1 \pm 3.5\%$ in the third phase, respectively. We noticed the worst performance in the prismatic-4 fingers for the amputee subjects, with 49.6±5.6% in the third phase (Figure 4.6c), and in prismatic-2 fingers for the able-bodied subjects, with $47.7 \pm 8\%$ in the third phase (Figure 4.6f). The prismatic-2 fingers and palm pinch were misclassified for one another in the third motion phase for the able-bodied subjects about $25 - 30\%$ (see Figure 4.6f). This indicates that the muscular activity during the preshaping of the fingers is similar for these grasp types. The reason for this could the similarity of the two grasp types, as they differ mainly on the configuration of the middle finger.

Figure 4.7a-c presents the evolution of average classification performance of the control group that consists of the eight able-bodied subjects and of the individual performance of all the amputee subjects, until 2s after the motion onset. For the cases of $4-$grasp and $5-$grasp types, the classification performance of each classifier follows the same profile: poor classification performance in the first phase of the motion, and the performance increases as the hand approaches the object. Subject TR1 achieved the best performance of all amputee subjects, with a performance comparable to that of the able bodied subjects, whereas TR2 had the lowest performance. TR3 and TR4 exceeded the level of $60 - 70\%$ in the accuracy at the end of the first phase and the beginning of the second phase, and they stayed at this level until the end of the third phase.

In the case of $3-$grasp types, TR3 and TR4 appeared to performance better than the control group in the first phase, reaching 80% of accuracy during the

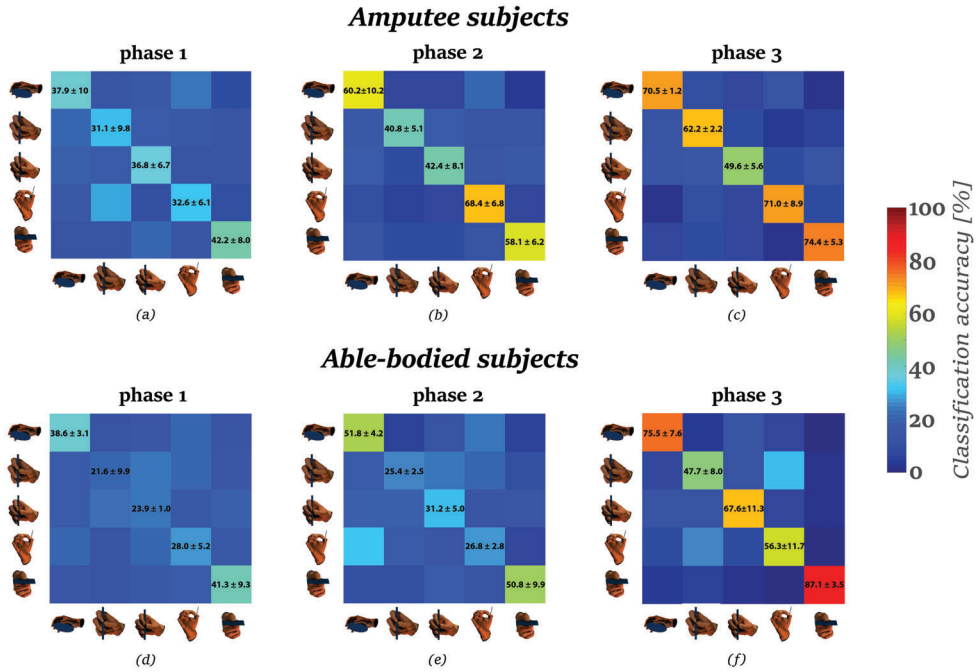

Figure 4.6: The confusion matrices for all the motion phases. The confusion matrices present the average classification accuracies and their standard deviations for the five grasp types. The matrices on the top correspond to the classification performances among the amputee subjects while the matrices on the bottom correspond to the classification performance of the able-bodied subjects. The horizontal axis of the confusion matrices correspond to the predictions while the vertical axis correspond to the ground-truth. The color of the tile was assigned according to the colormap of the classification accuracy on the right.

shift to the second phase. In the second phase, the performance among the subjects TR1, TR3 and TR4 reached an accuracy of $90 \pm 10\%$, higher than the corresponding performance of the control group ($76 \pm 20\%$). The classification accuracy in the third phase for the these amputee subjects stayed above 80%, though lower than the control group ($95 \pm 5\%$).

Reducing the Number of Channels

In this section, we compare classification performance for when only the forearm EMG is used with that of the complete muscle set. An SVM classifier with an RBF kernel was trained for each muscle set: the complete muscle set and the five muscles of the forearm. Figures 4.7d-e present the evolution of the classification accuracy for a duration of $2s$. As shown, using fewer EMG sites led to decreased performance for the amputee subjects. From the end of the second phase, the average classification accuracy decreased significantly from $67.2 \pm 8.4\%$ to $60 \pm 8.2\%$ when predicting among $5-$grasp types ($p < 0.01$, *t-value*=4.33). Although the reduction of the EMG sites available had an impact on the performance of amputee subjects, when only the muscles of the forearm are used the performance of able-bodied subjects was higher than when using the full muscle set.

Comparing the Performance of TMR versus Non-TMR Subjects

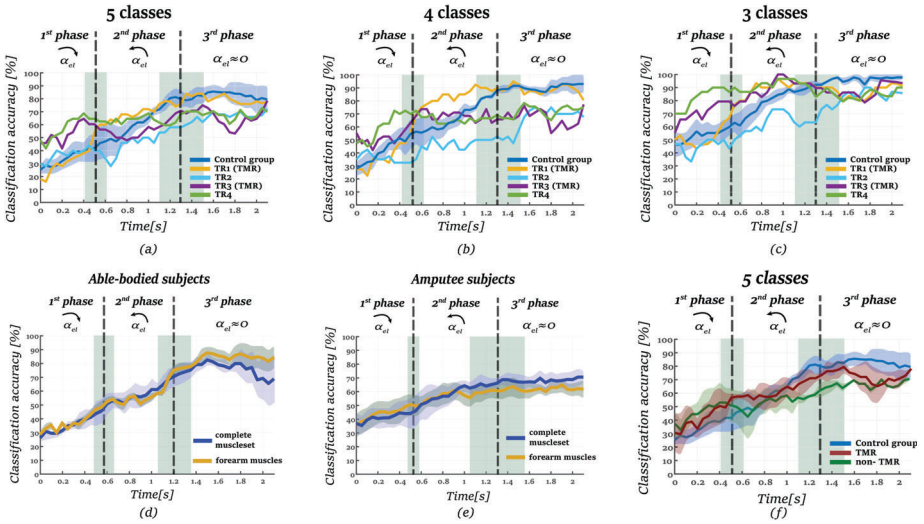

Figure 4.7: The evolution of classification performance and standard error through time for 2s after the motion onset. The vertical dashed lines correspond to the average moments of the shifts of between the phases while the shaded areas present the corresponding standard deviations accordingly. Figures a,b and c present the evolution of the classification performance of the control group and the amputee subjects for $5, 4$ and 3 classes accordingly. Figures d and e compare the classification performance on 5 classes when using the forearm muscles and complete muscle-set as an input to the classifier.

In this section, we compare the classification performance between TMR subjects (TR1 and TR3) and non-TMR subjects (TR2 and TR4). In the case of 5 classes, the average classification accuracies and standard errors in the first, second and third phases of the TMR subjects are $44.1 \pm 10.1\%$, $62.7 \pm 86.5\%$ and $74.9 \pm 6.1\%$, respectively. The corresponding performances of the non-TMR subjects in the three motion-phases are $47.6 \pm 8.9\%$, $54.9 \pm 7.5\%$ and $67 \pm 2.5\%$. The classification accuracies are also at the same level in the case of 4 classes. More specifically, the average classification accuracies and standard errors of the TMR subjects are $45.5 \pm 8.9\%$, $76.45 \pm 6.4\%$ and $77.7 \pm 8.4\%$ in the first, second and third phase, respectively. The corresponding performances of the non-TMR subjects in the three motion-phases are $48.33 \pm 10.7\%$, $58.3 \pm 6.9\%$ and $77.72 \pm 8.6\%$. In the case of $3-$grasp types, both the TMR and non-TMR groups have improved accuracies with respect to the other two cases (5 and 4 classes). In the first and third phase, the average classification accuracies of the non-TMR group are at the same level as the TMR group; $68.6 \pm 8.8\%$ and $64 \pm 14.4\%$ for the first phase and $87.6 \pm 3.4\%$ and $83.6 \pm 4\%$ for the third phase, respectively. However, the accuracy of the TMR subjects exceeds the one of the non-TMR subjects in the second phase; $90.2 \pm 4.6\%$ and $77.8 \pm 10.9\%$, respectively. As stated above, TR1 (a TMR-subject) has the better performance among the amputee subjects.

4.3.4 On-line Evaluation

To demonstrate the usability of our proposed approach for controlling a prosthetic hand, we present an on-line implementation of our approach. We followed the protocol described in Section IIE. One amputee subject took part in this validation. The subject performed reach-to-grasp motions while commanding the device to close in one of two grasp types: a power grasp or a prismatic-2 fingers grasp. In total, the subject performed two sets of 20 trials for each training approach: training over all phases or training only over the third phase.

An SVM with an RBF kernel was trained off-line, whereas the testing was performed on-line, where the subject performed 20 reaching motions for each of the aforementioned training approaches. As soon as the classifier reached the confidence threshold of 0.5, the corresponding motor commands were sent to the prosthetic hand to drive the fingers to their desired final posture. We assessed the performance through two metrics: classification accuracy and time to generate a confident prediction on grasp type. Results are shown in Figures 4.8b-c.

When trained with all three phases of the motion, the pattern recognition system showed a higher performance, in terms of the overall classification accuracy, compared to the one that used only the third phase. The overall classification accuracy, when using all three phases for training the system, was $80 \pm 5\%$; whereas the corresponding accuracy when the system was trained only with the third phase was $55 \pm 5\%$, see Figure 4.8c. When using only the third phase for training the system, it identified poorly the power grasp type, despite having similar performance for the prismatic-2 fingers grasp type.

The system that trained on all 3 phases was also faster at delivering a robust prediction. On average, it offered a confident prediction $25 - 40\%$ earlier than the system trained only on the 3rd phase. For the correctly classified trials, when the system trained over all the phases the time needed to exceed the confidence level was significantly lower($p = 0.0194$, *t-value*=2.49) than when it used only the third phase, 0.3 ± 0.10 and $0.42 \pm 0.12s$, respectively (Figure 4.8b). The pattern recognition system trained with all the phases reached the confidence threshold at $0.26 \pm 0.04s$ for the prismatic-2 fingers grasp; it was significantly faster ($p = 0.003$, *t-value*=3.49) than the system trained with only the third phase. Regarding the power grasp, the system trained with all the phases reached the confidence threshold faster, but not significantly ($p = 0.3841$, *t-value*=0.93), $0.37 \pm 0.13s$ than $0.48 \pm 0.18s$, respectively.

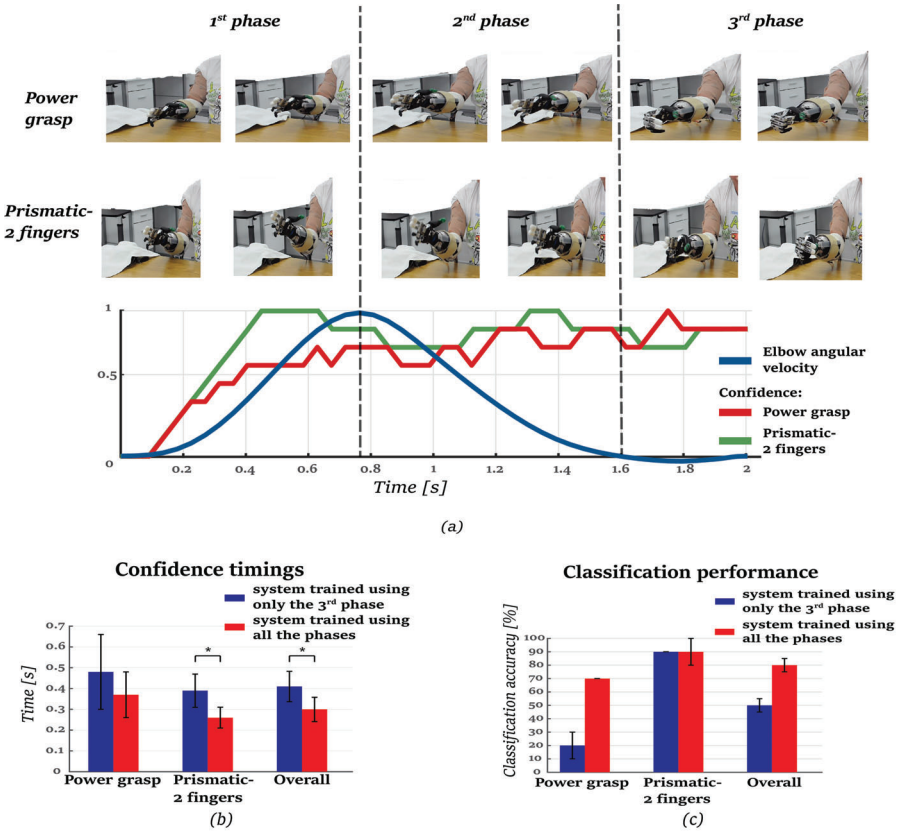

Figure 4.8: The results of the on-line evaluation. a) Screen-shots of two examples of the on-line implementation showing an activation of the prosthetic device during the second phase. The graph presents the confidence of the majority vote with the elbow's angular velocity profile. b) the average time and standard deviations until the confidence threshold was reached for the correctly classified trials. The pattern recognition system exceeds the confidence threshold of 0.5 significantly faster ($p = 0.019$) when trained including all the phases of the motion. c) the classification accuracy of the testing phase of the on-line evaluation. The pattern recognition system presents better accuracy when trained including all the phases of the motion.

4.4 Discussion

We present an approach for decoding the grasping intention during reach-to-grasp motions. Although the classification results for our proposed approach are comparable with previous studies (Daley et al. (2012); He et al. (2015); Peerdeman et al. (2011)), it is different for two main reasons. Previous studies examine the classification performance of different hand gestures, including wrist motion, hand open/close, a small number of grasp types (2-4), and in some cases the resting condition(Geng et al. (2017); Liu et al. (2014); Yang et al. (2017)). Whereas, we focus only on grasping gestures with different finger configurations. Most importantly, previous studies examined static hand-gestures, whereas we investigate the classification of EMG activity during dynamic motions. The inclusion of the reaching motion in the training procedure increases classification performance and confidence, enabling faster activation of the prosthetic device while yielding a seamless and intuitive interaction with the user.

When a hand reaches for an object, the velocity and acceleration profile of the motion are coordinated with the motion of the fingers and the wrist, and the fingers function in a synergistic manner (Wing and Turton (1986); Santello and Soechting (1998)). It is shown that the reach-to-grasp motion consists of many components (M. Jeannerod (1998); Supuk et al. (2005)). Specifically, the motion can be separated into two phases; (1) the reaching phase, when the hand approaches the object while the fingers are preshaping (Supuk et al. (2005)),and (2) grasping phase, where the hand has traveled the distance to the object and the fingers have taken their final form. This gradual molding of the fingers is revealed through different patterns of muscle activation visible during the reaching motion, which we noticed this in our analysis on able-bodied subjects. Although we cannot observe preshaping in amputees, we assume that this pattern of muscle activation would be preserved partially and that it would be revealed through different patterns of muscle contractions, as propagating in reach-to-grasp movement.

Taking inspiration from human behavior, we examine the classification performance with respect to the velocity of elbow extension. In particular, we segment the reach-to-grasp motion into three phases: (1) the first phase - where the velocity of the motion increases, (2) the second phase - where the velocity of the motion decreases, and (3) the third phase - when the reaching motion is complete. As the average activity of the EMG signals between the three phases is significantly different, training a classifier with only one phase could increase the difficulty of generalizing over the three phases. To highlight these differences, we model the first two principal components with Gaussian Mixture Models (GMMs) for each phase and show that phase models occupy different spaces and that they only partially overlap(Figure 4.4). Hence, classification during different phases of the reaching motion could reduce the variability of the EMG signals, thus increasing the classification accuracy. The lack of motion after the contraction of the muscles could lead to different EMG patterns. As shown in Figure 4.4, amputee subjects contract their forearm muscles even in the latter stages of the reaching motion, whereas the EMG of able-bodied subjects converges to lower levels in the final stages. Furthermore, in the case of able-bodied subjects, the fingers preshape during the early stages of the reaching motion (Supuk et al. (2005)) which results in earlier activation of the forearm muscles. As no preshape occurs in transradial amputees, they potentially contract the muscles but solely to close their phantom hand. This could lead to high accuracies in the predictions of the grasp types, even from the first phase with a smaller number of grasp types, as presented in Figures 4.7c and 4.8c.

Therefore, to increase the efficiency of the classification approach, it is important to look into the patterns of the muscular activation. The authors in Liu et al. (2014) point out that the muscle activation differs with respect to the arm position and that examining the EMG patterns is important. In this chapter, we elaborate on the EMG pattern during reach-to-grasp motions, both on

able-bodied subjects and individuals with amputation.

In our real-time evaluation, we intend to highlight the negative impact that the lack of good classification over the entire duration of the reaching motion could have in the natural coordination of motion of the prosthesis with the arm. More specifically, we compare the performance of a classifier when it is trained only with one phase (i.e., the third motion phase) against our approach that takes the overall motion into account. Previous approaches (Smith et al. (2016); Gonzalez-Vargas et al. (2015); Li et al. (2010)) train a pattern recognition system while maintaining the arm in a fixed position and monitoring the contraction of the muscles. This arm configuration is similar to our third phase, where the extension is complete and the arm remains in the same position. Our results show that the muscle contractions when the arm is fixed are different from the contractions when the arm extends hence the pattern recognition fails to generalize. This leads to low classification accuracy that results in a slower reaction of the prosthesis. This outcome is aligned with the findings of (Geng et al. (2017)), where a classifier that takes into account different arm positions outperformed a single-position classifier. The benefits of a dynamic training protocol are also shown in (Yang et al. (2017)). Our work is complementary to these approaches in that it focuses on the timing of classification. As in (Yang et al. (2017)), we address the problem of dynamically estimating the grasp type. To reduce the time needed for reaching a sufficient classification confidence, so as to provide faster reaction time, we focus on combining detection mechanisms.

Relating muscle activation of amputee subjects to the classification accuracy in Figure 4.4, we notice that as the activation level increases, the performance also increases. The evolution of the classification accuracy follow the same trend on all the subjects: lower classification in the first phase an higher in the second and third phase(Figure 4.7). Although it seems that forearm muscles are most important for classification performance, as they are responsible for finger motion, the muscles of the upper arm can help improve the classification performance. Our results show that, when we remove upper arm EMG data, there is a decrease in accuracy for our amputee subjects by 10% on average, see Figure 4.7e. This outcome is aligned with the findings of (Martelloni et al. (2009)), where it is shown that the activation of the proximal muscles is statistically different when the arm reaches to grasp objects with different characteristics or orientations. Although our experimental protocol constrains subjects to a single-hand orientation, the decreased accuracy when removing the upper-arm EMG indicates that the proximal muscles are important for an efficient classification accuracy during reaching.

We notice that there is an improvement on the performance of the individuals who undergo a TMR operation. More specifically, the classification accuracy on the TMR subjects becomes better than the non-TMR subject on the second motion phase, whereas it stays at the same level of performance in the third phase. These results are aligned with studies (Miller et al. (2008); Kuiken et al.

(2009)) that indicate the potential benefits of TMR on the classification accuracy. However, considering the small sample size of the group in our study, these results should be taken with a grain of salt. The improvements that TMR operations could provide on the performance of a myoelectric pattern-recognition system should be further investigated.

We compare four different classification methods, but find no significant differences in classification performance. LDA performs well: delivering similar results with SVM with either a linear or RBF kernel. The performance of the Echo State Network was on a level similar to the other classification methods. It is worth mentioning that no feature extraction is performed on the EMG before being inserted in the ESN. In this case, we let the random reservoir select the features and then train a linear regressor for classification. This indicates that a random projection of the EMG signals to a very high-dimensional space could be sufficient for achieving good classification results.

In this chapter, we present an approach to improving the reaction time of a hand prosthetic devices through a systematic assessment of the accuracy of a myoelectric pattern-recognition system over different phase periods during reach-to-grasp motions. The EMG signals are collected from seven muscles of the upper arm and five muscles of the forearm, as we focus on a potential application for individuals with transradial amputation. Our approach could be implemented for proximal amputations in cases where the user has an enhanced ability to control a myoprosthesis, e.g. after undergoing a TMR operation. TMR has been shown to increase the accuracy of a myoelectric pattern-recognition system also for the case of transhumeral amputation (Kuiken et al. (2009); Hargrove et al. (2017)). This improvement increases the number of degrees of freedom that individuals with transhumeral amputations can control. A potential extension of our approach to a proximal upper-limb amputation could be possible for individuals with TMR. This extension would, however, require further work in modeling the activation of the residual muscles of the upper arm during reach-to-grasp motions and in selecting a smaller number of grasp types, for increasing the classification confidence.

An important extension of our approach is the introduction of a robotic control scheme that derives from the natural motion of the human hand and that imparts a human-like behavior to the prosthesis. As the EMG activation is significantly different among the three phases of the motion, a combination of different classifier for each phase, or a combination of those, could improve the classification performance. This approach could also be applied in conjunction with a synergistic closure of the hand Santello and Soechting (1998), tackling the problem of the high dimensionality of the task.

4.5 Conclusion

In this chapter, we have presented an electromyography-based approach for decoding the grasping intention during reach-to-grasp motions. Four able-bodied subjects and four individuals with transradial amputation participated in our study. In order to examine the evolution of the classification accuracy over the reach-to-grasp motion, we have separated the motion into three phases: (1) the first phase- where the velocity of the motion increases, (2) the second phase- where the velocity of the motion decreases and (3) the third phase- when the reaching motion is complete. Our results have shown that it is possible to decode the grasping intention before the end of the reaching motion, especially during the second motion phase. The inclusion of the muscular activity of the upper arm to the pattern recognition algorithm increases its accuracy by 10% on average. As a proof of concept, we have evaluated our approach with an individual with a transradial amputation controlling a myo-prosthesis in real-time. The real-time evaluation shows a significant improvement in classification accuracy as well as in the reaction time of the device when all the motion phases are included in the training data. In the next chapter, we further investigate the concept of motion phases elaborating more on the distribution of the classes in each phase.

Chapter 5

Reach-to-grasp motions: Towards a Dynamic Classification Approach for Upper-Limb Prostheses

In this chapter, we take a closer look at the concept of motion phases, introduced in the previous chapter, and its potential to address the variability of the signals. In the previous chapter, we modeled the overall muscle activity of each motion phase with GMMs, as we intended to examine the differences among the phases. In an attempt to investigate the variability of the EMG signals to increase the performance of the pattern-recognition system, we focus on the differences among the classes (i.e., grasp types) and their evolution throughout the reach-to-grasp motion. Specifically, we project the EMG activity of each phase on the LDA space and model each class with Gaussian distributions. We use the Hellinger distance to quantify the similarity of distributions when projected on the overall LDA space (i.e., a common space including all the phases) and the individual space of each phase. The projection on the individual LDA space produces large values of the Hellinger distance and, hence, smaller overlaps among the classes.

5.1 Introduction

Low accuracy introduces delays in the operation of the myo-prosthesis and limits the coordination with the user's intention (Batzianoulis et al. (2018)). Therefore, in order to increase the efficiency of the system, it is crucial to address the variability of EMG signals.

Different arm positions and levels of activation are confounding factors that introduce signal variations and affect the performance of the pattern-recognition system (Lorrain et al. (2011); Liu et al. (2014)). The changes in EMG pattern characteristics during dynamic motions also lowers the accuracy of the system (Yang et al. (2017)). The introduction of dynamic, and more complicated, training protocols improves the accuracy of the system by including larger contraction intervals (Krasoulis et al. (2017)) and containing the EMG activity of the complete motion. In long intervals, however, the EMG signals become non-stationary, and this is reflected in the variation on EMG patterns.

To address the variability of the EMG signals over arm motions, the patterns over different motion phases should be further investigated, especially in individuals with amputation. The authors in Liu et al. (2014) show that the muscle

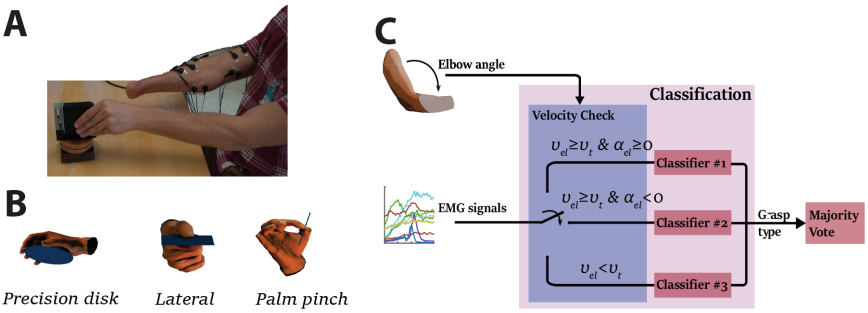

Figure 5.1: a) Experimental set-up for training the system with amputee subjects in data recordings. EMG-information from the amputated arm are recorded while the subject performs the reach and grasp motion with his/her intact arm, b) The selected three grasp types used in our classification, following the names and using figures from the taxonomy of Feix et al. (2015), c) An illustration of the classification approach with one classifier per phase. The classifier is selected with respect of the angular velocity (u_{el}) and angular acceleration (a_{el}) of the elbow joint. For each time window, the angular velocity on the elbow (u_{el}) is compared with a velocity threshold (u_t). If the angular velocity is less than the threshold, the arm has completed its extension and the classifier of the third phase is selected. Otherwise, the motion phase is defined by the angular acceleration (a_{el}). If the angular acceleration is greater than zero then the classifier of the first phase is selected. Accordingly, if the angular acceleration is less than zero then the classifier of the second phase is selected.

activation differs with respect to the arm position, and that examining the EMG patterns is important. In this chapter, we elaborate on the EMG pattern during reach-to-grasp motions in individuals with amputation.

We offer an approach to modeling the stochastic nature of the EMG pattern, and relate this to the evolution of the muscular activity during the three typical phases underlying a reach and grasp motion. Specifically, we separate the motion into three phases and model the muscular activity of each class (i.e., grasp type) with Gaussians after performing Linear Discriminant Analysis (LDA). We analyze the result of the LDA projection and relate this to the muscular activity. Moreover, we examine the classification accuracy when training three LDA classifiers: one for each phase. We compare it with the accuracy of an LDA classifier over all phases. We evaluate the approach off-line with four individuals with transradial amputations. This chapter corresponds to the following publication:

Iason Batzianoulis, I., Simon, A., Hargrove, L. and Billard. *Reach-to-grasp motions: Towards a dynamic classification approach for upper-limp prosthesis*, in Proceeding of the 9th International IEEE EMBS Conference on Neural Engineering, 2019, San Francisco, CA, USA.

5.2 Methods

5.2.1 Experimental protocol

Four individuals with below-elbow amputations participated in the experiment. All the participants gave written consent, and the experiments were performed at the Shirley Ryan Abilitylab in Chicago under a protocol approved

by the Northwestern University Institutional Review Board (IRB). Two of the amputee subjects had undergone a TMR surgery.

During the experiment, the subjects sat in front of a table, faced a computer screen, and held their elbow at a 90^o angle. The subjects would start their self-paced motion when cued by the experimenter, grasping the object with their intact hand and, simultaneously, imitating the motion with their phantom limb, see Figure 5.1a.

5.2.2 Apparatus

Custom computer software (Kuiken et al. (2009)) was used for signal acquisition, with EMG signals acquired at $1000Hz$ with a $30 - 350Hz$ band-pass filter using TI ADS1298 biosignal amplifiers. The EMG activity of *5* muscles of the residual arm was recorded: *Flexor Digitorum Superficialis (FDS), Extensor Digitorum Communis (EDC), Flexor Carpi Ulnaris (FCU), Extensor Carpi Ulnaris (ECU), Flexor Carpi Radialis (FCR).* To construct a linear envelope, full-wave rectification was performed, followed by smoothing with a low-pass seventh-order Butterworth filter with cut-off frequency at 20Hz. Finally, each channel was normalized by the maximum value recorded across the trials. A goniometer was placed on the elbows for measuring the onset and extension of the elbow.

5.2.3 Phases of the motion and classification method

Taking inspiration from the behavior reported in Rand et al. (2008), we divided the reach-to-grasp motion into three phases with respect to the extension of the elbow joint. The first phase is defined as the interval from motion onset, i.e., when the angular velocity of the elbow joint exceeds a velocity threshold, until the angular velocity of the elbow reaches its maximum. The second phase is the interval between the aforementioned maximum angular velocity and the end of the reaching motion, i.e., when the angular velocity of the elbow drops below a velocity threshold. We defined the third phase as the phase after the completion of the elbow extension. In particular, we selected 25% of the duration of the reaching motion selected after the velocity drops below a threshold. The velocity threshold was set at 10% of the maximum angular velocity recorded for each subject.

For each grasp type, 10 trials were randomly selected as the testing sets. The remaining 20 trials of each grasp type constituted the training and validation sets.

The preprocessed EMG signals were analyzed using a sliding time-window of $150ms$ with an increment of $50ms$. Three features were extracted from each time window: the average (Ave), the number of slope changes (SC) and the

waveform length (WFL). The features of each EMG channel were concatenated and introduced to an LDA classifier. Due to its performance and robustness, LDA is one of the most commonly used classification algorithms for biomedical signals. LDA finds a linearly optimal combination of the features in order to separate between classes. A fitting function estimates the parameters of a Gaussian distribution for each class and finds the probability of each point belonging to a class.

In our approach, instead of building one model for all time -windows, we train three classifiers with respect to the angular velocity of the elbow joint. Specifically, we create one model for the phase with increasing angular velocity, a second model for the phase with decreasing angular velocity and a third model for the phase when the angular velocity is below the threshold. We set this threshold as the 10% of average of the peak velocity recorded from all training trials. We assume that by building a classifier for each phase, the muscular activity of the trials of the same grasp type will be more proximal to its average, which will decrease the variability of the data and, hence, improve classification performance. Figure 5.2 presents an illustration of the approach. We compare this approach (lda_I) with the performance of one LDA classifier for all the phases (lda_A).

To further investigate the three phases, we use the squared Hellinger distance to quantify the similarity of the distributions of the classes (i.e., grasp types). The squared Hellinger distance (H^2) between two multivariate Gaussian distributions $P \sim \mathcal{N}(\mu_1, \Sigma_1)$ and $Q \sim N(\mu_2, \Sigma_2)$ is given by the formula:

$$H^2(P,Q) = 1 - \frac{det(\Sigma_1)^{1/4} det(\Sigma_2)^{1/4}}{det(\frac{\Sigma_1+\Sigma_2}{2})^{1/2}} e^d \tag{5.2.1}$$

where $d = \left\{ -\frac{1}{8}(\mu_1 - \mu_2)^T \left(\frac{\Sigma_1+\Sigma_2}{2}\right)^{-1} (\mu_1 - \mu_2) \right\}$

The Hellinger distance is a type of f-divergence metric, with 0 and 1 bringing its lower and upper bound, respectively. It reaches its maximum value (1) when the distributions do not overlap. In our case, a small Hellinger distance would indicate that the means of the distributions would be close to each other. Hence, a lager overlapping would occur between them, leading subsequently to poor classification. Whereas, large values close to 1 would indicate that the distributions are well separated from each other.

5.3 Results

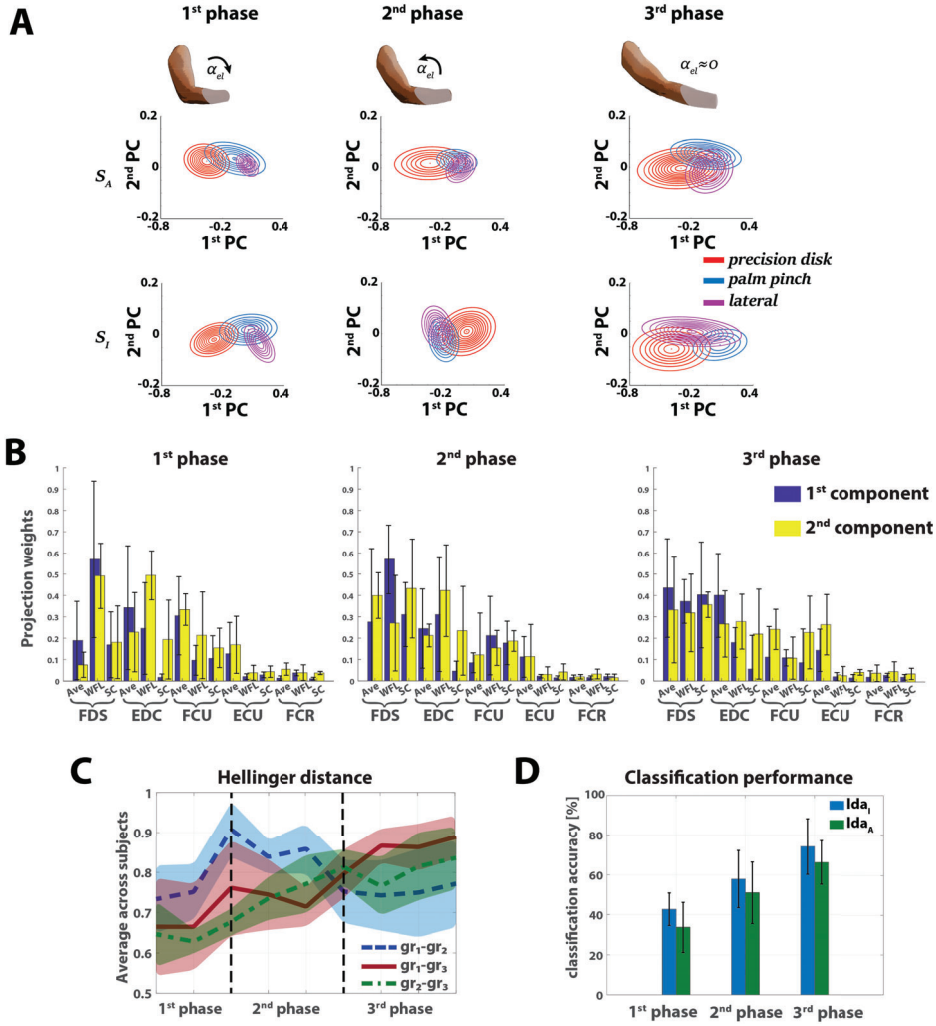

Figure 5.2: a) The Gaussian distributions of the classes (i.e. grasp types) for each phase of the subject 1. The red color corresponds to precision disk, whereas the blue and magenta color corresponds to palm pinch and lateral grasp. The three graphs on the top show the Gaussian distributions over the space of all the phases (S_A). The three graphs on the bottom present the Gaussian distributions on the space of each phase separately (S_I) b) The average across the subjects and the standard deviation of the projection weights after LDA and c) The average Hellinger distance across subjects between classes on all the phases. gr_1, gr_2 and gr_3 correspond to precision disk, palm pinch and lateral grasp respectively d)The average classification accuracy and standard deviation across subjects on the three motion phases.

5.3.1 Phases of the motion and Hellinger distance

Figure 5.2a presents the Gaussian distribution of the classes on each phase for the subject 1. The three graphs on the top the Figure 5.2a correspond to the distributions of the classes when the data are projected to the space of all phases (S_A), whereas the three graphs on the bottom correspond to the distributions with the data projected on the space of each phase separately (S_I). We observe that the overlapping among the distributions on the S_A space is larger than the S_I space for all the phases. A representative example of this is the distribution of lateral grasp in the first motion phase, which is completely overlapped by the

distribution of the palmar pinch on space S_A. However, the distribution of the lateral grasp is partially overlapped by the one of the palmar pinch on the space S_I.

The projection weights on the new hyperplane after LDA are presented in Figure 5.2b for all the motion phases. The distribution of weights is different in each phase; the wavelengths of the muscles FDS and EDC have larger values on the 1^{st} phase, whilst the weight of the average value of FDS increases significantly on the 2^{nd} and 3^{rd} phase. The distribution of weights is more balanced in the 3^{rd} phase across the muscles FDS, EDC, FCU and ECU. FCR has the smallest value among the muscles in all the phases. This could be explained by the fact that FDS and EDC are primarily responsible for the motion of three fingers; index, middle and ring fingers.

The Hellinger distance, presented in Figure 5.2c, indicates that the distributions of the classes are better separated in the late stages of the reaching motion. More specifically, H^2 increases in all the phases for the pairs precision disk-lateral grasp and lateral grasp-palm pinch. The H^2 between the class distributions of the precision disk and the lateral grasp has a large value between the 1^{st} and 2^{nd} phase, whilst it decreases in the 2^{nd} and increasing in the 3^{rd} phase.

5.3.2 Classification performance

In this subsection, instead of building one classifier for all the phases, we trained one classifier for each phase. Figure 5.2d shows the average classification accuracy and standard deviation among subject for each phase. The approach with the three classifiers (lda_I) outperforms the one classifier in all the phases(lda_A). Specifically, lda_I has an accuracy of $42.7 \pm 8.2\%$, $57.8 \pm 14.4\%$ and $74.2 \pm 14\%$ in the first, second and third phase accordingly. Whereas, lda_A presents an accuracy of $33.6 \pm 12.5\%$, $51 \pm 15.4\%$ and $66.2 \pm 11\%$ for each phase accordingly. Two-sample t-tests on the classification performances for each phase failed to reject the null hypothesis, revealing not significant improvement on the performance (the $p-values$ are $0.61, 0.87$ and 0.75 for each phase accordingly).

5.4 Discussion

Following the previous chapter and (Batzianoulis et al. (2018)), we explore the concept of motion phases on the EMG signals and its potential to address the variability of the signals. We extend our previous analysis, providing insights on the LDA projection and quantifying the similarity of the distributions of the classes (i.e., grasp types) with the Hellinger distance.

Different arm movements reflect on different patterns in muscular activity in able-bodied individuals (Liu et al. (2014)). These different EMG patterns

are produced due to gravity and inertia compensation, but also the fingers' motions during the hand preshape. Our work is complementary to previous approaches, thus focusing on the EMG patterns on individuals with below-elbow amputation, where no finger motion occurs. Moreover, we offer insights into the EMG patterns of each class (i.e., grasp type) and quantify their evolution over time.

Previous studies (Liu et al. (2014); Yang et al. (2017); Krasoulis et al. (2017); Gu et al. (2018)) have shown that the arm motion introduces variations in the EMG patterns and affects dramatically the classification accuracy. Our outcomes are aligned with these findings: The arm extension in the reach-to-grasp motion creates confounds in the EMG activity that influence the classification performance regardless of the fact that our experimental protocol involves the extension of the arm towards a specific direction.

Specifically, the different projection weights (see Figure 5.2b) reveal that the EMG activity differs in each phase. During the reaching motion (phase 1 and 2), a dynamic contraction of the muscles occurs to compensate the gravity and inertia of the arm. This factor increases the overlapping of the class-distributions (see Figure 5.2a) and results in small values of the Hellinger distance (see Figure 5.2c). In the case the user wears a prosthetic device, the gravity compensation of a larger weight could have a greater effect on the EMG patterns and result in even harder separation of the classes. As no pre-shape occurs in transradial amputees, they potentially contract the muscles but solely to close their phantom hand. This leads to the generation of more stationary EMG signals from the forearm muscles close to end of reaching motion and after it (e.g., late phase 2 and phase 3). As the muscle contractions become gradually isometric, the Hellinger distance (see Figure 5.2c) presents increased values in two of the three cases, hence the classes become more separable. An interesting extension of this work would involve the use of Hellinger distance as a component of an objective function for separating the classes among each other.

The changes on the EMG patterns over the motion phases have an effect on the classification performance. To examine the improvement of the classification accuracy, we compared the performance when an LDA classifier is trained for each phase with the performance of one LDA classifier in all the phases. The former approach with the three classifiers presents a higher accuracy for all the phases, indicating an improved encapsulation of the EMG patterns on each motion phase. Although the improvement is important, the performance is not significantly better.

A direct extension of the proposed approach would be the introduction of the kinematics of the arm, towards a multi-sensor pattern-recognition system. An on-line implementation of this work would include the angular position or velocity as a parameter of the system. This would provide information regarding the motion phase in real-time for selecting the proper classifier. The introduction of different hand orientations and an additional wrist control could be a further

expansion of the approach.

Furthermore, the introduction of different motions, besides reach-to-grasp motions, could be an interesting extension of this work. In this case, the motion phases could be employed for segmenting the overall motion, whilst a second decoder, running in the background, could identify the overall motion intention. In particular, the background decoder would predict the state of the motion, such as reach-to-grasp, reach-no-grasp, arm-flexion or arm-adduction/ abduction, and selects the corresponding classification method to use. Introducing, however, more components to the system would increase its complexity. The investigation of the trade-off between control-complexity and convenience could be an interesting topic of research.

5.5 Conclusion

In this chapter, we have presented a close investigation of the distribution of classes inside the motion phases. We have quantified the overlap among the classes with the Hellinger distance and notice larger values, hence smaller overlaps among the classes with the segmentation to motion phases. The better separation of the classes affected positively the accuracy of a LDA classifier, thus improving the accuracy by $6 - 10\%$ on average. These findings indicate that a system that switches the classifiers according to the arm kinematics could improve the performance and, hence, the efficiency of a myo-prosthesis.

In the following chapter, we summarize the main contributions of the thesis and discuss future research directions that derive from this study.

Chapter 6

Conclusion

In this chapter, we summarize our key contributions in the thesis. We discuss the limitations of the present study and potential directions for future research.

6.1 Main Contributions

To the best of our knowledge, this is the first approach to enabling real-time decoding of grasp intention during the reaching phase. It is based on a key observation from biology; the activation of the hand muscles follows specific temporal patterns with an early preshape. We have exploited machine-learning techniques to model these different stages of activation from EMG, and we have shown that this could be used at run-time to decode on-line the different grasps. Furthermore, we have shown that this decoding remains successful when used with amputees, as it can detect the preshape muscular activity from the residual muscles.

In Chapter 3, we have presented an approach for decoding the grasping intention from the muscle activity during the reaching phase. We have also compared the performance of the pattern recognition system with the hand's preshape and noticed a successful decoding before the preshape occurrence. Initially, we assumed that the muscle activity of the residual arm could be efficient for identifying the grasping intention with amputee individuals. In Chapters 4 and 5, we have focused on the evaluation of this assumption by testing four individuals with below-elbow amputations. In order to examine the evolution of the classification accuracy over the reach-to-grasp motion, we have introduced the concept of motion phases. This concept was the key to examining properly the significant differences in the muscle activity over the stages of the reach-to-grasp motion and to defining the stage where the classification accuracy is efficient for on-line decoding. Most importantly, this thesis highlights the requirement of including the complete motion for addressing the variability of the EMG signals during reaching. The real-time evaluation of this approach in Chapter 4 has shown a significant improvement in classification accuracy, as well as in the reaction time of the device.

Different arm positions affect the EMG patterns significantly (Liu et al. (2014)) resulting in a greater variability on the EMG signals. The inclusion of

different static arm postures can increase the generability of the classifier (Geng et al. (2017)), though this could still be limited over the dynamic muscle contractions that occur in reach-to-grasp motions. This thesis offers a solution to bypassing the problem of the arm-position sensitivity of the classifier, by exploiting the ability of machine-learning algorithms to embed local models for the arm motion in the reaching phase. By addressing the sensitivity of the classifier to the arm motion, we can predict correctly the grasp type before the end of the reaching motion.

Yang et al. (2017) show that using a dynamic training protocol could rather improve the performance of the pattern recognition system. We have confirmed this finding and expanded it in the decoding of the grasping intention in the reaching phase of the motion. We have focused, in contrast to other studies (Yang et al. (2017); Krasoulis et al. (2017)), on the effect of poor classification performance on the delayed prosthesis activation and its coordination with the arm motion. Furthermore, in a first attempt to include the arm kinematics in our system, we have investigated the improvement on the performance of a pattern-recognition system when a series of classifiers were employed, depending on the angular velocity of the elbow joint.

6.2 Limitations and Future Work

We have focused on the decoding of the grasping intention thus on the final configuration of the fingers. Hence, we did not consider decoding the wrist motion, a topic already well covered in the literature.

The introduction of different hand orientations, however, would increase the functionality of the system because the wrist dexterity is an important addition for prostheses Montagnani et al. (2015). Studies (Young et al. (2013); Fougner et al. (2014)) have shown that it is possible to successfully decode the wrist flexion/extension and rotation from the EMG activity. The wrist motion is generally decoded by introducing either additional classifiers Jiang et al. (2018) or classes Li et al. (2010) into the pattern recognition system. Nevertheless, the inclusion of an additional component increases the complexity of the system and could result in fatigue for the user.

As the results have shown in the Chapter 4, including the reaching motion in the training set improves the classification accuracy during the reaching motion. Additionally, the performance of the pattern-recognition system in the real-time control of a prosthesis indicates that the high accuracy produces high confidence on the detection of the grasping type and enables an early activation of the prosthesis. However, improvements on the pattern-recognition system are not always noticeable from the users when controlling a prosthesis in daily tasks. Due to the small sample size of our study, it is difficult to reach concrete conclusions towards this direction. A usability study with a larger number of participants,

controlling in real-time a prosthesis, would reveal the potential applicability of the approach to the control of a prosthesis.

In Chapters 3 and 4, we have evaluated the approaches with real-time control for a robot hand and a myo-prosthesis, respectively. To demonstrate a fast activation of the device, the pattern-recognition system commands the robot to close once the classification confidence is above a threshold. This strategy decreases the chances of grasping an object, as the device could obtain the final configuration before reaching the object. To avoid this inconsistency the device must be in perfect coordination with the motion of the arm or be aware of the location of the object. Here, we will discuss different ways to address this limitation in the following parts.

Gradual formation of the fingers during the reaching phase

Our work substantially improves the coordination of the prosthesis with the user. However, the prosthesis controller could be even more involved with the arm kinematics. An important extension would be the integration of arm motion in the system, by introducing a gradual formation of the robotic fingers while reaching.

There are a few studies that attempt to improve the coordination of upper-limb prosthesis with the motion of the body. In Legrand et al. (2018) and Merad et al. (2018), the authors model the inter-joint coordination of the arm to control the phantom joints in order to relax the device's dependency on the muscular activity and offer a more intuitive control. Specifically, they model the coupling between the shoulder and elbow joints of able-bodied individuals and use the information from the shoulder motion of an individual with transhumeral amputation as input to control the elbow joint of a prosthesis. These approaches are limited to the control of the elbow joint and omit any relation between the arm motion (i.e., flexion/extension) and the hand closure. Nevertheless, they indicate that the employment of the inter-joint kinematic relations could enhance the functionality of a prosthesis and inspire alternative control methods.

The authors in Markovic et al. (2015) and Ghazaei et al. (2017) use computer vision techniques in order to provide a form of hand preshape that occurs during reaching with respect to the object characteristics. They propose finite-state machine approaches to triggering the activation of the vision system by the muscular activity. Also, they produce a hand preshape that depends on the object classification and close the hand with another trigger that comes from the muscular activity. Although these approaches introduce a hand preshape to the prosthesis, the closure of the hand has a very limited coordination with the extension of the arm. The aforementioned approaches do not encapsulate the natural coupling and the dynamic relation between the hand and the arm.

Dynamical systems (DS) have been successful in modeling human motions (Bullock and Grossberg (1988); Diedrichsen and Dowling (2009)) and generating them in robot motion (Schaal et al. (2000); Gribovskaya et al. (2010); Shukla

and Billard (2012)). A key feature of the dynamic system is that it generates the next state with respect to the current state. The dynamic model encapsulates the motion primitives of the given demonstrations and is able to reproduce the dynamic of the task; such a task could be a reach-to-grasp motion. The dynamic behavior of this task could be analyzed into two motions: the extension of the arm and the open/closure of the hand. As these motions occur in coordination, the underlying coupling could be also learned by a coupled dynamical-system approach. In this scenario, the master dynamical system would derive from the arm motion, and the slave dynamical system would derive from the motion of the fingers. As the master DS generates the next state of the robot (e.g., the next position of the end effector), the next state of the fingers would be generated from the slave DS through the learned coupling function. In this way, the motion of the fingers would be in coordination with the arm motion as the hand approaches an object, thus offering a gradual convergence to the targeted fingers' configuration.

As we focus on the case of hand prostheses for transradial amputation, the kinematics of the residual arm could correspond to the master system. In this case, the next fingers' positions will be generated in coordination with the position of the arm through the coupling function. This approach could also offer a solution for the case of transhumeral prostheses, enabling a coordination between the elbow joint and the hand closure.

Integration with computer vision and other sensory inputs

When humans engage in object manipulation tasks, eye movements are also related with the motion of the hand (Biguer et al. (1982)). The gaze fixates on the object of interest, and this fixation generally precedes the reaching motion. This principle has inspired various methods in robot control for grasping strategies (Levine et al. (2018)) and obstacle avoidance (Lukic et al. (2012)). In the case of neuroprosthetic control, the gaze of the user can be used to identify the object of interest before the onset of the reaching motion. Furthermore, the use of stereovision could enable the localization of the object and the extraction of object's characteristics (such as the size of the object) to direct the hand prosthesis to close accordingly (Markovic et al. (2014)). Stereovision, as well, can potentially enable an estimation of the distance from the object. In this case, the hand prosthesis could perform a gradual closing with respect to the distance from the object.

It is clear that the coupling between the motion of the residual arm and the prosthetic hand is crucial for a seamless coordination and intuitive control. As already discussed in the previous subsection, the principal input of this coupling should derive from the kinematics of the residual arm. The introduction of sensory inputs, such as goniometers or Inertia Measurement Units (IMUs), could enable the on-line tracking of the arm kinematic. Studies have integrated IMUs with EMG to control hand and wrist motions, either by introducing the signals

either to individual classifiers (Bennett and Goldfarb (2018)) or combining them as input to the same classifier (Kyranou et al. (2016)). In our case, the input from the IMU could be used to control the closure of the hand prosthesis.

Tactile sensing and feedback to the user

When manipulating an object, the tactile sensing plays an important role in achieving secure grasps. It is shown that the mechano-receptors on the non-hairy part of the human hand is the most important information for grasping, whereas proprioception and vision provide less essential information (Johansson and Flanagan (2009)). Despite the importance of the tactile sensing, the benefits of it are demonstrated only in experimental prostheses (Osborn et al. (2016); Imbinto et al. (2018)). In contrast, tactile sensing becomes a key component in robotic grasping (Sun et al. (2016); Li et al. (2016)). The integration of tactile sensing with the grasping intention from the EMG signals could be combined in a shared-control framework. In this framework, the high-level information of grasping intention is derived from the user whilst the grasping stability is secured from the robot controller with the employment of tactile sensing.

Furthermore, tactile sensing could provide valuable feedback to the user thus restoring partially this ability (Valle et al. (2018); Raspopovic et al. (2014)). This feedback could also involve a sensing of slippage or even a measure of grasp stability encoded in the returned signal. The recent developments in the restoration of tactile sensing are very promising and could become a key component of hand prostheses in the future.

Automated feature extraction

Furthermore, this thesis has presented one of the first attempts to automated feature extraction from the EMG signals. In contrast to traditional approaches, where the researcher selects *a priori* the extracted features, we took advantage of the echo property of ESN for extracting the relative information from the signals. The classification accuracies, produced by ESN, have been comparable with the ones produced by other classification methods with *a priori* feature extraction. Therefore, this type of automated feature extraction could act as an alternative to traditional feature extraction. This outcome also indicates a potential next step of this work. One possible direction is the systematic comparison of the classification performance between ESN, without any *a priori* feature extraction, and methods that use a diverse selection of features; In our work, we focused on three time-domain features due to their advantages in low computational time. However, the enrichment of the approach with other type of features, such as frequency-domain and auto-regressive features, might have resulted in a better classification accuracy. Hence, this comparison would reveal the strengths and weaknesses of the method and its potential.

Another possible direction is the employment of other types of neural net-

works, such as RNN and CNN, for automated feature extraction. Specifically, RNN have shown promising performance on time-series classification on sequences of images and speech (Keren and Schuller (2016)). Recently, Côté-Allard et al. (2019) trained a CNN for decoding hand-gestures with EMG datasets that are available online and noticed a better classification accuracy than LDA. This outcome is another indication that alternative methods for feature extraction could be equally or even more powerful than traditional selection of features.

6.3 Concluding Summary

This thesis offers an alternative method of the pattern-recognition system for controlling hand myo-prosthesis. We focused on decoding the grasping intention, from the EMG activity, during the reach-to-grasp motion. Our results showed that it is possible to decode accurately the grasping intention for 5 grasp types, from able-bodied individuals, during the hand's pre-shaping phase. The early and accurate prediction of the grasp type enabled us to activate the motion of a robotic hand in the early stages of the reaching motion.

In our evaluation with four individuals with below-elbow amputation, we separated the overall motion into three phases. When the number of grasp types was reduced to three, we noticed that the residual EMG activity is efficient for producing high classification accuracy in the second motion phase. Furthermore, we tested our approach in real-time control of a prosthesis. The high accuracy of our method resulted in high confidence in the pattern-recognition system during the reaching motion and enabled the activation of the prosthesis before the end of the reaching motion, hence improving the coordination with the motion of the arm.

Furthermore, we noticed that the overlap among the distributions of the classes becomes smaller when we performed LDA on each motion phase individually than on the overall motion. Therefore, training a LDA classifier for each motion phase resulted in an improved classification accuracy.

This thesis contributes to the enhancement of the coordination between the user's intention and the hand prosthesis by improving the performance of the pattern-recognition system. The EMG patterns, developed during the reaching motion, are examined for the first time, together with their effect on the classification performance. Additionally, we have introduced the concept of motion-phases on the EMG activity and explored its benefits on the control of a prosthesis. We have demonstrated that the high accuracy of our method enables a fast reaction of the prosthesis and provides an improved coordination with the motion of the user's residual arm.

Appendices

Appendix A

Supplementary Materials for Chapter 4

In this section, we present additional results regarding the muscular activity of the motion phases. Figure A.1 shows the location of the electrodes and muscles set which is selected in Chapter 4.

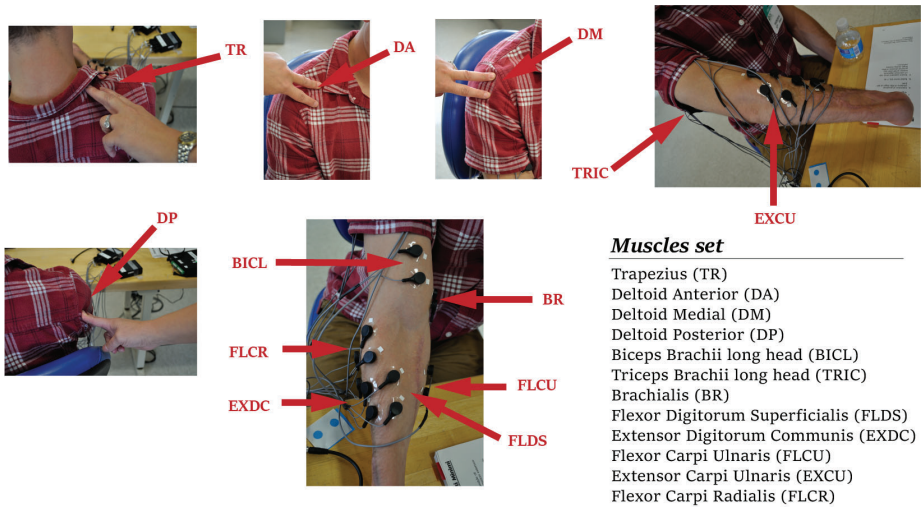

Figure A.1: The location of the electrodes and the muscles set of this study.

Figures (A.2) and (A.3) presents the average EMG activity the muscles of each group in normalized time. The green vertical like shows the moment that the angular velocity of elbow joint reached its maximum, while the shaded area around it corresponds to its standard deviation of the moment the maximum velocity occurred. The activation of the more distal muscles in able-bodied subjects occurs in an earlier phase than in amputees. The muscular activity of the forearm muscles of ABD 2, 3 and 4 is reaching its peak from $20-60\%$ of the motion, while only the forearm muscles of ABD5 and TR4 are activating in the early stages of the reaching motion. Moreover, the EMG activity of the forearm muscles is decreasing as the motion is getting closer to completion on the able-bodied subjects. On the other hand, the EMG activity of forearm muscles of the amputee subjects increases, either gradually during the reaching motion (TR1,TR3, TR4-chapter 4) or more rapidly in the end of the motion (TR2). The different timing of activation could have an impact to the classification performance as we see later in the document. The more proximal muscles stay in

the same level of activation after the maximum angular velocity is reached.

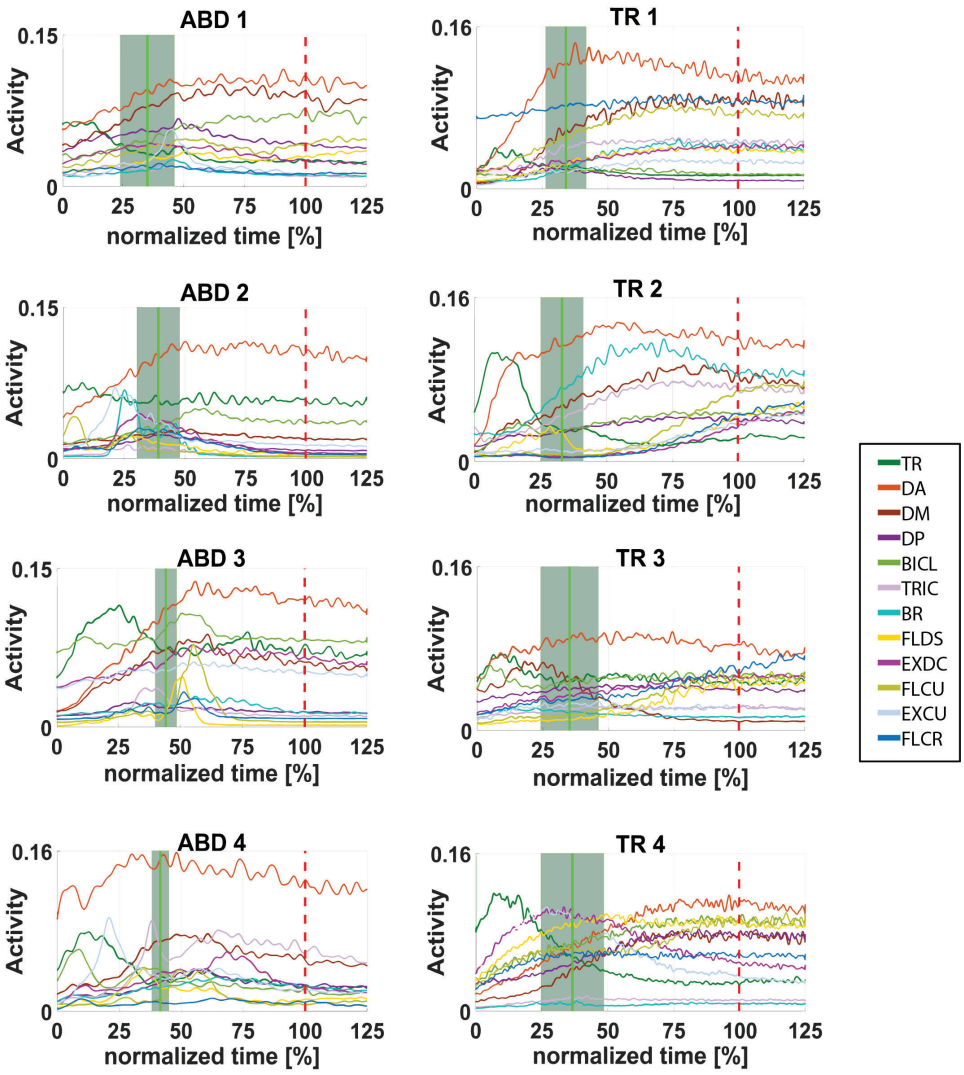

Figure A.2: The linear envelope of the EMG signals of the able-bodied subjects (left) and amputee subjects (right).

Figures A.4, A.5 and A.6 present the Gaussian models of the phases on the first two principal components for the complete muscle-set and the muscles of the forearm respectively for able-bodied (Figures A.4 and A.5) and amputee subjects (Figure A.6). Although some models are partially overlapping, the means of the models are different with each other in all the subjects, regardless the muscle-set. In able-bodied subjects (Figure A.4 and A.5), the models of the third phase are concentrated on the area around the origin and their corresponding standard deviations are smaller than the standard deviation of the models of the other two phases. The larger overlapping was noticed on the models of first and third phases for the complete muscle-set of the subjects ABD1 and ABD2 and between all the models of the forearm muscles of ABD3. While

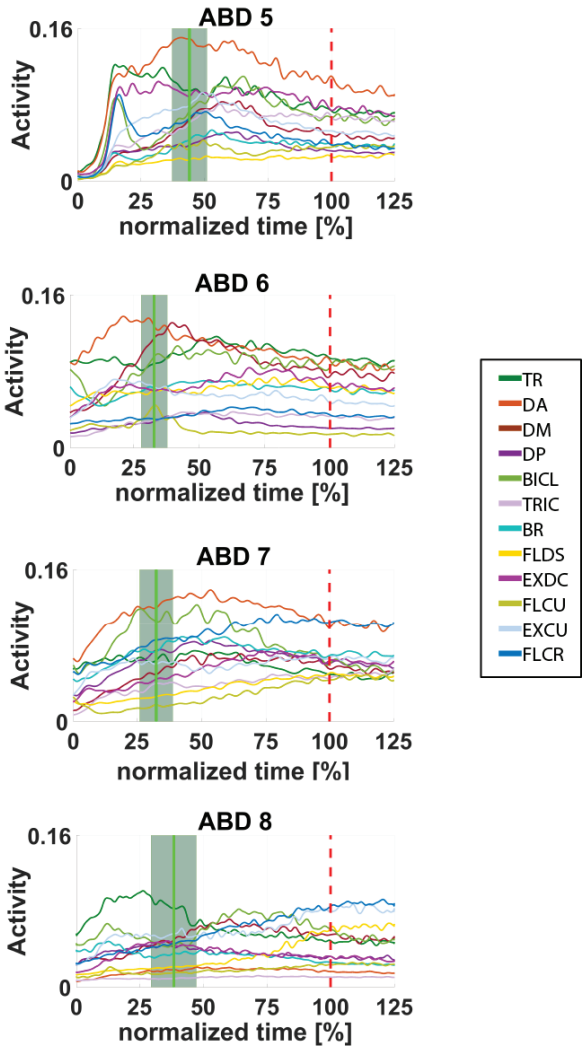

Figure A.3: The linear envelope of the EMG signals of able-bodied subjects 5-8.

the models of the third phase are concentrated around the origin, similarly to the able-bodied subjects, they cover a larger area than the corresponding models of the able-bodied subjects. A larger overlapping area is noticed between the models of the first and second phase for all the amputee subjects, while the models of the third phase are more distant form the other two.

Similar results are noticed regarding the phases of the motion for the amputee subjects (Figure A.6). More particularly, the models of the second and third phase are partially overlapping for TR2 and TR3. The models of the third phase of the forearm muscles of TR2 and TR3 occupy a larger area than the other two, while the models occupy approximately equal space when the complete muscle-set in taken into account. Regarding the subject TR1, the models of the second and third phase are overlapping more extensively than the other subjects.

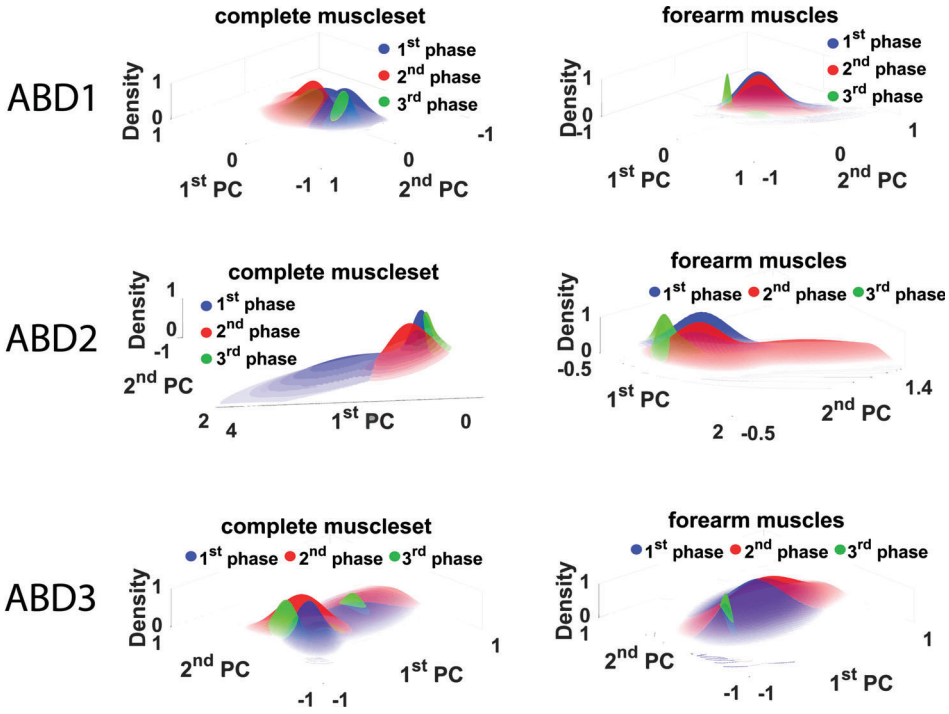

Figure A.4: A representation with Gaussian Mixture Models (GMMs) of the EMG activity of the three phases projected on the first two components of third phase after performed Principal Component Analysis (PCA). The analysis was performed on the complete muscle set (N = 12) and when using only the muscles of the forearm (N = 5). The blue color corresponds to the first phase, the red color to the second phase and the green color to the third phase. The results presented in this figure regard the EMG activity of able-bodied subjects 1-3.

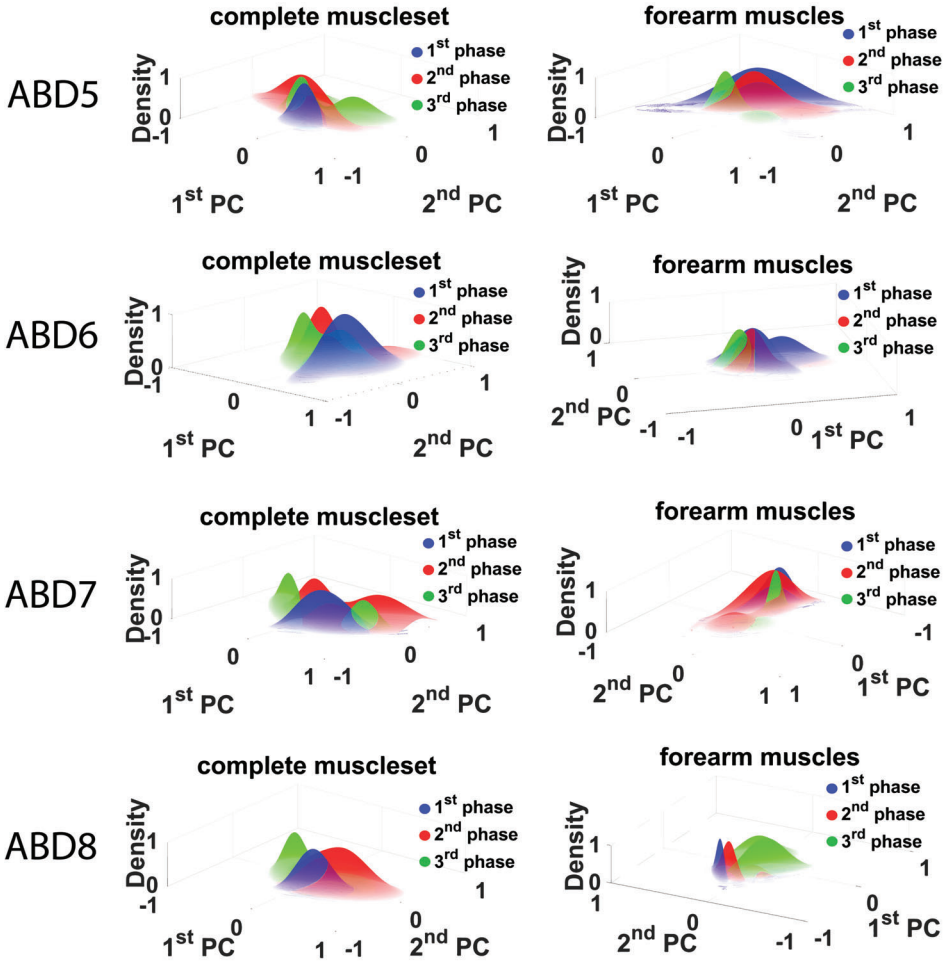

Figure A.5: A representation with Gaussian Mixture Models (GMMs) of the EMG activity of the three phases projected on the first two components of third phase after performed Principal Component Analysis (PCA). The analysis was performed on the complete muscle set (N = 12) and when using only the muscles of the forearm (N = 5). The blue color corresponds to the first phase, the red color to the second phase and the green color to the third phase. The results presented in this figure regard the EMG activity of able-bodied subjects 5-8.

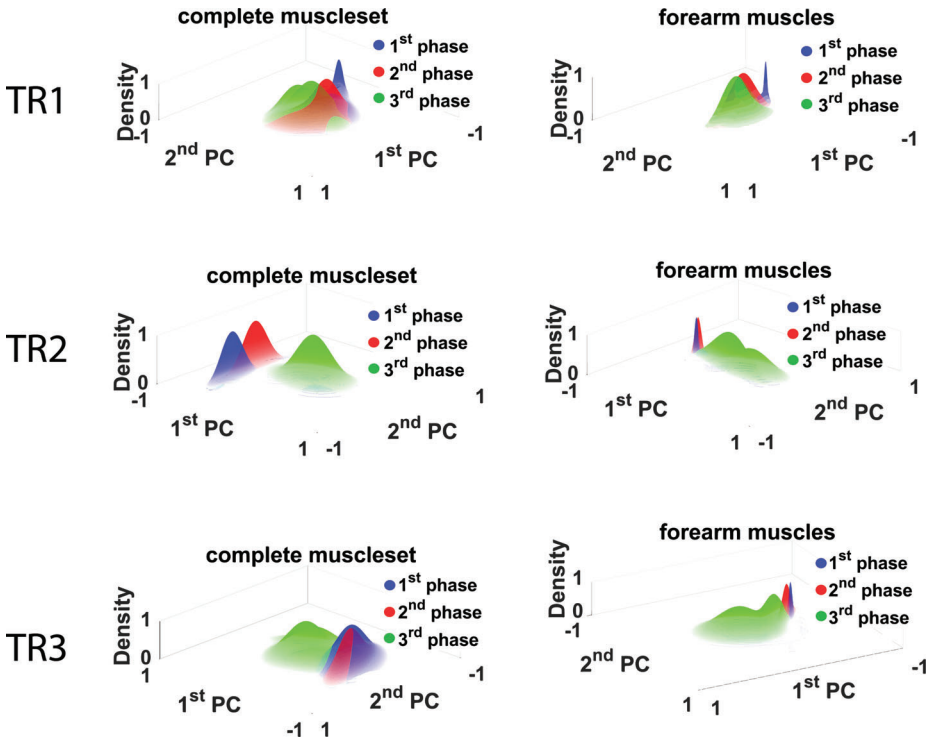

Figure A.6: A representation with Gaussian Mixture Models (GMMs) of the EMG activity of the three phases projected on the first two components of third phase after performed Principal Component Analysis (PCA). The analysis was performed on the complete muscle set (N = 12) and when using only the muscles of the forearm (N = 5). The blue color corresponds to the first phase, the red color to the second phase and the green color to the third phase. The results presented in this figure regard the EMG activity of amputee subjects.

Appendix B

Student Projects Supervised by the Author

In this appendix, we provide a list of the projects supervised by the author.

Semester Project[1], Fall 2016

Student: Paul Rolland

Title: Motion onset detection of the arm from EMG signals using Machine Learning methods

Description

As we have discussed in this thesis, it is crucial for the the prosthesis to follow the user's intention seamlessly. Besides expressing the grasping intention, the device should also be able to identify the moments to stay idle without performing any type of motion. This project provided a solution to the identification of the idle state for the device by predicting the onset as well as the end of the motion from the EMG signals. The accurate estimation of the motion onset could avoid any untimely activation of the device whilst the estimation of the end of the motion would signal the device keep the same configuration constant.

In this project, a method based on SVM was developed as decoding method. Specifically, the EMG signals were pre-processed and divided into time windows. A PCA was performed on the resulted signals before introducing them to the SVM classifier. Two different classifiers were trained in this project; one for the prediction of the motion onset and one for the prediction of the end of the motion. The results showed high accuracy on the prediction of the motion onset, while the estimation of the end of the motion had significantly lower performance.

Semester Project[2], Fall 2017

Student: Teo Gaudin

Title: Analysis of error-related potential elicited by the motion of a robotic arm

Description:

[1] This project was co-supervised by Denys Lamotte

When humans work together with robots, the interaction between them should involve a smooth coordination. The robot should be able to understand the intention of the user in order to follow smoothly her/his motion. This principle is applied not only to the case of prosthesis but also in any type of human-robot interaction (HRI). Examples of this interaction can be found in industrial sites, where humans and a robots work together for moving and assembling various objects. In addition, a key component of robotic rehabilitation systems is the seamless interaction with the user, especially when the user has limited motor functionality. In this case the robotic system should be able to identify the user's intention from biomedical signals, such as Encephalography (EEG). A very useful type of brain signal in this case is the Error Potential.

The Error Ponential is occured in the middle-central region of the brain and is associated with erroneous observations during an execution of a task. This type of signals could be employed to identify mistakes and errors in the robot motion. This project investigated this control principle. It involved a design of experimental protocol in which the user was observing various erroneous robot motions while its brain activity was monitored. Specifically, the end-effector of a robot arm was oscillating between two points while a randomly introduced noise was diverging the end-effector from its normal route. The results showed an elicitation of Error Potential brain signals when the end-effector was diverging its route approximately $0.5s$ after the onset of the divergence. This was an indication that those type of signals could be used as a control input for correcting the motion of the robot according to the user's preference.

Semester Project, Spring 2018

Student: Antoine Weber

Title: A fast decode of grasping intention from the muscular activity

Description:

Following the contributions of this thesis, this semester project focused on the identification of the grasp type from the muscle activity when the object was placed on different locations but also on the identification of reach-no-grasp motion. The experimental protocol involved two grasp types; power grasp and thumb-2-fingers and a reach but no grasp motion, where the user performed a reaching motion (i.e. arm extension) without grasping the object. In addition, a systematic comparison was conducted on the performance of four classification methods; ESN, LDA, SVM with RBF kernel and GMM. All the classification methods showed high accuracy in the estimation of the grasp type and the no-grasp condition. However, ESN classifier appeared the best performance while the LDA classifier appeared the poorest performance among all the methods.

[2]This project was co-supervised by Dr. Iñaki Iturrate

Furthermore, the reach-to-grasp motion was separated into three phases, as in Chapter 4, and one classifier was trained for each phase, as in Chapter 5. A comparison between the performance of this approach with the one of a classifier trained on all the phases accumulated showed higher accuracy in the earlier stages. Specifically, the results showed an accurate prediction after $0.6s$ from the motion onset regardless the location of the object and the grasping/no-grasping condition. This project indicated that this approach could be extended to other hand postures which are irrelevant to grasp types.

Semester Project, Spring 2018

Student: Sinan Gokce

Title: Activating grasp with a prior from the muscular activity

Description

Besides the accurate identification of the grasping intention, a prosthetic device should be able to grasp an object securely. A secure grasp involves the application of the proper force from the fingers to the object for primary compensating for its weight, but also adapt to various perturbations. However, applying "blindly" the maximum possible force could result in damaging or even breaking the object. To avoid these events, the prosthetic hand should close compliantly around the object while gradually making contact with it. In this scenario, the integration of the prosthesis with tactile sensors offers a solution on the identification of the contact points.

This project developed a control method for compliant closure of a robot hand for three grasp types; power grasp, thumb-2-fingers and lateral grasp. Specifically, the robot hand was covered with tactile sensors for detecting the pressure on each of its phalanges while a proportional controller was used to drive the fingers to each desired configuration. Once a contact was detected on a phalanx, the corresponding finger joint stopped its motion. Furthermore, the project proposed an approach for collision avoidance among the fingers when transitioning from one grasp type to another. This method introduced a small re-opening stage in the transition for avoiding singular positions and collision between the fingers.

Semester Project[3], Fall 2018

Student: Manu Srinath Halvagal

Title: A Study of User Response to Errors in Robot Motion

Description:

Robotic assistive devices for the patients with motor disabilities require a smooth interaction with the user. Generally, the system makes use of the biomedical signals of the user to identify her/his intention and translates it to motion

commands for the robot. In cases where the EMG activity is very limited, the system employs machines learning methods to decode the relevant information from the brain activity. One way for the system to learn the desired robot motion is by using the Error Related Potentials (ErrP) of the brain. In this scenario, the robot corrects its motion according to the existence or absence of ErrPs following a learning-from-error approach. Thus, the machine learning system should be able to learn the boundaries between the desired and rejected motions in real-time. This project attempted to develop a learning scheme for successfully training a classifier to recognize the desired robot motion on-line based on the user's input.

Specifically, the experimental protocol involve a robot arm performing an obstacle avoidance motion following different trajectories. In addition, a user was set to decide to keep or reject the robot trajectory. Approaches based on SVMs and logistic regression were evaluated on a simulated on-line learning. The results showed that the classifiers converge after approximately 10 trials to the desired robot motion. After the number of trials was reached, the user was not required to correct the robot motion.

Semester Project, Fall 2018
Student: Valentin Morel
Title: Object localization using gaze tracking
Description:

The gaze could be used as an intuitive control input for robotic assistive systems. For example, in users with limited motor functionalities for the upper limb, the gaze could be used to identify the object of interest so that a robot could bring the object to the user. In those scenarios, the gaze can be an important component of the system providing useful information for the coordination with the user.

The goal of this project was to develop a system that detects the object of interest based on the gaze and send the coordinates of this object to a robot. The robot, then, could use this information to generate trajectories for reaching and grasping the object. Specifically, the user was wearing a headset to track the pupils to interpolate the gaze focal point of the candidate. Computer vision methods were used to process the acquired images and Support Vector Regression was used to calibrate the motion of pupils with the focal point. In addition, a systematic evaluation was conducted to identify the limitations of the system.

Master Thesis[4], Fall 2018

[3]This project was co-supervised by Prof. Aude Billard

Student: Shupeng Wei

Title: Learning Robot Optimal Trajectories Online Using Inverse Reinforcement Learning

Description:

There is a growing interest on robotic assistive devices for people with motor disabilities. In the cases where the patient has limited functionality of the upper limb, a robotic device could assist the patient on daily pick-and-place tasks. Since the patient would depend mostly on the robotic system to execute those task, the robotic system should adapt to the preferences of the user. Let's examine a case where a patient with limited functionality in upper and lower extremity uses a wheelchair with a robot arm mounted on it. The user communicates with the robot arm through an interface and commands the robot to reach and grasp an object. However, there is an obstacle between the robot arm's initial position and the position of the obstacle. In this case, the robotic system should generate a trajectory for the end effector of the robot to by-pass the obstacle. A trajectory that passes very close to the obstacle could create a great uncertainty on the side to the user, while a trajectory passing very far from the obstacle could drive the end effector outside its workspace or hit an object undetected from the robotic system. Both these scenarios constitute an undesired robot operation from the user's perspective. The use of learning by demonstration methods and kinesthetic teaching could be very constraint in this case due to the limited motor functonality of the patient. Thus, the desired trajectories should be learned using alternative methods of training.

This project addresses the problem of learning the desired trajectories using Inverse Reinforcement Learning (IRL) techniques. Specifically, the project involves a user directing a robot arm to perform an obstacle avoidance task while the trajectories are generated from a modulated dynamical system. However, this modulation may not be the desired according to the user. In this case, the user could correct the robot motion from a joystic and decide in the end of the motion to accept or not the resulted trajectory as demonstration. Using the selected demonstrations, a reward function is been built using the principle of Maximum Entropy. After the computation of the desired trajectory, the modulation of the dynamical system is found using the Gradient Descent. The results show that only a small number of demonstrations are required for the system to be trained and, thus, require no correction from the user.

[4]This project was co-supervised by Prof. Aude Billard

References

V. Agostini and M. Knaflitz. An algorithm for the estimation of the signal-to-noise ratio in surface myoelectric signals generated during cyclic movements. *IEEE Transactions on Biomedical Engineering*, 59(1):219–225, 2012.

Sebastian Amsuess, Peter M Goebel, Ning Jiang, Bernhard Graimann, Liliana Paredes, and Dario Farina. Self-correcting pattern recognition system of surface emg signals for upper limb prosthesis control. *IEEE Transactions of Biomedical Engineering*, 61(4), 2014.

Sebastian Amsuess, Ivan Vujaklija, Peter Goebel, Aidan D Roche, Bernhard Graimann, Oskar C Aszmann, and Farina Dario. Context-dependent upper limb prosthesis control for natural and robust use. *IEEE Transactions of Neural Systems and Rehabilitation Engineering*, 2016.

Iason Batzianoulis, Sahar El-khoury, Silvestro Micera, and Aude Billard. Emg-based analysis of the upper limb motion. In *10th ACM/IEEE International Conference on Human-Robot Interaction (HRI)*, 2015.

Iason Batzianoulis, Sahar El-Khoury, Elvira Pirondini, Martina Coscia, Silvestro Micera, and Aude Billard. Emg-based decoding of grasp gestures in reaching-to-grasping motions. *Robotics and Autonomous Systems*, 2017.

Iason Batzianoulis, Nili Krausz, Ann Simon, Levi Hargrove, and Aude Billard. Decoding the grasping intention from electromyography during reaching motions. *Journal of NeuroEngineering and Rehabilitation*, 2018.

Iason Batzianoulis, Ann Simon, Levi Hargrove, and Aude Billard. Reach-to-grasp motions: Towards a dynamic classification approach for upper-limp prosthesis. In *9th International IEEE EMBS Conference on Neural Engineering*, 2019.

Daniel A Bennett and Michael Goldfarb. Imu-based wrist rotation control of a transradial myoelectric prosthesis. *IEEE Transactions on Neural Systems and Rehabilitation Engineering*, 26(2), 2018.

Elaine Biddis. *Need-Directed Design of Prostheses and Enabling Resources in Amputation, Prosthesis Use, and Phantom Limb Pain: An Interdisciplinary Perspective*. Springer, 2010.

B Biguer, M Jeannerod, and C Prablanc. The coordination of eye, head, and

arm movements during reaching at a single visual target. *Experimental Brain Research*, 46(2), 1982.

Raoul M Bongersa, Frank T J M Zaala, and Marc Jeannerod. Hand aperture patterns in prehension. *Human Movement Science*, 31, 2012.

Reza Boostani and Mohammad Moradi. Evaluation of the forearm emg signal features for the control of a prosthetic hand. *Physiological measurement*, 24: 309–19, 06 2003.

D Bullock and S Grossberg. Neural dynamics of planned arm movements: Emergent invariants and speed-accuracy properties during trajectory formation. *Psychological Review*, 95(1):49–90, 1988.

I M Bullock, J Z Zheng, S De La Rosa, C Guertler, and A M Dollar. Grasp frequency and usage in daily household and machine shop tasks. *IEEE Transactions on Haptics*, 2013.

J Carpaneto, K H Somerlik, T B Krueger, T Stieglitz, and S Micera. Natural muscular recruitment during reaching tasks to control hand prostheses. In *IEEE RAS & EMBS International Conference on Biomedical Robotics and Biomechatronics*, 2012.

Erina Cho, Richard Chen, Lukas-Karim Merhi, Zhen Xiao, Brittany Pousett, and Carlo Menon. Force myography to control robotic upper extremity prostheses: A feasibility study. *Frontiers in Bioengineering and Biotechnology*, 2016.

C. Cipriani, C. Antfolk, M. Controzzi, G. Lundborg, B. Rosén, M. C. Carrozza, and F. Sebelius. Online myoelectric control of a dexterous hand prosthesis by transradial amputees. *IEEE Transactions on Neural System and Rehabilitation Engineering*, 2011.

M. Cognolato, M. Atzori, D. Faccio, C. Tiengo, F. Bassette, R. Gassert, and H. Muller. Hand gesture classification in transradial amputees using the myo armband classifier* this work was partially supported by the swiss national science foundation sinergia project 410160837 meganepro. In *2018 7th IEEE International Conference on Biomedical Robotics and Biomechatronics (Biorob)*, pages 156–161, 2018.

U. Côté-Allard, C. L. Fall, A. Drouin, A. Campeau-Lecours, C. Gosselin, K. Glette, F. Laviolette, and B. Gosselin. Deep learning for electromyographic hand gesture signal classification using transfer learning. *IEEE Transactions on Neural Systems and Rehabilitation Engineering*, pages 1–1, 2019.

Heather Daley, Kevin Englehart, Levi Hargrove, and Usha Kuruganti. High density electromyography data of normally limbed and transradial amputee subjects for multifunction prosthetic control. *Journal of Electromyography and Kinesiology*, 22(3), 2012.

S.A. Dalley, H.A. Varol, and M. Goldfarb. A method for the control of multi-

grasp myoelectric prosthetic hands. *IEEE Transactions on Neural Systems and Rehabilitation Engineering*, 2012.

El-Khoury S de Souza, R L and, J Santos-Victor, and Aude Billard. Towards comprehensive capture of human grasping and manipulation skills. In *Thirteenth International Symposium on the 3-D Analysis of Human Movement*, 2014.

Gurpreet S Dhillon, Stephen M Lawrence, Douglas T Hutchinson, and Kenneth W Horch. Residual function in peripheral nerve stumps of amputees: implications for neural control of artificial limbs. *The Journal of Hand Surgery*, 2004.

J Diedrichsen and N Dowling. Bimanual coordination as task-dependent linear control policies. *Human Movement Science*, 28(3), 2009.

Edoardo D'Anna, Francesco Maria Petrini, Fiorenzo Artoni, Igor Popovic, Igor Simanić, Stanisa Raspopovic, and Silvestro Micera. A somatotopic bidirectional hand prosthesis with transcutaneous electrical nerve stimulation based sensory feedback. *Scientific Reports*, 2017.

Eric J Earley, Levi J Hargrove, and Todd A Kuiken. Dual window pattern recognition classifier for improved partial-hand prosthesis control. *Frontiers in Neuroscience*, 2016.

Sahar El-khoury, Iason Batzianoulis, Chris Wilson Antuvan, Sara Contu, Lorentzo Masia, Silvestro Micera, and Aude Billard. Emg-based learning approach for estimating wrist motion. In *37th International Conference of the IEEE Engineering in Medicine and Biology Society (EMBC)*, 2015.

Kevin Englehart and Bernard Hudgins. A robust, real-time control scheme for multifunction myoelectric control. *IEEE Transactions of Biomedical Engineering*, 50(7), 2003.

D. Farina, N. Jiang, H. Rehbaum, A. Holobar, B. Graimann, H. Dietl, and O. C. Aszmann. The extraction of neural information from the surface emg for the control of upper-limb prostheses: Emerging avenues and challenges. *IEEE Transactions on Neural Systems and Rehabilitation Engineering*, 22(4): 797–809, 2014.

Todd R Farrell and Richard F Weir. The optimal controller delay for myoelectric prostheses. *IEEE Transactions on Neural Systems and Rehabilitation Engineering*, 2007.

T. Feix, H.-B. Schmiedmayer J. Romero, A. M. Dollar, and D. Kragic. The grasp taxonomy of human grasp types. *IEEE Transactions on Human-Machine Systems*, 46(1), 2015.

N Fligge, H Urbanek, and P van der Smagt. Relation between object properties and emg during reaching to grasp. *Journal of Electromyogry Kinesiology*, 2000.

Anders L Fougner, Oynvid Stavdahl, and Peter J Kyberd. System training and assessment in simultaneous proportional myoelectric prosthesis control. *Journal of Neuroengineering and Rehabilitation*, 11(75), 2014.

Alan E Freeland and Rick Psonak. Traumatic below-elbow amputations. *Orthopedics*, 2007.

O Fukuda, T Tsuji, M Kaneko, and A Otsuka. A human-assisting manipulator teleoperated by emg signals and arm motions. *IEEE Transactions on Robotics and Automation*, 2003.

Y Geng, O W Samuel, Y Wei, and G Li. Improving the robustness of real-time myoelectric pattern recognition against arm position changes in transradial amputees. *BioMed Research International*, 2017.

M Gentilucci, F Benuzzi, L Bertolani, E Daprati, and M Gangitano. Language and motor control. *Experimental Brain Research*, 133, 2000.

Ghazal Ghazaei, Ali Alameer, Patrick Degenaar, Graham Morgan, and Kianoush Nazarpour. Deep learning-based artificial vision for grasp classification in myoelectric hands. *Journal of Neural Engineering*, 14(3):036025, 2017.

D S Gonzales and C Castellini. A realistic implementation of ultrasound imaging as a human-machine interface for upper limb amputees. *Frontiers in Neurorobotics*, 2013.

Jose Gonzalez-Vargas, Strahinja Dosen, Sebastian Amsuess, Wenwei Yu, and Dario Farina. Human-machine interface for the control of multi-function systems based on electrocutaneous menu: Application to multi-grasp prosthetic hands. *PlosOne*, 2015.

J González, Y Horiuchi, and W Yu. Classification of upper limb motions from around-shoulder muscle activities: Hand biofeedback. *Open Medical Informatics Journal*, 2010.

D. Graupe and W. K. Cline. Functional separation of emg signals via arma identification methods for prosthesis control purposes. *IEEE Transactions on Systems, Man, and Cybernetics*, 5(2):252–259, 1975.

E Gribovskaya, S M Khasnari-Zadeh, and A Billard. Learning nonlinear multivariate dynamics of motion in robotic manipulators. *International Journal of Robotics Research*, 30(1), 2010.

Y Gu, D Yang, Q Huang, W Yang, and L Liu. Robust emg pattern recognition in the presence of confounding factors: features, classifiers and adaptive learning. *Expert Systems with Applications*, 96, 2018.

W. Guo, X. Sheng, H. Liu, and X. Zhu. Toward an enhanced human–machine interface for upper-limb prosthesis control with combined emg and nirs signals.

IEEE Transactions on Human-Machine Systems, 47(4):564–575, 2017.

Patrick Haggard and Alan Wing. Coordinated responses following mechanical perturbation of the arm during prehension. *Experimental Brain Research*, 1995.

Patrick Haggard and Alan Wing. On the hand transport component of prehensile movements. *Journal of Motor Behavior*, 29(3):282–287, 1997.

L J Hargrove, G Li, K B Englehart, and B S Hudgins. Principal components analysis preprocessing for improved classification accuracies in pattern-recognition-based myoelectric control. *IEEE Transactions on Biomedical Engineering*, 56(5):1407–1414, 2009.

Levi J Hargrove, Laura A Miller, Kristi Turner, and Todd A Kuiken. Myoelectric pattern recognition outperforms direct control for transhumeral amputees with targeted muscle reinnervation: A randomized clinical trial. *Scientific Reports*, 2017.

J He, D Zhang, N Jiang, X Sheng, D Farina, and X Zhu. User adaptation in long-term, open-loop myoelectric training: implications for emg pattern recognition in prosthesis control. *Journal of Neural Engineering*, 2015.

H J Hermens, B Freriks, C Disselhorst-Klug, and G Rau. Development of recommendations for semg sensors and sensor placement procedures. *Journal of Electromyogry Kinesiology*, 2000.

Y Huang, K B Englehart, B Hudgins, and A D C Chan. A gaussian mixture model based classification scheme for myoelectric control of powered upper limb prostheses. *IEEE Transactions on Biomedical Engineering*, 2005.

I Imbinto, F Montagnani, M Bacchereti, C Cipriani, A Davalli, R Sacchetti, E Gruppioni, S Castellano, and M Controzzi. Thes-finger: A synergetic externally powered digit with tactile sensing and feedback. *IEEE Transactions on Neural Systems and Rehabilitation Engineering*, 26(6), 2018.

Fumiaki Iwane, Manu Srinath Halvaga, Iñaki Iturrate, Iason Batzianoulis, Ricardo Chavarriaga, Aude Billard, and José del R. Millán. Inferring subjective preferences on robot trajectories using eeg signals. In *9th International IEEE EMBS Conference on Neural Engineering*, 2019.

H. Jaeger. The "echo state" approach to analyzing and training recurrent neural networks. GDM Report 148, German National Research Institute for Computer Science, 2001.

Mark Jeannerod. The timing of natural prehension movements. *Journal of Motor Behaviour*, 16(3), 1984.

Johnny LG Jiang, Ning Vest-Nielsen, Silvia Muceli, and Dario Farina. Biomimetic intraneural sensory feedback enhances sensation naturalness, tac-

tile sensitivity, and manual dexterity in a bidirectional prosthesis. *Neuron*, 100(1), 2018.

M W Jiang, R C Wang, J Z Wang, and D W Jin. A method of recognizing finger motion using wavelet transform of surface emg signal. In *IEEE Engineering in Medicine and Biology 27th Annual Conference*, 2005.

Ning Jiang, Ivan Vujaklija, Hubertus Rehbaum, Bernhard Graimann, and Dario Farina. Is accurate mapping of emg signals on kinematics needed for precise online myoelectric control? *IEEE Transactions on Neural System and Rehabilitation Engineering*, 2014.

R S Johansson and J R Flanagan. Coding and use of tactile signals from the fingertips in object manipulation tasks. *Nature Reviews Neuroscience*, 10(9), 2009.

L A Jones and S J Lederman. *Human Hand Function*. Oxford University Press, Oxford, UK, 2006.

Z Ju and H Liu. Human hand motion analysis with multisensory information. *IEEE/ASME Transactions on Mechatronics*, 2014.

K K. Oltstlie, B Garfelt, and P Skjeldal, O and. Magnus. Adult acquired major upper-limb amputation in norway: Prevalence, demographic features and amputation specific features. *Disability and Rehabilitation*, 2011.

G Kanitz, C Cipriani, and B B Edin. Classification of transient myoelectric signals for the control of multi-grasp hand prostheses. *IEEE Transactions on Neural Systems and Rehabilitation Engineering*, 26(9):1756–1764, 2018. ISSN 1534-4320. doi: 10.1109/TNSRE.2018.2861465.

G. Keren and B. Schuller. Convolutional rnn: An enhanced model for extracting features from sequential data. In *2016 International Joint Conference on Neural Networks (IJCNN)*, pages 3412–3419, 2016.

Z O Khokhar, Z G Xiao, and C Menon. Surface emg pattern recognition for real-time control of a wrist exoskeleton. *BioMedical Engineering OnLine*, 9: 41–57, 2010.

Rami N Khushaba, Sarath Kodagoda, Maen Takruri, and Gamini Dissanayake. Toward improved control of prosthetic fingers using surface electromyogram (emg) signals. *Expert Systems with Applications*, 39(12), 2012.

K Kita, R Kato, H Yokoi, and T Arai. Development of autonomous assistive devices-analysis of change of human motion patterns. In *IEEE International Symposium on Robot and Human Interactive Communication (RO-MAN)*, 2006.

A Krasoulis, I Kyranou, M S Erden, K Nazarpour, and S Vijayakumar. Improved prosthetic hand control with concurrent use of myoelectric and inertial

measurements. *Journal of NeuroEngineering and Rehabilitation*, 2017.

N E Krausz, D Lamotte, I Batzianoulis, L Hargrove, S Micera, and A Billard. Gaze and emg coordination during targeted pick-and-place tasks for upper-limb prosthesis control. In *38th International Conference of the IEEE Engineering in Medicine and Biology Society (EMBC)*, 2016.

T. A. Kuiken, L. A. Miller, K. Turner, and L. J. Hargrove. A comparison of pattern recognition control and direct control of a multiple degree-of-freedom transradial prosthesis. *IEEE Journal of Translational Engineering in Health and Medicine*, 4:1–8, 2016.

Todd A Kuiken, Blair A Li, Guanglin amd Lock, Robert D Lipschutz, Laura A Miller, Stubblefield Kathy A, and Kevin Englehart. Targeted muscle reinnervation for real-time myoelectric control of multifunction artificial arms. *JAMA*, 301, 2009.

Iris Kyranou, Agamemnon Krasoulis, Kianoush Erden, Mustafa Suphi adn Nazarpour, and Sethu Vijayakumar. Real-time classification of multimodal sensory data for prosthetic hand control. In *IEEE International Conference on Biomedical Robotics and Biomechatronics (BioRob)*, volume 11, 2016.

O Lambercy, L Dovat, H Yun, S K Wee, C WK Kuah, K SG Chua, R Gassert, T E Milner, C L Teo, and E Burdet. Effects of a robot-assisted training of grasp and pronation/supination in chronic stroke: a pilot study. *Journal of NeuroEngineering and Rehabilitation*, 2011.

M Legrand, M Merad, E de Montalivet, A Roby-Brami, and M Jarasse. Movement-based control for upper-limb prosthetics: Is the regression technique the key to a robust and accurate control? *Frontiers in Neurorobotics*, 2018.

T. Lenzi, J. Lipsey, and J. W. Sensinger. The ric arm- a small anthropomorphic transhumeral prosthesis. *IEEE Transactions on Mechatronics*, 2016.

D Leonardis, M Barsotti, C Loconsole, M Solazzi, M Troncossi, C Mazzotti, V P Castelli, C Procopio, G Lamola, C Chisari, M Bergamasco, and A Frisol. An emg-controlled robotic hand exoskeleton for bilateral rehabilitation. *IEEE Transactions on Neural System and Rehabilitation Engineering*, 2015.

Sergey Levine, Peter Pastor, Alex Krizhevsky, Julian Ibarz, and Deirdre Quillen. Learning hand-eye coordination for robotic grasping with deep learning and large-scale data collection. *International Journal of Robotics Research*, 37(4), 2018.

D. Li, M. Han, and J. Wang. Chaotic time series prediction based on a novel robust echo state network. *IEEE Transactions on Neural Networks and Learning Systems*, 23(5), 2012.

Guanglin Li, Aimee E Schultz, and Todd A Kuiken. Quantifying pattern

recognition-based myoelectric control of multifunctional transradial prostheses. *IEEE Transactions on Neural Systems and Rehabilitation Engineering*, 18(185), 2010.

Miao Li, Kaiyua Hang, Danica Kragic, and Aude Billard. Dexterous grasping under shape uncertainty. *Robotics and Autonomous Systems*, 75:352–364, 2016.

M V Liarokapis, P K Artemiadis, K J Kyriakopoulos, and E S Manolakos. A learning scheme for reach to grasp movements: On emg-based interfaces using task specific motion decoding models. *IEEE Journal of Biomedical and Health Informatics*, 2013.

D Liu, J Zhang, X Sheng, and X Zhu. Quantification and solutions of arm movements effect on semg pattern recognition. *Biomedical Signal Processing and Control*, 2014.

T Lorrain, N Jiang, and Dario Farina. Influence of the training set on the accuracy of surface emg classification in dynamic contractions for the control of multifunction prostheses. *Journal of NeuroEngineering and Rehabilitation*, 2011.

L Lukic, J Santos-Victor, and A Billard. Learning coupled dynamical systems from human demonstration for robotic eye-arm-hand coordination. In *IEEE-RAS International Conference on Humanoid Robots (Humanoids)*, 2012.

P. Weiss M. Jeannerod, Y. Paulignan. Grasping an object: one movement, several components. In *Novartis Foundation Symposium*, 1998.

J Ma, N V Thakor, and F Matsuno. Hand and wrist movement control of myoelectric prosthesis based on synergy. *IEEE Transactions on Human-Machine Systems*, 45(1):74–83, 2015. ISSN 2168-2291. doi: 10.1109/THMS.2014.2358634.

M Markovic, S Dosen, D Popovic, B Graimann, and D Farina. Sensor fusion and computer vision for context-aware control of a multi degree-of-freedom prosthesis. *Journal of Neural Engineering*, 15, 2015.

Marko Markovic, Strahinja Dosen, Christian Cipriani, Dejan Popovic, and Dario Farina. Stereovision and augmented reality for closed-loop control of grasping in hand prostheses. *Journal of Neural Engineering*, 11, 2014.

Chiara Martelloni, Jacopo Carpaneto, and Silvestro Micera. Characterization of emg patterns from proximal arm muscles during object- and orientation-specific grasps. *IEEE Transactions On Biomedical Engineering*, 2009.

R. Menon, G. Di Caterina, H. Lakany, L. Petropoulakis, B. A. Conway, and J. J. Soraghan. Study on interaction between temporal and spatial information in classification of emg signals for myoelectric prostheses. *IEEE Transactions on Neural Systems and Rehabilitation Engineering*, 25(10):1832–1842, 2017.

E Merad, M de Montalivet, A Toullet, N Martinet, A Roby-Brami, and M Jarasse. Can we achieve intuitive prosthetic elbow control based on healthy upper limb motor strategies? *Frontiers in Neurorobotics*, 2018.

Laura A Miller, Kathy A Stubblefield, Robert D Lipschutz, Blair A Lock, and Todd A Kuiken. Improved myoelectric prosthesis control using targeted reinnervation surgery: A case series. *IEEE Transactions on Neural System and Rehabilitation Engineering*, 2008.

Federico Montagnani, Marco Controzzi, and Christian Cipriani. Is it finger or wrist dexterity that is missing in current hand prostheses? *IEEE Transactions on Neural Systems and Rehabilitation Engineering*, 23(4), 2015.

S Muceli and D Farina. Simultaneous and proportional estimation of the hand kinematics from emg during mirrored movements at multiple degrees of freedom. *IEEE Transactions of Neural System and Rehabilitation*, 20(3), 2012.

G R Naik and H T Nguyen. Nonnegative matrix factorization for the identification of emg finger movements: Evaluation using matrix analysis. *IEEE Journal of Biomedical and Health Informatics*, 19, 2015.

Ganesh R Naik, Ali H Al-Timemy, and Hung T Nguyen. Transradial amputee gesture classification using an optimal number of semg sensors: An approach using ica clustering. *IEEE Transactions on Neural Systems and Rehabilitation Engineering*, 24(8), 2016.

D Nishikawa, W Yu, H Yokoi, and Y Kakazu. Emg prosthetic hand controller using real-time learning method. In *IEEE International Conference on Systems, Man, and Cybernetics, (SMC)*, 1999.

D. Novak, X. Omlin, R. Leins-Hess, and R. Riener. Effectiveness of different sensing modalities in predicting targets of reaching movements. In *International Conference of the IEEE EMBS*, 2013.

Domen Novak and Robert Riener. A survey of sensor fusion methods in wearable robotics. *Robotics and Autonomous Systems*, 2014.

R C Oldfield. The assessment and analysis of handedness: the edinburgh inventory. *Neuropsychologia*, 1971.

kristin Oltstlie, Ingrid Marie Lesjo, Rosemary Joy Franklin, Beate Garfelt, Ola H Skjeldal, and Per Magnus. Prosthesis rejection in acquired major upper-limb amputees: a population-based survey. *Disability and Rehabilitation*, 2012.

R R Osborn, L Kaliki, A B Soares, and N V Thakor. Neuromimetic event-based detection for closed-loop tactile feedback control of upper limb prostheses. *IEEE Transactions on Haptics*, 9(2), 2016.

G Ouyang, X Zhu, Z Ju, and H Liu. Dynamical characteristics of surface emg signals of hand grasps via recurrence plot. *IEEE Journal of Biomedical and*

Health Informatics, 2014.

Y Paulignan, C MacKenzie, R Marteniuk, and M Jeannerod. The coupling of arm and finger movements during prehension. *Experimental Brain Research*, 79:431–435, 1990.

B Peerdeman, D Boere, H Witteveen, R H Veld, H Hermens, S Stramigioli, H Rietman, P Veltink, and S Misra. Myoelectric forearm prostheses: State of the art from a user-centered perspective. *Journal of Rehabilitation Research and Development*, 2011.

Angkoon Phinyomark, Pornchai Phukpattaranont, and Chusak Limsakul. Feature reduction and selection for emg signal classification. *Expert Systems with Applications*, 39(8):7420 – 7431, 2012.

Katherine A Raichle, Marisol A Hanley, Ivan Molton, Nancy J Kadel, Kellye Campbell, Emily Phelps, Dawn Ehde, and Douglas G Smith. Prosthesis use in persons with lower- and upper-limb amputation. *Journal of Rehabilitation Research and Development*, 2008.

Miya K Rand, Y P Shimansky, Abul B M I Stelmach, and HossainGeorge E Stelmach. Quantitative model of transport- aperture coordination during reach-to-grasp movements. *Experimental Brain Research*, 188, 2008.

S Raspopovic, M Capogrosso, F M Petrini, M Bonizzato, J Rigosa, G Di Pino, J Carpaneto, M Controzzi, T Boretius, E Fernandez, G Granata, C M Oddo, L Citi, A L Ciancio, C Cipriani, M C Carrozza, W Jensen, E Guglielmelli, T Stieglitz, P M Rossini, and S Micera. Restoring natural sensory feedback in real-time bidirectional hand prostheses. *Science Translational Medicine*, 2014.

Linda Resnik, He (Helen) Huang, Anna Winslow, Dustin L. Crouch, Fan Zhang, and Nancy Wolk. Evaluation of emg pattern recognition for upper limb prosthesis control: a case study in comparison with direct myoelectric control. *Journal of NeuroEngineering and Rehabilitation*, 15(1):23, 2018.

Agnés Roby-Brami, Nezha Bennis, Mounir Mokhtari, and Pierre Baraduc. Hand orientation for grasping depends on the direction of the reaching movement. *Brain Research*, 869(1):121 – 129, 2000.

M. Santello and J. F. Soechting. Gradual molding of the hand to object contours. *Journal of Neurophysiology*, 79(3), 1998.

M Santello, M Flanders, and J F Soechting. Postural hand synergies for tool use. *The Journal of Neuroscience*, 1998.

C Sapsanis, G Georgoulas, A Tzes, and D Lymberopoulos. Improving emg based classification of basic hand movements using emd. In *IEEE Engineering in Medicine and Biology 35th Annual Conference*, 2013.

S Schaal, S Kotosaka, and D Sternad. Nonlinear dynamical systems as movement primitives. In *IEEE international conference on humanoid robotics*, 2000.

Erik Scheme, K Biron, and Kevin Englehart. Improving myoelectric pattern recognition positional robustness using advanced training protocols. In *33rd Annual International Conference of the IEEE EMBS*, 2011.

F Sebelius, M Axelsson, N Danielsen, J Schouenborg, and T Laurell. Real-time control of a virtual hand. *Technology and Disability*, 2005.

P Shenoy, K J Miller, B Crawford, and R P N Rao. Online electromyographic control of a robotic prosthesis. *IEEE Transactions on Biomedical Engineering*, 2008.

A Shukla and A Billard. Coupled dynamical system based arm-hand grasping model for learning fast adaptation strategies. *Robotics and Autonomous Systems*, 60(3), 2012.

L. H. Smith and T. A. Kuiken L. J. Hargrove, B. A. Lock. Determining the optimal window length for pattern recognition-based myoelectric control: Balancing the competing effects of classification error and controller delay. *IEEE Transactions on Neural Systems and Rehabilitation Engineering*, 19(2), 2011.

Lauren H Smith, Todd A Kuiken, and Levi J Hargrove. Evaluation of linear regression simultaneous myoelectric control using intramuscular emg. *IEEE Transactions of Biomedical Engineering*, 2016.

R J Smith, F Tenore, D Huberdeau, R Etienne-Cummings, and N V Thakor. The coupling of arm and finger movements during prehension. In *IEEE Engineering in Medicine and Biology 30th Annual Conference*, 2008.

Y Su, M H Fisher, A Wolczowski, G D Bell, D J Burn, and R X Gao. Towards an emg-controlled prosthetic hand using a 3-d electromagnetic positioning system. *IEEE Transactions on Instrumentation and Measurement*, 56(1), 2007.

Fuchun Sun, Chunfang Liu, Wenbing Huang, and Jianwei Zhang. Object classification and grasp planning using visual and tactile sensing. *IEEE Transactions in Robotics*, 46(7), 2016.

T Supuk, T Kodek, and T Bajd. Estimation of hand preshaping during human grasping. *Medical Engineering and Physics*, 2005.

Melanie G Urbanchek, Benjamin Wei, Ziya Baghmanli, Kristoffer Sugg, and Paul S Cederna. Long-term stability of regenerative peripheral nerve interfaces. *Plastic and Reocnstractive Surgery*, 128(4S), 2011.

Giacomo Valle, Alberto Mazzoni, Francesco Iberite, Edoardo D'Anna, Ivo Strauss, Giuseppe Granata, Marco Controzzi, Francesco Clemente, Giulio Rognini, Christian Cipriani, Thomas Stieglitz, Francesco Maria Petrini,

Paolo Maria Rossini, and Silvestro Micera. Biomimetic intraneural sensory feedback enhances sensation naturalness, tactile sensitivity, and manual dexterity in a bidirectional prosthesis. *Neuron*, 100(1):37 – 45.e7, 2018.

Jinsung Wang and George E Stelmach. Coordination among the body segments during reach-to-grasp action involving the trunk. *Experimental Brain Research*, 1998.

T W Williams. Control of powered upper extremity prostheses. In Meier RH and Atkins DJ, editors, *Functional restoration of adults and children with upper extremity amputation*, pages 207–224. Demos Medical Publishing, Inc., New York, 2004.

A. M. Wing and A. Turton. Grasp size and accuracy of approach in reaching. *Journal of Motor Behavior*, 1986.

M. Xu and M. Han. Adaptive elastic echo state network for multivariate time series prediction. *IEEE Transactions on Cybernetics*, 2016.

D Yang, Y Gu, L Jiang, L Osborn, and H Liu. Dynamic training protocol improves the robustness of pr-based myoelectric control. *Biomedical Signal Processing and Control*, 2017.

Aaron J Young, Lauren H Smith, Elliott J Rouse, and Levi J Hargrove. Classification of simultaneous movements using surface emg pattern recognition. *IEEE Transactions on Biomedical Engineering*, 60(5), 2013.

A Ziai and C Menon. Comparison of regression models for estimation of isometric wrist joint torques using surface electromyography. *Journal of NeuroEngineering and Rehabilitation*, 2011.

K Ziegler-Graham, E J MacKenzie, P L Ephraim, and T G Travison. Estimating the prevalence of limb loss in the united states: 2005 to 2050. *Archives of Physical Medicine and Rehabilitation*, 2008.

Iason Batzianoulis

Curriculum Vitae

Education

2015 - present Advisor	**PhD, Robotics,** Ecole Polytechnique Fédérale de Lausanne (EPFL), Lausanne, Switzerland Prof. Aude Billard
Sept - Dec 2016	**Visiting Scholar,** Northwestern University and Shirley Ryan AbilityLab, Chicago, Il, USA
Mar - Dec 2014	**Research Assistant**, Ecole Polytechnique Fédérale de Lausanne (EPFL), Lausanne, Switzerland
2003 - 2012	**Diploma of Electrical and Computer Engineer,** Aristotle University of Thessaloniki (AUTH), Thessaloniki, Greece

Skills

Machine Learning	Proficient on the application and development of multiple learning approaches, including dimentionality reduction, linear and non-linear classification and regression, artificial neural networks, data modeling, kernel methods, convex optimization, deep learning (beginner level)
Robot Control	Robotic arm kinematics, object manipulation with robotic hand, linear and non-linear dynamical systems, development of real-time applications, learning by demonstration
Biomedical Signals	Electromyography, Eye-gaze analysis, signal processing, human arm and hand anatomy, Encephalography (beginner level)
Programming	C, C++, Python, Matlab, Java, modern source control (Git)
Software Packages	MS office, MS Visual Studio, Qt creator, MS Windows, Linux, OpenCV, libSVM, scikit-learn, SciPy, NumPy, ROS, Adobe Photoshop, Adobe Illustrator

Projects

PhD thesis

a. ***Fast decoding of grasping intention from Eletromyography***
Designed a classification approach for the identification the grasping type from the muscular activity of the arm. This approach tackles the uncertainty of the noisy Electromyographic signals with the use of Echo State Networks, handling the signals as time series.

b. ***Real-time control and evaluation with end-users***
Developed a real-time pattern recognition system for controlling a hand myo-prosthesis. A systematic performance comparison was conducted among different ML methods, such as Support Vector Machines, Linear Discriminant Analysis and Echo State Networks. The approach satisfies the requirements of a real-time application for a rapid and accurate prediction.

c. ***Evolution of the Gaussian models in muscle activity during the reaching phase***
Developed a method for increasing the classification accuracy of a decoder by examining the evolution of the EMG activity when modeled as Gaussian distributions. A quantification of the similarity among the Gaussian models was performed with the Hellinger distance, a type of f-divergence measure.

Other

a. ***Object recognition for picking and placing tasks***
The computer vision system locates different objects on the robot workspace and classifies online. A Principal Component Analysis performs a dimensionality reduction whereas the classification is based on Gaussian Mixture Models.

Av. de Sévelin 2B, 1007 Lausanne, Switzerland

+41 (0) 76 698 24 11 iason.batzianoulis@epfl.ch Iason Batzianoulis yias

Other

b. ***Learning optimal robot trajectories from brain activity***
The optimal parameters for the robot motion were identified with Inverse Reinforcement Learning methods. The robotic system uses error-related potentials from the brain activity of the user for modifying the robot trajectories.
c. ***Eye-gaze and Electromyography coordination***
A Support Vector Regressor was built for relating the arm extension with the muscular activity. The gaze fixation on objects was monitored to evaluate the relation with the motion onset of the arm, for examining potential uses on robot control.

Publications

Journal papers

2018 **Batzianoulis** et al., "*Decoding the Grasping Intention from Electromyography during Reaching Motions*", Journal of NeuroEngineering and Rehabilitation, vol. 15 (57)

2017 **Batzianoulis** et al., "*EMG-Based Decoding of Grasp Gestures in Reaching-to-Grasping Motions*", Robotics and Autonomous Systems, vol. 91

Conference papers

2019 **Batzianoulis** et al., "*A dynamic approach for decoding the grasping intention*", in the proceedings of the IEEE EMBS International Conference on Neural Engineering, San Francisco, CA, USA

2018 F. Iwane, M. Halvagal, I. Iturrate, **I. Batzianoulis** et al., "*Learning subjectively optimal trajectories from EEG error potentials: A pilot study*", in the proceedings of the International Conference on Robot Learning, Zurich, Switzerland

2016 N. Krausz, D. Lamotte, **I. Batzianoulis** et al., "*Gaze and EMG coordination during targeted pick-and-place tasks for upper-limb prosthesis control*", in the proceedings of the 38th International Conference of IEEE Engineering in Medicine and Biology Society EMBC, Orlando, FL, USA

2015 **Batzianoulis** et al., "*EMG-Based Analysis of the Upper Limb Motion*", in the proceedings of the 10th ACM IEEE International Conference on Human-Robot Interaction, Portland, OR, USA

S. El-Khoury, **I. Batzianoulis** et al., "*EMG-based learning approach for estimating wrist motion*", in the proceedings of the International Conference of IEEE Engineering in Medicine and Biology Society (EMBC), Milan, Italy

Soft skills

Interpersonal — Teamwork, creative and highly motivated, decision making, criticial thinking
Hardworking, excellent ability to adapt to new envirnments

Leadership — Project managment, ability to frame accuratelly a problem and guide group members
Tutoring and teaching (teaching assistantship for 3 years, supervision of 8 student projects)

Languages

English — C2 level in speaking, reading, writing and scientific writing
French — A1 level in speaking, (currently learning)
Greek — Native language

Extracurricular activities

Artistic — Photography and graphics design
Sports — Football, basketball, hiking

Av. de Sévelin 2B, 1007 Lausanne, Switzerland
+41 (0) 76 698 24 11 iason.batzianoulis@epfl.ch Iason Batzianoulis yias

**Ce document a été imprimé au Centre d'impression EPFL,
imprimerie climatiquement neutre, certifiée myClimate.**